UNIVERSITÄT ZU LÜBECK

From The Department of Dermatology

of University of Lübeck

Director: Prof. Dr. med. Detlef Zillikens

Contribution of cytokines to the pathogenesis of epidermolysis bullosa acquisita

Dissertation

for Fulfillment of

Requirements

for the Doctoral Degree

of the University of Lübeck

From the Department of Natural Sciences

Submitted by

Unni Krishna SRL Samavedam, MSc. MRes.

From Kakinada, India

Lübeck 2013

IM FOCUS DAS LEBEN

First referee:-	Prof.Dr.R.Ludwig
Second referee:-	Prof.Dr.J.Stein
Additional referee:-	Prof.Dr.E.Hartmann
Chairman:-	Prof. Dr. J.Westermann
Date of oral examination:-	17.10.2013
Approved for printing:-	22.10.2013, Lübeck

TABLE OF CONTENTS

1. Summary

Cytokines are crucial regulators of immune functions. While an integral part of the host response, aberrant cytokine responses are linked to pathogenesis of chronic inflammatory diseases. Cytokine modulating strategies are successfully implemented in treatment of many inflammatory conditions. Despite aberrant cytokine expression, cytokine-targeting therapies have not been established in autoimmune bullous dermatoses (AIBD), most likely due to lack of functional data and / or redundant functions within the cytokine family. This study focuses on systematic analysis of the contribution of two cytokines, namely GM-CSF and IL-6, to the pathogenesis of autoantibody-induced tissue injury in the animal models of a prototypic AIBD, epidermolysis bullosa acquisita (EBA). In experimental EBA, GM-CSF and IL-6 serum cytokine levels correlated with disease activity. Functional analysis revealed a complex and unexpected contribution of these cytokines to the pathogenesis: as expected by correlating serum levels, GM-CSF inhibition significantly reduced skin blistering and/or was effective in a therapeutic setting. At the functional level, GM-CSF modulated reactive oxygen species (ROS) release from immune-complex-activated neutrophils and their migration. Furthermore, GM-CSF$^{-/-}$ mice immunized with COL7 developed significantly lower antibody titers which were associated with reduced neutrophil numbers in draining lymph nodes. An identical effect on autoantibody production was observed in neutrophil depleted wild type mice. Additionally, neutrophil depletion in GM-CSF$^{-/-}$ mice, led to an even stronger inhibition of autoantibody production, indicating that GM-CSF and neutrophils have overlapping and distinct functions in modulating autoantibody production in a CD4 dependent B cell immune response. Interestingly, IL-6, the other cytokine studied in the present thesis, showed a surprising effect in experimental EBA. In sharp contrast to other autoimmune diseases, inhibition of IL-6 functions led to enhanced blistering, while treatment with recombinant IL-6

almost completely protected from disease. At the molecular and functional levels, IL-6 led to increased IL-1Ra concentrations in serum and skin and protected from apoptosis and proteolysis in the skin through *classical IL-6 signaling*. In summary, this study provides new insights into the complex cytokine network regulating autoantibody-induced tissue injury, which will facilitate selection of novel therapeutic targets for patients with EBA and other AIBD.

2. Appendix

2.1. List of abbreviations

AIBD	autoimmune bullous disease
AUC	area under the curve
BALB/c	inbred mouse strain
BMZ	basement membrane zone
BP	bullous pemphigoid
BP 180	180-kD bullous pemphigoid antigen
BP 230	230-kD bullous pemphigoid antigen
BPAG1	bullous pemphigoid antigen 1
BPAG2	bullous pemphigoid antigen 2
C (domain)	collagenous (domain)
C3	complement component 3
C57Bl/6J	inbred mouse strain
CaCl2	calcium chloride
CD	cluster of differentiation
CMP	cartilage matrix protein
COL7	Type VII collagen
COL17	Type XVII collagen

DEJ	dermal-epidermal junction
DIF	direct immunofluorescence
EBA	epidermolysis bullosa acquisita
ECM	extracellular matrix
EDTA	ethylene-diamine-tetra-acetic acid
ELISA	enzyme-linked immunosorbent assay
FITC	fluorescein isothiocyanate
g	gram
gp130	glycoprotein 130
GST	glutathione S transferase
H&E	haematoxylin and eosin
H2b	mouse major histocompatibility complex haplotype 2b
H2s	mouse major histocompatibility complex haplotype 2s
HD	hemidesmosome
HLA	human leukocyte antigen
HRP	horseradish peroxidase
IC	immune complex
IF	immunofluorescence
IgG	immunoglobulin G
IgG1	immunoglobulin G1

IgG2a	immunoglobulin G2a
IgG2b	immunoglobulin G2b
IgG2c	immunoglobulin G2c
IgG3	immunoglobulin G3
iIF	indirect immunofluorescence
kg	kilogram
LD	lamina densa
LL	lamina lucida
M	molar(mole/liter)
m	milli (10^{-3})
µ	micro (10^{-6})
MHC	major histocompatibility complex
MS	multiple sclerosis
n	nano (10^{-9})
NaCl	sodium chloride
NC (domain)	non-collagenous (domain)
OD	optical density
PBS	phosphate buffered saline
PBST	phosphate buffered saline-tween
RA	rheumatoid arthritis

ROS	reactive oxygen species
RT	room temperature
SLE	systemic lupus erythematosus
vWFA2	von Willebrand factor A-like domain 2

2.2. List of tables

2.3. List of figures

3. Introduction

3.1. Skin: Structure and functions

The skin is the largest organ of the body, accounting for approximately 16% of the body weight, with a surface area of 1.8m². The skin fulfills several functions, the most important by forming a physical barrier to the environment, allowing and limiting the inward and outward passage of water, electrolytes and various substances while providing protection against micro-organisms, ultraviolet radiation, toxic agents and mechanical insults (1). To accomplish these functions, skin is in a constant state of change and cells of the outer layers are continuously shed and replaced by inner basal cells that are moving up to the surface.

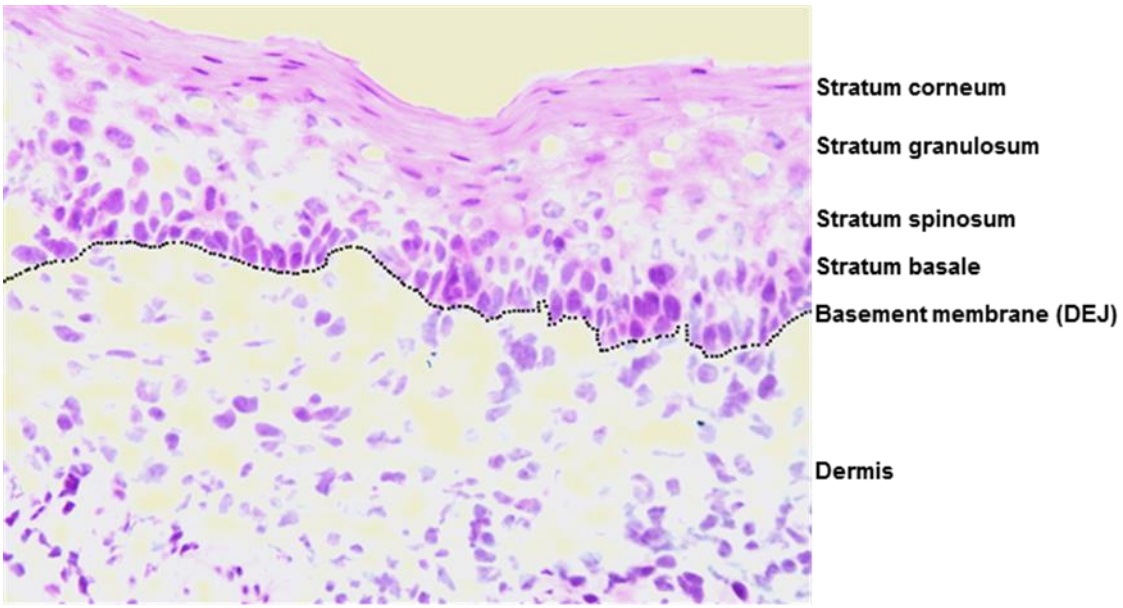

Figure 1. Histological structure of the mouse skin

Epidermis contains outermost layer of corneocytes and organelles granular (2-3 layers), spinosum cell (5-10 layers) and basal cells (single layer). Black line indicates the dermal-epidermal junction (DEJ). Hematoxylin stained cross-section of skin magnified to 200x.Section obtained from control mouse used in this thesis.

Structurally there are three main layers in the skin (table 1): the epidermis, dermis and subcutis. The basement membrane connects epidermis and dermis and forms the

dermal-epidermal junction (DEJ). Dermal papillae of the dermis are small inter-digitations that extended into epidermis. Papillae increase the surface area between the dermis and epidermis along with increasing the exchange of oxygen, nutrients, and waste products between these two layers of the skin.

Layer	Sub-layers	Components and Description
Epidermis	Stratum corneum	Hexagonal-shaped, non-viable cornified cells (corneocytes) along with keratin
	Stratum granulosum	Flatten basal cells with basophilic keratohyalin granules called as Odland bodies or ketatosomes
	Stratum spinosum	Cells of Langerhans and supra-basal (Prickle) cells. They are larger than basal cells and contain a small amount of chromatin in their circular nuclei
	Stratum basale	Innermost layer, comprises dividing and non-dividing keratinocytes, melanocytes, dendritic cells and Merkel cells, The basal cells have desmosomes (for cell-cell attachment), gap junctions (for cell communication), and hemidesmosomes (attachment with BM)
Basement membrane (BM)	Lamina lucida	Consists of laminin 332. Type XVII collagen (BP180) bridges the lamina lucida to connect hemidesmosomes directly with the lamina densa
	Lamina densa	Consists mainly of fibronectins, heparin sulphate proteoglycan, type IV collagen and laminin 5 (laminin 332)
	Sub-lamina densa	Connects around collagen type I and III in the dermis linking it to the lamina densa. Consists of anchoring fibrils, collagen VII, microfilaments
Dermis	Papillary layer	Loosely arranged collagen fibers (type I collagen), fibroblasts and macrophages Contains sweat glands, hair roots, nervous cells and fibers, blood and lymph vessels
	Reticular layer	Connected with papillary layer through collagen fibers (type III collagen)
Subcutis	-	Connective tissue (fibroid septum) and fat cells

Table 1: Layers of skin

Keratinocytes are connected to each other by desmosomes (cell-cell) and hemidesmosomes connect basal keratinocytes to the basement membrane (DEJ) (1). Basal cell cytokeratins such as keratin filaments and tonofilaments, distally connect with hemidesmosomes and desmosomes to form a rigid and robust cellular cytoskeleton (1). Regulation of the adhesive interactions between hemidesmosomes and the basement membrane is essential in various normal biological processes such as wound healing and morphogenesis. Gene expression defects in this region leads to genetic disorders of skin, such as non-junctional Epidermolysis bullosa (2) and Epidermolysis bullosa hereditaria (3).

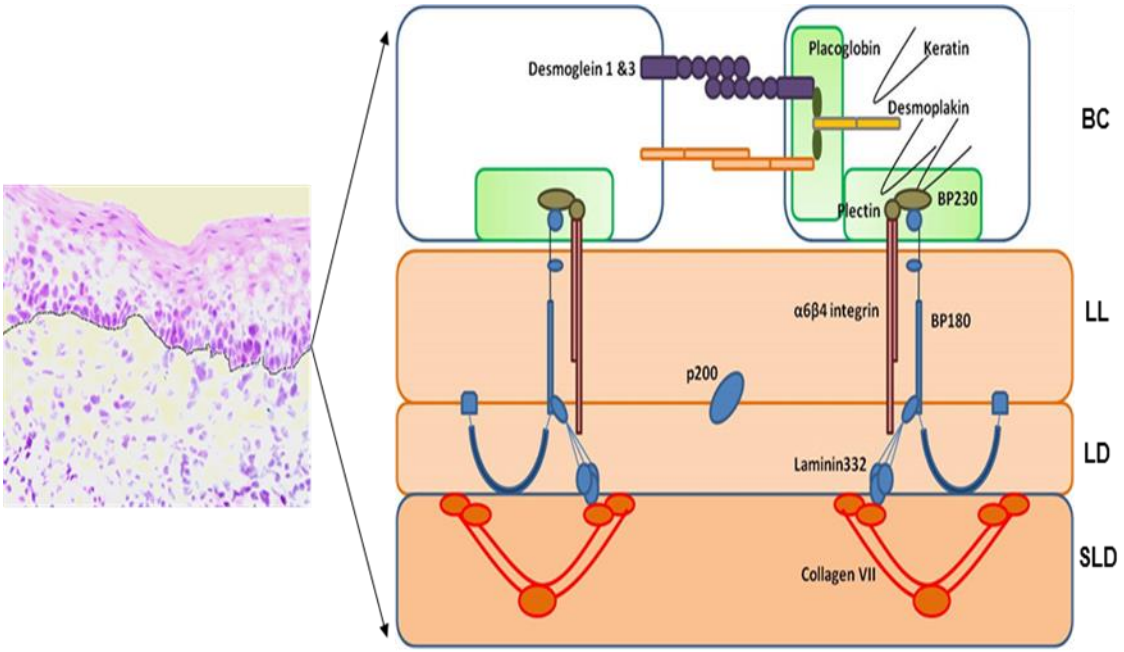

Figure 2. Structure of basement membrane and dermal epidermal junction

BC: basal keratinocytes, LL: lamina lucida, LD: lamina densa, SLD: sublamina densa

3.2. Autoimmune skin blistering diseases (AIBD)

Nobel Laureate Paul Ehrlich first predicted the concept of autoimmunity in 1900. He described it as *'horror autotoxicus'*, that autoimmunity was 'dysteleological' such that 'contrivances' must exist to prevent immune reactions from harming the body itself, thereby concluding that the normal protection mediated by host immune system work wrong and then the immune system can attack self tissues resulting in autoimmune disease (4). Discovery of nephrotoxic antisera, production of hemolysins and spermatolysins in 1900 by Lindemann and others confirmed the existence of autoimmune reactions in the human system (5). Landsteiner, a co-reporter of the first autoimmune disease, described syphilitic patients would react to extracts of normal organs and organs that contain spirochetes, suggesting that hemolysin of cold hemoglobinuria develops exclusively in syphilis patients (6). Later on, many researchers identified the contribution of autoimmune nature of the immune system (7). These lead to defining the criteria for autoimmune diseases by Witebsky in 1957 (8). Finally, In 1965, the International Conference on *Autoimmunity — Experimental and Clinical Aspects,* convened by the New York Academy of Sciences, led to public acknowledgment and consensus on the reality of autoimmunization as an important cause of human disease (9).

Since then many autoimmune diseases have been identified and are classified as either organ-specific or systemic autoimmune diseases. Autoimmune bullous dermatoses (AIBD) are chronic inflammatory, organ-specific (skin) disorders, characterized by mucocutaneous blistering and autoantibodies to desmosomal or hemidesmosomal antigens (10). Depending on the targeted autoantigen, AIBDs are classified into two distinct groups. A brief classification of these diseases shown in table 2.

Disease group	Disease name	Target antigen
Pemphigus	Pemphigus vulgaris	Desmoglein 1 and 3, plakoglobin, E-cadherin, α9-acetylcholinreceptor, pemphaxin
	Pemphigus foliaceus	Desmoglein 1, plakoglobin
	Paraneoplastic pemphigus	Desmoglein1,2 & 3, envoplakin, periplakin, 170 kD antigen, BP230, plectin, desmoglein 1
	IgA Pemphigus	Desmocollin 1, desmoglein 3
Pemphigoid	Bullous pemphigoid	BP180 NC16A, BP230
	Pemphigoid gestationis	BP180 NC16A, BP230
	Linear IgA disease	LAD-1, BP230 (IgA)
	Mucous membrane pemphigoid	BP180, laminin 332, α6β4 integrin, laminin 311, BP230
	Cicatricial pemphigoid	BP180, laminin 332,laminin 311, BP230
	Lichen planus pemphigoides	BP180 NC16A, BP230
	Anti-laminin γ1/p200 pemphigoid	Laminin γ1 (p200 protein)
	Epidermolysis bullosa acquisita	Type VII collagen (IgG / IgA)
Dermatitis herpetiformis		Epidermal/tissue transglutaminase, endomysium, gliadin

Table 2- Classification of AIBD

BP-Bullous pemphigoid, NC- non-collagenous domain, LAD-Linear IgA bullous dermatosis antigen

More specifically, AIBDs are classified as pemphigus, when autoantibodies target desmosomal proteins that connect neighboring keratinocytes, or pemphigoid group in which hemidesmosomal proteins are targeted (10, 11). Lever WF, in 1953, first differentiated these diseases by their histological hallmarks during their pathogenesis (12) In dermatitis herpetiformis, autoantibodies typically bind to epidermal and tissue *transglutaminase* (13). The presence of autoantibodies in the serum of specific target antigens forms the gold standard diagnostic tool for the identification of autoimmune diseases (14–17).

3.3. Epidermolysis bullosa acquisita (EBA): Autoimmunity to type VII collagen

Epidermolysis bullosa acquisita (EBA) is a chronic AIBD clinically characterized by features resembling those of hereditary dystrophic epidermolysis bullosa on the skin and mucosal surfaces (13). Later, EBA was distinguished from other bullous diseases on the basis of distinctive clinical and histological features such as, clinical lesions, adult onset, negative family record and exclusion of other AIBDs (14). EBA is a clinically heterogeneous disease and patients may present with an inflammatory or non-inflammatory phenotype. The inflammatory type is characterized by cutaneous inflammation resembling bullous pemphigoid, linear IgA disease, mucous membrane pemphigoid or Brunsting–Perry pemphigoid (15). In contrast, patients with non-inflammatory or mechanobullous EBA, show skin fragility, trauma-induced blisters and erosions localized to the extensor skin surface, healing with scars and milia (11, 14).

Autoantibodies to type VII collagen (COL7) detected in EBA patients have been shown to induce skin blistering (11). EBA is diagnosed by the presence of sub-epidermal blisters and tissue-bound and circulating autoantibodies to the dermal–epidermal junction in patients (16, 17). Patient's serum contains autoantibodies which recognize the 290-kD type VII collagen, the major component of anchoring fibrils of the DEJ (18). The pathogenesis of the disease includes complement activation, predominantly through the alternative pathway (19). The release of pro-inflammatory cytokines, such as interleukin-1 (IL-1), contributes to the autoantibody-induced tissue injury and inhibition of IL-1 function hinders EBA induction *(personal communication, Hengameh Sadeghi)*. The pro-inflammatory milieu in EBA leads to a CD18-dependent recruitment of neutrophils into the skin (20) through activation of Fc receptor-complexes in mice and humans (21, 22). This activation, leads to a) recruitment of neutrophils to the skin

(23), b) release of reactive oxygen species from the neutrophils and c) proteases including *elastase* and *gelatinase-B*, causing tissue damage (20, 24). Human EBA could be detected in serum samples by more specific and sensitive assays that are developed recently (25).

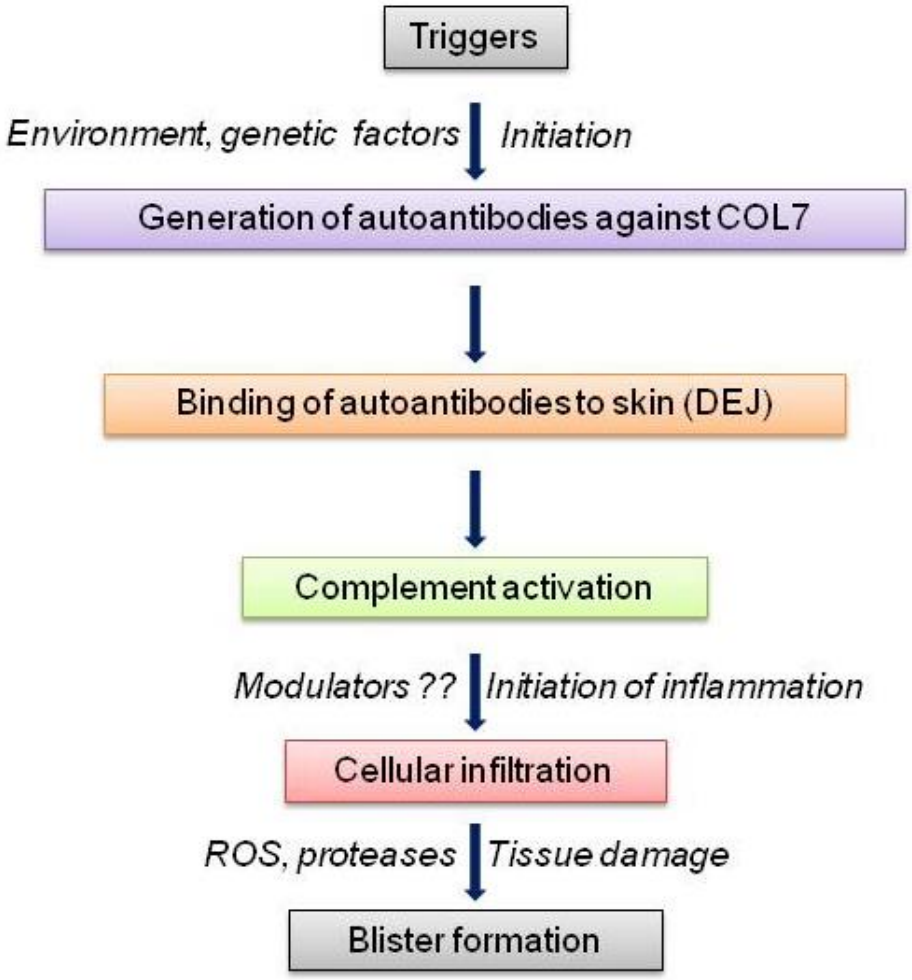

Figure 3. Schematic representation of autoantibody mediated tissue injury in EBA

In EBA, autoantibodies against COL7 are generated in the initiation phase of the disease and they bind to COL7 at DEJ. This leads to complement activation via alternative pathway, which initiates the inflammation. Later, cellular infiltration (mainly neutrophils) takes place leading to tissue damage and blister formation.

3.4. Experimental models for EBA

To understand the pathogenesis of EBA, experimental models (*in vitro*, *ex vivo* and *in vivo)* have been developed. In an *in vitro* assay model, the release of reactive oxygen species (ROS) from immuno complex-activated neutrophils is determined by the measurement of luminol based chemiluminescence (22). In *exvivo* model (cryosection assay), the quantification of the dermal-epidermal separation is performed by using human or mouse skin cryosections, incubated with sera derived from patients (26). Initial efforts to generate animal models (26, 27) were barely successful due to complex interactions and differences between mouse and human COL7 structures. In 2005 and 2006, animal models representing clinical and histological features of human EBA were successfully developed (28) and the disease can be induced either by transfer of anti-COL7 antibodies, or by immunization of mice with immune-dominant fragments of COL7 (29, 30).

In the passive antibody transfer model, Sitaru and colleagues immunized rabbits with recombinant proteins located within the NC1 domain of COL7. Injection of the total immune IgG isolated from these rabbits into C57Bl/6 or BALB/c mice induced subepidermal skin blisters, reproducing human EBA at clinical, histological, electron microscopically, and immunopathological levels (29). After administration of these polyclonal antibodies into mice at different doses, subepidermal blisters and erosions were observed after 2–4 days in a dose dependent manner along with the presence of circulating autoantibodies against COL7. Deposition of C3 and anti-COL7 antibodies at the DEJ was also detected using immunoflourescence. Affinity purified IgG, but not $F(ab)_2$ fragments, from human EBA patients, was used to generate clinical EBA lesion in mice (31). In 2005, Woodley and colleagues generated rabbit anti-human COL7 IgG, which induced experimental EBA in hairless SKH1 mice (32). This blister-inducing activity of anti-COL7 IgG was confirmed by other experiments such as injection of

affinity-purified anti-COL7 or affinity-purified anti-CMP antibodies from EBA patients' sera injected into adult hairless mice (31, 33). Moreover, injection of rabbit IgG directed against the Fn3-like repeats of COL7 into hairless mice also shown blistering activity. (34) Furthermore, rabbit anti-mouse vWFA2 IgG into several, but not all, strains of in- and out-bred mice *(personal communication, Hiroaki Iwata)*, and injection or rabbit anti-human COL7 IgG into COL7-humanized mice induces EBA (35, 36). Most of these antibody-transfer models of EBA mimic the inflammatory variant of the disease. However, in some experimental models, nail loss is additionally observed (31, 32), which is characteristic of mechano-bullous EBA.

Furthermore, an immunization-induced (active) disease model for EBA also was established in order to understand and control the disease induction and to test pharmacological interventions (30). In this model, mice were immunized with a recombinant peptide fragment from the immunogenic NC-1 domain of murine COL7. This method produced circulating autoantibodies against murine COL7 in the mouse itself together with deposits of anti-COL7 IgG antibodies and C3 at the DEJ, closely resembling the human disease. Subsequently, a dependency on T cells was identified, as mice lacking T cells ($SJL^{nu/nu}$ mice) were resistant to disease induction, and adoptive transfer of lymphocytes from immune-competent SJL mice into $SJL^{nu/nu}$ mice lead to EBA in the recipient mice (37). Induction of antibodies with a distinct specificity in the active immunization model was linked to the MHC haplotype in experimental EBA (38). In addition, this model was also used to identify several quantitative trait loci (QTLs) located on mouse chromosomes 9, 12, 14, and 19, whereas maximum disease severity was linked to QTLs on chromosomes 1, 15, and 19, showing the non-MHC dependence of the disease (39). Recently, a new epitope derived polyclonal antibodies targeting VWFA-2 domain of murine COL7 have also been shown pathogenically

relevant in both passive transfer *(personal communication, Hiroaki Iwata)* and immunization-induced models (40).

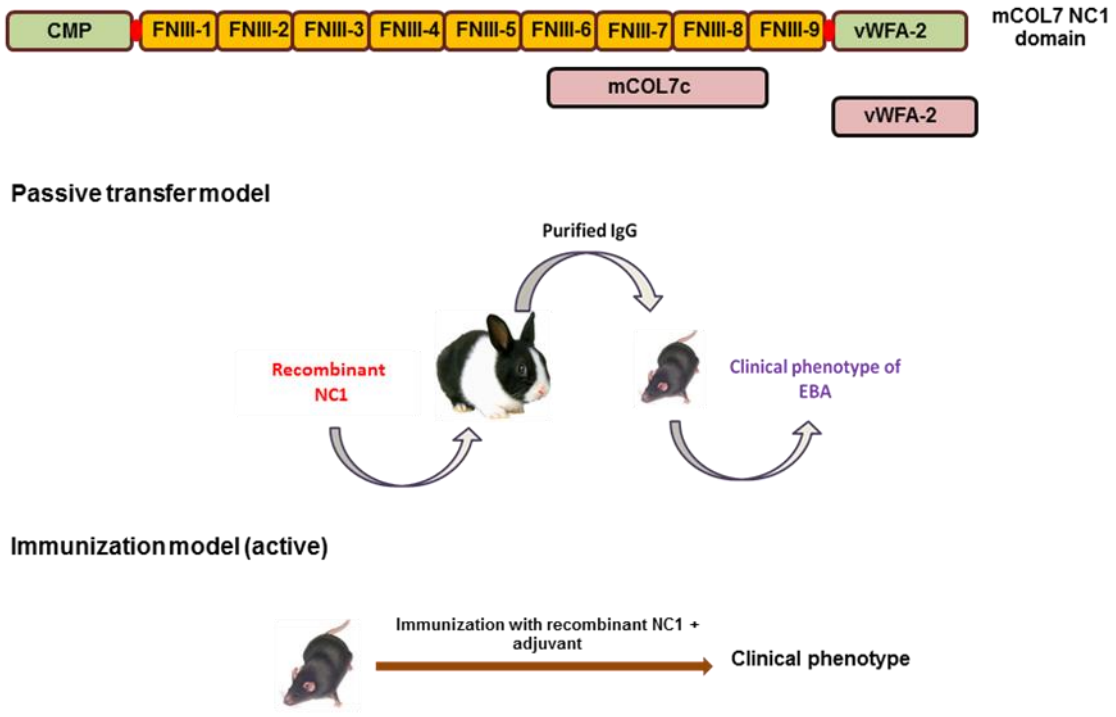

Figure 4. Animal models of EBA

In passive transfer model, rabbits were immunized with recombinant NC1 protein (mCOL7c or vWFA2) and rabbit IgG was purified. This purified IgG was later injected into mice to induce EBA. In immunization model (active model), mice were directly immunized with recombinant NC1 (mCOL7c or vWFA2) together with adjuvant (TiterMax), leading to EBA phenotype.

3.5. Cytokines

The term cytokine, or immune-cytokines, was initially used to separate a group of immune-modulatory proteins, also termed as immune-transmitters, from other growth factors or regulatory peptide factors that modulate the proliferation and bioactivities of non-immune cells (41). These are produced by different cells, especially cells of the immune system, either as a response to an immune stimulus or as an intracellular signal after certain stimulation (42). Cytokines have a multitude of different biological effects and are very important both in the innate and adaptive immunity (43). They can modulate the functions and activation of various cells at pico-molar (pM) concentrations. Cytokines can target various cell types and the activity on cells depends on the expression of cytokine specific receptors on the cell membrane (41). The cytokines can be classified as interleukins (leukocyte modulation), growth factors (growth and maturation of immune cells) and chemokines although all these have interactive and multifunctional roles in immune system together with the positive and negative impact (44).

Cytokines can function pro- as well as anti-inflammatory depending on the condition by which they are released from the cells (45). Some cytokines, such as interleukin-1 (IL-1), interleukin-2 (IL-2), tumor-necrosis factor-α (TNF-α) and interferons, are considered as pro-inflammatory in terms of disease pathogenesis and are also well known for the promotion of immune and inflammatory responses against infections. Some cytokines, such as interleukin-10 (IL-10) play mainly as immune suppressive, also regulates the pathogenesis of infections (46). However, the balance and combination of cytokines exert variable effects in resolving inflammatory exudates, cell–cell interactions lead to the generation of active signals that limit further cell recruitment to the tissue and thereby promoting a return to homeostasis in the evolution of autoimmune diseases (47). This combination of cytokine mediated

activation leads to specialized signaling pathways, including nuclear factor-κB (NF-κB)-regulated processes (which can be either stimulatory or inhibitory), depending on the ligand and the cellular process by which the pathway is activated (48). In some autoimmune diseases such as rheumatoid arthritis (RA), multiple sclerosis (MS), cytokines such as interleukin-1 (IL-1) and TNF-α have been implicated as pro-inflammatory (49) and treatment options to block these cytokines have been successfully implemented to treat patients especially for TNF-α.

3.6. Cytokine modulating therapies in other chronic inflammatory diseases

Cytokine modulation, such as using TNF-α blockers, IL-1, and IL-6 and GM-CSF (in clinical trials) have been successfully implemented in other chronic inflammatory diseases. In rheumatoid arthritis (RA), treatment with TNF-α blockers such as infliximab, etanercept and adalimumab have shown profound therapeutic activities (50–52). In the case of psoriasis models, TNF-α blockade greatly improved therapeutic options (53). In Crohn's disease, adalimumab treatment effectively controlled inflammation (54, 55). Treatment with Interleukin-1 blockers such as anakinra, a recombinant human interleukin 1 receptor antagonist, showed a trend towards clinical benefit in RA patients (56, 57). In other inflammatory diseases such as post-infarction remodeling, neonatal onset multisystem inflammatory disease, severe atopic dermatitis, Muckle-Wells Syndrome, amyotrophic lateral sclerosis, primary sjøgrens syndrome and type-1 diabetes, effect of anakinra treatment is under evaluation (58). Similarly, IL-6 blockade also showed clinical significance in various inflammatory diseases (59).

However, with the exception of a single study pointing to the involvement of IL-1 and TNF-α in the pathogenesis of pemphigus vulgaris (60), no functional data has been published regarding the contribution of cytokines to the pathogenesis of the AIBD, other than reported in this thesis. Due to rising incidence and mortality (61, 62), adverse events induced by the current corticosteroid-based immunosuppressive therapy, as well as rapid relapse after withdrawal of therapy (62, 63), there is a great medical need for alternative treatment options for patients with AIBD.

3.7. Cytokines in experimental EBA: Previous studies

Using passive transfer model of EBA, susceptible mice strains (C57Bl/6 or BALB/c) were injected with normal rabbit (NR) IgG, comparable and equally distributed serum concentrations of 23 different cytokines were identified. In comparison, induction of experimental EBA by repetitive injection of anti-COL7 IgG lead to a statistically significant increase of different cytokine serum concentrations in BALB/c or C57Bl/6 mice, respectively. Furthermore, when serum was obtained at different time points from C57Bl/6 mice, 10 out of 23 tested cytokine concentrations correlated with clinical disease activity (shown as **BOLD** in table 3). Out of these 10 significantly correlating cytokines, given the availability of therapeutic inhibitors and implications in the pathogenesis of various inflammatory conditions (64–69), Granulocyte-Macrophage colony stimulating factor (GM-CSF) and IL-6 has been selected for the present study to analyze functional and pathological relevance in experimental models of EBA.

Cytokine	BALB/c NR-IgG	BALB/c pIgG	C57Bl/6 NR-IgG	C57Bl/6 pIgG	Correlation (r)	p value
TNF-α	**50 ± 9**	**106 ± 21**	**238±77**	**819±573**	**0.571**	**0.026**
MIP1-α	**24 ± 8**	**530 ± 232**	**15±4**	**561±331**	**0.908**	**0.0006**
MIP1-β	50 ± 11	2,461 ± 1,681	110 ± 50	3270 ± 1770	no correlation	--
GM-CSF	**5 ± 5**	**229 ± 81**	**13.5±10**	**654 ±158**	**0.910**	**0.00021**
G-CSF	61 ± 12	515 ± 495	43±11.5	1383±1097	no correlation	--
IL-1α	**23 ± 8**	**530 ± 232**	**40±10**	**1,520 ± 221**	**0.583**	**0.0224**
IL-1β	**253 ± 58**	**4,758 ± 2,662**	**860 ± 260**	**5,861 ± 3897**	**0.597**	**0.018**
IL-2	-	-	NA	NA	no correlation	--
IL-3	-	-	50 ± 31	180 ± 89	no correlation	--
IL-4	**10 ± 2**	**174 ± 54**	**26 ± 10**	**240 ± 110**	**0.813**	**0.004**
Il-5	41 ± 10	275 ± 149	ND	ND	ND	--
IL-6	**50 ± 11**	**1,464 ± 830**	**110 ± 60**	**2,120 ±1590**	**0.724**	**0.0022**
IL-8	NA	NA	NA	NA	ND	--
KC[1]	38 ± 13	151 ± 34	71±60	430±257	no correlation	--
IL-9	218 ± 117	234 ± 61	720 ±450	1040±580	no correlation	--
IL-10	**68 ± 27**	**2,210 ± 743**	**35 ± 23**	**5,750 ±2480**	**0.689**	**0.00453**
IL-12p40	ND	ND	1,000±380	2,690 ± 1761	no correlation	--
IL-12p70	ND	ND	239±196	5,757±2826	no correlation	--
IL-13	130 ± 62	2,450 ± 576	350 ± 240	6,250 ±3710	no correlation	--
IL-17	**1 ± 1**	**645 ± 390**	**1±1**	**496±169**	**0.907**	**0.00002**
Eotaxin	2,258 ± 517	2,131 ± 583	3870 ± 3510	9,210±3890	no correlation	--
RANTES	**289 ± 96**	**2,853 ± 1,523**	**659±230**	**2,280±1362**	**0.577**	**0.024**
IFN-γ	50 ± 9	106 ± 21	205±134	356±144	no correlation	--
MCP-1	ND	ND	660 ±46	2,030 ± 1060	no correlation	--

Table 3: Cytokine profiles in mice after induction of experimental EBA by passive transfer. Experimental EBA was induced in BALB/c and C57Bl/6 mice by passive transfer of COL7 specific antibodies. All concentrations were indicated, as pg/ml. Cytokines with statistical significance ($p<0.05$) and correlation in C57Bl/6 mice and serum levels were shown as **BOLD (student t-test)** NR-normal rabbit,[1)] Significant increase of KC serum concentrations in mice injected with anti-COL7 IgG on day 6, NA- Not applicable, ND- Not detectable. (Part of the data reproduced from publication related to thesis (70)).

In the current study, I focused on the contribution of two cytokines namely GM-CSF and IL-6 to the pathogenesis of EBA. Both cytokines showed a higher level of expression in sera, both in human as well as in experimental models (Please check in results).

3.8. Granulocyte-Macrophage colony stimulating factor (GM-CSF)

Colony stimulatory factors (CSFs) are a family of cytokines, which mediate recruitment of hematopoietic cells to sites of inflammation and infection (71–73). Members of the CSF family are broadly classified into 3 major CSFs, Csf1 (G-CSF), Csf2 (GM-CSF) and Csf3 (M-CSF). Out of these family members, Csf2 (Granulocyte-Macrophage colony stimulating factor, GM-CSF) is the most potent of all CSFs and has been implicated as a main CSF for the recruitment of neutrophils and macrophages to sites of inflammation. In RA and other chronic and/or autoimmune diseases, CSFs were found to be associated with neutrophil activation and disease pathogenesis (74). GM-CSF is a multi-potent stimulatory factor, which is also required for the development of early megakaryocytic and eosinophilic progenitor cells along with granulocyte and macrophage development. GM-CSF is secreted as a glycosylated protein and consists of a single polypeptide chain (75). The GM-CSF receptor consists of a specific GM-CSF binding subunit (CSF2Rα) and a common signal-transduction subunit (CSF2Rβ) which is shared with other cytokines, including IL-3 and IL-5 in humans (76, 77). GM-CSF is able to stimulate different cells of the hematopoietic lineage along with M-CSF. Both CSFs show similar functions but there are lots of variations in the ability to stimulate different cell types. Macrophage polarization (78) has been proposed which is dependent on the amount of M-CSF and GM-CSF in the blood. GM-CSF priming stimulates the production of pro-inflammatory cytokines such as IL-1 and TNF-α from the granulocytes and macrophages. In granulocytes, GM-CSF stimulates the release of arachidonic acid metabolites and increase generation of reactive oxygen species (ROS) (79, 80). Recent studies on GM-CSF-deficient mice (GM-CSF$^{-/-}$) showed no effect on myeloid-cell development, although effecting the maturation of macrophages in lung (81) and defects in thymic ontogeny (82). Several recent findings identified GM-CSF as a clear pro-inflammatory mediator on macrophage and

neutrophils. Level of GM-CSF in the inflammatory conditions have been found to be increased at tissue and mRNA expression levels in tumor cells and in macrophage respiratory burst (83–85). It has been suggested that in autoimmune diseases, migration of neutrophils and macrophages is controlled by the level of GM-CSF. At the tissue level, GM-CSF forms a density gradient that helps with the migration of polymorphonuclear (PMN) cells towards the inflammasome and forms CSF network which facilitates and aggravates the disease (86–88). Experiments on collagen induced arthritis model (CIA) confirmed the role of GM-CSF as a pro-inflammatory mediator. Mice deficient in GM-CSF failed to develop CIA and blocking of GM-CSF using monoclonal antibodies also showed similar results (67, 68, 74, 89). Experiments on the mono-articular model of arthritis, the disease severity was lower in GM-CSF$^{-/-}$ mice (89). The same study suggested that GM-CSF activity might be downstream of IL-1 action. In EAE (experimental autoimmune encephalomyelitis), the disease was increased after administration of GM-CSF which activates the proliferation of microglial cells and helps in the disease progression (90). Functional blocking antibodies against GM-CSF in EAE experiments confirmed the role of GM-CSF in autoimmune diseases as pro-inflammatory cytokine (91). In other models of disease, such as nephritis or alveolar diseases (92, 93), the requirement of GM-CSF in disease development was also shown. In contrast, administration of GM-CSF in the psoriasis model showed decrease in the disease severity (94). GM-CSF is also used in clinics to increase the number of neutrophils after chemotherapy and for the recruitment of myeloid stem cells. It is also employed as an alternative method for bone-marrow cell shift in clinical transplantation (95). In contrast, mouse models of Crohn's disease and colitis, GM-CSF demonstrated significant benefit in decreasing the intensity of the disease (96, 97). As GM-CSF has predominant pro-inflammatory effects, it was also hypothesized to contribute to blister formation in experimental models of EBA by mediating neutrophil activation and recruitment.

3.9. Interleukin (IL)-6

Interleukin-6 is a well-known acute phase response protein and was first described as a T-cell-derived B cell stimulatory factor 2 (BSF-2) (98). It has been established that IL-6 has many biological functions, including development of immune cells along with increased production of acute phase proteins by liver cells (99). Elevated levels of IL-6 were observed in many inflammatory diseases. Furthermore, IL-6 is also known to be associated with mortality and aging (100). IL-6 also aids leukocyte recruitment to sites of inflammation (101). Also, in particular, IL-6 modulates T cell resistance against apoptosis, along with induction of T-helper cells and Th17 cells (102). It was also shown that anti-IL6 receptor (anti-IL-6R) treatment was able to suppress T cells and IL-2 production (103). Levels of IL-6 in normal conditions are not detectable. Elevated levels of IL-6 were associated with insulin resistance and type 2 diabetes (104). It also plays major role in the increased levels of iron regulatory hormone hepcidin in hypoferremia of inflammation (105).

Interleukin-6 is known as multifunctional NF-kB regulator and functions through 80kD IL-6 binding type I transmembrane glycoprotein termed IL-6 receptor (IL-6R, CD126) and the type-I transmembrane signal transducer protein gp130 (CD130) (106) and via activation of JAK/STAT, ERK and PI3 signaling cascades. These signaling events are termed as *classical signaling*. The signal transducer protein, gp-130 is expressed on all cell types whereas the expression of the IL-6R is restricted to monocytes, macrophages, neutrophils, B-cells, subpopulations of T-cells. Non-lymphoid cells such as hepatocytes also express gp-130 (107). Along with IL-6, gp130 is also used by the other family members IL-11, IL-27, leukemia inhibitory factor (LIF), cardiotropin-like cytokine (CLC), oncostatin M(OSM), ciliary neurotrophic factor(CNTF), cardiotropin-1 (CT-1) and neuropoietin (NPN) (108). Beside the membrane-bound IL-6R form, two soluble isoforms of IL-6R (sIL-6R), which lack cytoplasmic and transmembrane

domains, are detectable in the plasma of healthy individuals. Release of soluble IL-6R is linked to the regulatory functions of immune responses induced by IL-6 stimulation (109). Presence of sIL-R in the serum activates the cells, which do not express the IL-6R on their surface. This process is termed as *trans-signaling* (110). Generation of soluble form of the IL-6 receptor increases the range of IL-6 target cells. Experiments with IL-6 transgenic mice and IL-6/sIL-6R double transgenic mice demonstrated the determinative role of IL-6 *trans-signaling* in the regulation of liver regeneration (111). In other terms, anti-inflammatory activities of IL-6 are mediated by *classic signaling* whereas pro-inflammatory responses of IL-6 are mainly directed by *trans-signaling pathway of IL-6* (112). Alongside of soluble IL-6R, soluble form of the signal transducer protein gp130 (sgp130) was also detected in the human circulation (113) and is mainly produced by alternative splicing rather than limited proteolysis (114). Development and application of chimeric sgp-130Fc which acts as a potent inhibitor of IL-6 *trans-signaling* showed beneficial effects in preventing may experimental models of diseases (114–116).

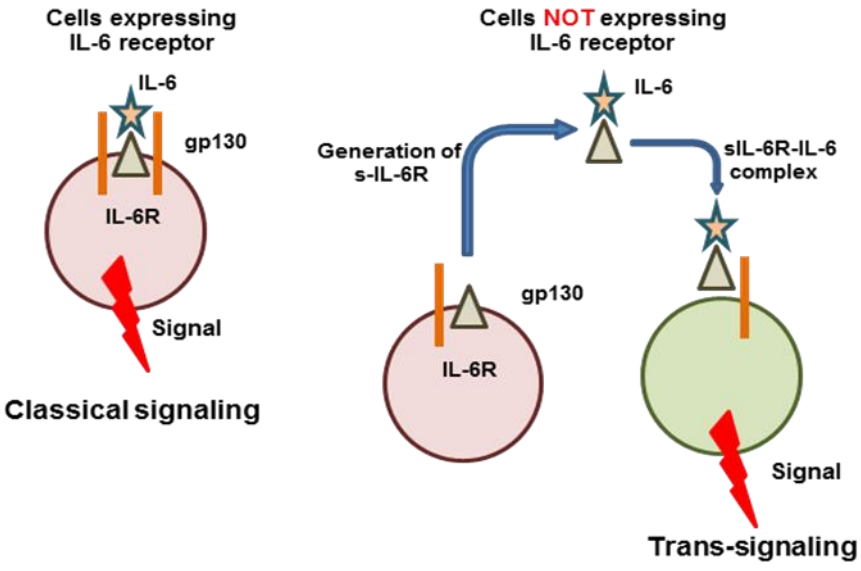

Figure 5. Signaling pathways of IL-6

In classical signaling, cells that can express both IL-6R and gp-130 can induce IL-6 mediated downstream signaling. In trans signaling, sIL-6R is released into serum and forms complex with IL-6. This complex activates the cells, which do not express the IL-6R on their surface. Figure adopted and modified from Stefan Rose-John *et al;* ***J. Leukoc. Biol. 80:*****227–236, 2006.**

While IL-6 is only expressed at low levels in health, elevated IL-6 concentrations are observed in many inflammatory diseases and often correlate with disease activity; for example in rheumatoid arthritis, Crohn's disease, asthma, and psoriasis (117–120). The importance of IL-6 in contributing to the pathogenesis of inflammatory disease is supported by the therapeutic effect of tocilizumab in patients with rheumatoid arthritis (64). Furthermore, inhibition of IL-6 demonstrates the significant role of this cytokine in several animal models of inflammatory diseases (65, 121–124). Interestingly, most of these pro-inflammatory effects of IL-6 are mediated by IL-6 *trans-signaling* (112) as the protection from experimental arthritis in IL-$6^{-/-}$ mice could be only restored by the injection of a fusion protein of IL-6 and the sIL-6R (hyper-IL-6), but not by IL-6 alone (125). Treatment of experimental arthritis in wild type mice with a fusion protein consisting of the entire extracellular portion of gp130 fused to the Fc region of human IgG1 (sgp130) lead to a similar (protected) phenotype as observed in IL-$6^{-/-}$ mice (108, 115, 125, 126).

Even though, IL-6 is widely known as a pro-inflammatory cytokine, in some experimental models, IL-6 shown to be effective in preventing the disease. In viral-induced autoimmunity, IL-6 is suggested to be anti-inflammatory by regulating the early immune response (127). In animal models of endotoxic lung or endotoxemia, studies revealed that endogenous IL-6 plays a crucial anti-inflammatory role in both local and systemic acute inflammatory responses by controlling the level of pro-inflammatory cytokines such as TNF-α and MIP-2 (128). Impaired immune and acute-phase responses were observed mice lacking IL-6 and failed to control V*accinia* and *Listeria monocytogenes* infections (129, 130). Moreover, IL-6 is known to induce the production of IL-1 receptor antagonist (IL-1Ra) and Tumor necrosis factor (TNF)soluble receptor-1 (sTNF-R1), which are antagonists for IL-1 and TNF-α, respectively. Administration of recombinant IL-6 in human cancer patients, leads to

increased levels of these antagonists (131). Serum levels of IL-1Ra were found to correlate with serum IL-6 concentrations in children with juvenile chronic arthritis (132) which could suggest the regulatory role of IL-6 in immune response. Increased levels of IL-1Ra along with IL-6 in circulation could suggest IL-1Ra is regulated by proinflammatory cytokines as an acute-phase protein (133). Recently, IL-6 was introduced as the first myokine, defined as a cytokine that is produced and released by contracting skeletal muscle fibers, exerting its effects in other organs of the body (134). Absence of SOC3 (Suppressor of Cytokine Signaling 3) increased the pro-inflammatory nature of IL-6 (135). Interleukin-6 is also known to increase the expression of *tissue inhibitor of metalloproteinase-1* (Timp-1), which will antagonize the *collagenase* production and helps in the tissue angiogenesis (136–139). Simultaneously, IL-6 also induces the expression of B-cell lymphoma 2 (Bcl-2) which is a well-known apoptotic regulator. Bcl-2 regulates cell death by controlling the mitochondrial membrane permeability and acts via BAX (Bcl-2-associated X protein) protein expression (140, 141).

4. Aim of the study

Despite the noted aberrant (increased) expression of cytokines in AIBD, including EBA (table 3) little to no data on the functional role of cytokines in AIBD had been published. Only one study documented a decrease of skin blisters in TNF-α deficient mice after transfer of IgG from pemphigus patients (60). As cytokine-modulating therapies have greatly improved the treatment of other chronic inflammatory diseases, the aim of this study was to evaluate the functional relevance of cytokines in AIBD. EBA was selected as a disease model, as the laboratory established the respective animal models, which in contrast to other models of the AIBD, reflect the entire pathogenesis of the diseases, including loss of tolerance and autoantibody-induced tissue injury. This allows investigating the effect of cytokine modulating therapies at all stages of disease development. GM-CSF and IL-6 were selected, as

- Increased expression was noted in experimental EBA
- Neutrophils, which are the among the main cells affected by GM-CSF are required to induce blister formation
- Increased IL-6 levels were also observed in EBA patients (please see results)

Based on these findings, the work aimed to challenge the following hypothesis:

- GM-CSF activates neutrophils, promoting recruitment and enhanced activation, leading to increased blistering in experimental EBA
- IL-6 has predominant pro-inflammatory events. Hence, IL-6 also contributes to autoantibody-induced tissue injury

These hypotheses were initially evaluated in antibody-transfer (passive model) EBA. Based on the obtained results, the effect of GM-CSF inhibition was further evaluated in mice with already established immunization-induced (active model) EBA.

5. Materials and methods

5.1. Materials

5.1.1. Equipment in laboratory

Name of equipment	Provider
Bio-photometer 8.5mm	Eppendorf AG, Hamburg, Germany
Centrifuge (BIOFUGE Fresco)	Haereus Instruments GmbH, Hanau, Germany
Centrifuge (Varifuge 3.0 R)	Haereus Instruments GmbH, Hanau, Germany
Cold room(4°C)	Viessmann GmbH&Co.KG, Allendorf, Germany
Cryostat (Leica CM 3050S)	Leica Mikrosysteme Vertrieb GmbH, Wetzlar, Germany
Deep freezer-C660 (-80°C)	New Brunswick Scientific, England
Dry heat sterilizer	Binder GmbH, Tuttlingen, Germany
ELISA plate reader	Perkin Elmer, CA, USA
ELISA plate washer	TECAN, Maennedorf, Switzerland
Pipettes	Eppendorf AG, Hamburg
Microscopy (Olympus BX40)	Olympus Deutschland GmbH, Hamburg, Germany
Microtome	Leica Mikrosysteme Vertrieb GmbH, Wetzlar, Germany
pH-meter (ph526)	MultiCal WTW, Weilheim, Germany
Refrigerator (4°C) / freezer (-20°C)	Liebherr International AG, Bulle, Switzerland
SDS ABI 7900 system	Applied Biosystems, Darmstadt, Germany
Vortex	Genie 2 Scientific Industries, Bohemia, New York, USA

Table 4: Equipment in the laboratory used in this thesis

5.1.2. Consumable materials

Name	Provider
1.5ml/2.0ml tubes	Sarstedt AG&Co., Nuembrecht, Germany
Amicon Ultra-15 Centrifugal Filter Units	Merck Millipore, Darmstadt, Germany
Cover glasses (24x60mm)	Gerhard Menzel, Glasbearbeitungswerk GmbH&Co. KG, Braunchweig, Germany
Dark chamber	Werner Hassa GmbH, Lübeck, Germany
Disposable cuvettes	BRAND GmbH, Wertheim, Germany
Disposable needle (BD Microlance 3, 26Gx1/2)	Becton Dickinson GmbH, Heidelberg, Germany
Disposable syringe-1ml (BD PlastipakTM)	Becton Dickinson GmbH, Heidelberg, Germany
Disposable syringe-20ml (BD DiscarditTM II)	Becton Dickinson GmbH, Heidelberg, Germany
EDTA-syringes	Sarstedt AG&Co., Nuembrecht, Germany
ELISA plate (Maxisorb®)	Nunc, Roskilde, Norway
ELISA plate seal	Sarstedt AG&Co., Nuembrecht, Germany
Fliter Minisart-Sterile (0.20µm)	Sarstedt AG&Co., Nuembrecht, Germany
Protein G sepharose columns	Amersham Biosciences, Heidelberg, Germany
SuperFrost/Plus- slide glasses	Gerhard Menzel, Glasbearbeitungswerk GmbH&Co. KG, Braunchweig, Germany
Tissue-Tek® O.C.T. Compound	Sakura Finetek Europe B.V. Alphen aan den Rijn, Netherland
Tissue-Tek® Cryomold	Sakura Finetek Europe B.V. Alphen aan den Rijn, Netherland

Table 5: Consumable materials used in this thesis work

5.1.3. Chemical substrates and kits

Name	Provider
1-step Turbo™- ELISA	Thermo Scientific, Rockford, USA
ABC Peroxidase Staining Kit	Thermo Scientific, Rockford, USA
Alkaline phosphatase-conjugated streptavidin	Jackson Immuno Research Laboratory Inc., Suffolk, UK
Biotin-free BSA	Roth, Karlsruhe, Germany
BSA	Sigma-Aldrich, Hamburg, Germany
Dako Dual Endogenous Enzyme Block	DakoCytomation, Hamburg, Germany
DAPI (4',6-Diamidino-2-Phenylindole, Dihydrochloride)	Life Technologies GmbH, Germany
DyLight488	Thermo scientific, Rockford, IL
Distilled Water	Pharmacy UKSH, Campus Lübeck, Germany
Eosin	Merck KgaA, Darmstadt, Germany
Ethanol	Pharmacy UKSH, Campus Lübeck, Germany
Glycerol	Roth, Karlsruhe, Germany
Haematoxylin	Merck KgaA, Darmstadt, Germany
Mouse IL-4 ELISA kit	eBioscience Inc, Germany.
Mouse IL-10 ELISA kit	eBioscience Inc, Germany.
Mouse TGF-β ELISA kit	eBioscience Inc, Germany.
InnuPrep RNA Mini Kit	Analytic Jena AG, Germany
Ketamine hydrochloride	Sigma-Aldrich, Hamburg, Germany
Kineret® (Anakinra)	Biovitrum AB, Stockholm, Sweden

Luminol (5-Amino-2,3-dihydro-1,4-phthalazinedione)	Sigma-Aldrich Biochemie GmbH, Germany
N-formyl-Methionyl-Leucyl-Phenylalanine(fMLP)	Sigma-Aldrich Biochemie GmbH, Germany
Peroxidase substrate, Histoprime® HistoGreen	AbCys s.a, Paris, France
Polymorphoprep™	Axis-Shield, Heidelberg, Germany
Quantikine® mouseIL-1Ra ELISA kit	R&D Systems
qPCR Master Mix Plus	Eurogentec GmbH, Cologne, Germany
R.T.U. VECTASTAIN® Elite ABC Reagent	Vector Laboratories, CA, USA
Roti®-Histofix 4% (Phosphate-buffered formaldehyde solution)	Roth, Karlsruhe, Germany
Mouse sTNF-R1 ELISA kit	Hycult Biotech, The Netherlands
TaqMan probe™	Biomers.net, Ulm, Germany
TiterMax™	ALEXIS Biochemicals, Lörrach, Germany
TUNEL In situ Cell Death Detection Kit	Roche Deutschland Holding GmbH,Germany
VECTA MOUNT™ permanent mounting medium	Vector Laboratories, CA, USA
Vector, pGEX-6P-1	Amersham Biosciences, Heidelberg, Germany
Xylazine hydrochloride	Sigma-Aldrich, Hamburg, Germany
Xylene	Sigma-Aldrich Chemie GmbH, Deisenhofen, Germany

Table 6: Chemical substrates and kits used in this thesis work

5.1.4. Antibodies

Antibody name	Provider
Anti-mouse Ly6G antibodies (1A8) purified	BioXCell, West Lebanon, USA
Anti-Mouse GM-CSF Functional Grade Purified (MP1-22E9)	eBioscience, Frankfurt, Germany
Biotin Rat anti-Mouse IgG1 (A85-1)	BD Pharmingen, Heidelberg, Germany
Biotin Rat anti-Mouse IgG2a (R19-15)	BD Pharmingen, Heidelberg, Germany
Biotin Rat anti-Mouse IgG2b (R12-3)	BD Pharmingen, Heidelberg, Germany
Biotin Rat anti-Mouse IgG3 (R4-82)	BD Pharmingen, Heidelberg, Germany
Donkey anti-goat secondary antibody (HRP)	Santacruz Biotechnology INC. USA
FITC Goat anti-Mouse C3 IgG	Cappel MP Biomedicals LLC, OH, USA
Goat-anti-rabbit immunoglobulins (FITC)	DakoCytomation, Hamburg, Germany
Goat polyclonal Antibody to Rabbit IgG - H&L (TR)	Abcam plc, Cambridge, UK
Goat anti-mouse GM-CSF antibody (A-6)	Santacruz Biotechnology INC. USA
Goat anti-rat secondary antibodies-HRP	BioLegend GmbH, Germany
Goat anti-mouse IgG-HRP	Santacruz Biotechnology INC. USA
Normal rabbit serum	C.C.Pro, Oberdorla, Germany
Rabbit Anti-Mouse Immunoglobulins (FITC)	DakoCytomation, Hamburg, Germany
Rat IgG2a k Isotype control (eBR2a)	eBioscience, Frankfurt, Germany
Rat anti-Mouse Ly6G/6c antibodies (PE) (RB6-8C5)	BD Pharmingen, Heidelberg, Germany
Rat anti-mouse IL-6 monoclonal antibody (MP5-20F3)	BioTechServives, Henningsdorf, Germany
Recombinant IL-6 (142)	Kindly provided by Prof. Rose-John, Kiel
sgp-130Fc (114, 142)	Kindly provided by Prof. Rose-John, Kiel
Rat anti-human IL-6 antibodies (MQ2-13A5)	BioLegend GmbH, Germany

Table 7: List of antibodies used in this thesis

5.1.5. Buffers

Name of buffer	Preparation
PBS (phosphate buffered saline)	8g/L NaCl, 0.2g/L KCl, 1.44g/L Na_2PO_4/K_2HPO_4 in distilled water, adjust pH at 7.2 with phosphoric acid
PBST (phosphate buffered saline-Tween20)	0.05ml Tween 20 in 1L PBS (1x)
Glycine buffer	7.52g of glycine in 1L of distilled water. Adjusted pH to 2.8 with 1N HCl
TRIS-buffer	181.71g of TRIS base in 1L of distilled water. Adjusted pH to 8.8 with 1N HCl
NaCl	58.44g of NaCl in 1L of distilled water
Carbonate buffer (Adsorption buffer)	5.3g of Na_2CO_3, 5.04g of $NaHCO_3$ dissolved in 1L of distilled water. Adjusted pH to 9.6 with 1N HCl
20% Ethanol	20ml of absolute ethanol in 80ml of distilled water

Table 8: List of buffers used in this thesis work

5.2. Methods

5.2.1. Studies with human material

Blood for isolation of polymorph nuclear cells (PMNs) was obtained from EDTA anti-coagulated blood drawn from healthy blood donors. For determination of cytokine concentrations, serum from EBA patients (n=17) were used, fulfilling the following criteria: (i) presentation with skin lesions resembling EBA (143), (ii) linear IgG and/or IgA deposition in direct immunofluorescence (IF) microscopy (18, 32), (iii) an u-serrated pattern in direct IF microscopy and/or detection of autoantibodies against COL7 by western blotting (144). Serum from healthy blood donors (n=21) served as reference. Skin biopsies from EBA patients fulfilling above criteria were obtained for analysis of IL-6 expression by immunohistochemistry (IHC). EBA sera and skin sections were obtained form a biobank at the Department of Dermatology in Lübeck, as well as from a group of cooperation partners in Department of Dermatology, University of Groningen, University Medical Center Groningen, Groningen, Netherlands. Skin specimen from plastic surgery served as a reference. All experiments using human samples were approved by the local ethics committee and performed according to the Declaration of Helsinki. All patients and control blood donors gave their written informed consent prior to study participation.

5.2.2. Mice

C57Bl/6 (B6), B6.SJL-H2s (B6.s), BALB/c and IL-$6^{-/-}$ mice on the C57Bl/6 genetic background were obtained from Charles River Laboratories (Sulzfeld, Germany). GM-CSF deficient mice (GM-$CSF^{-/-}$) were kindly provided by Prof. Jeff Whitsett (Division of Pulmonary Biology, Cincinnati Children's Hospital, 3333 Burnet Ave, Cincinnati, OH 45229). For experiments, mice aged 8-12 weeks were used. Mice were held at specific pathogen free conditions, and fed standard mouse chow and acidified drinking water

ad libitum. All clinical examinations, biopsies and bleedings were performed under anesthesia using intraperitoneal (i.p.) administration of a mixture of ketamine (100µg/g) and xylazine (15µg/g). Local authorities of the Animal Care and Use Committee (Kiel, Germany) approved animal experiments performed in this thesis. Brief descriptions of mice used in this thesis are given below.

5.2.2.1. C57Bl/6J mice

C57BL/6J is the most widely used inbred strain and the first to have its genome sequenced. These are commonly referred as B6 mice. These mice are mostly used in the generation of transgenic mice. Other characteristics include susceptibility to autoimmune diseases such as diet-induced obesity, type 2 diabetes, and atherosclerosis, eye diseases such as microphthalmia. These mice are also resistant to audiogenic seizures and have hereditary hydrocephalus. This strain was initially created Dr. CC Little from the mating of female 57 with male 52 from Miss Abbie Lathrop's stock. The same cross gave rise to the C57L and C57BR strains (145). Furthermore, these mice are highly susceptible to induction of antibody-transfer induced EBA (details below).

5.2.2.2. B6.s mice

These mice are congenic to H2s-MHC locus. Mice congenic for H2 haplotypes are widely used in immunologic research and their immune response often differs from the recipient strain. This mouse can be used to support research in many areas including Immunology, Inflammation and Autoimmunity Research for identification and characterization of CD antigens, antigen receptors, and histocompatibility markers (146). These mice found to be highly susceptible to immunization-induced EBA (details below).

5.2.2.3. IL-6$^{-/-}$ (deficient) mice

These mice are knockout for IL-6 and show defects in responses to various viruses and in inflammatory responses to tissue damage or infection (147). Targeted mutation for IL-6 was designed by Manfred Kopf and Georges Kohler at Max Planck Institut Fur Immunbiologie, Freiburg Germany. A targeting vector designed to place a neomycin resistance cassette into the first coding exon (exon 2) of the targeted gene. This construct was electroporated into 129S2/SvPas-derived D3 embryonic stem (ES) cells (129). Mutant mice on a C57BL/6 genetic background were sent to The Jackson Laboratory.

5.2.2.4. GM-CSF$^{-/-}$ (deficient) mice

GM-CSF deficient mice (GM-CSF$^{-/-}$) were kindly provided by Prof. Jeff Whitsett, Division of Pulmonary Biology, Cincinnati Children's Hospital, 3333 Burnet Ave, Cincinnati, OH 45229 (148–150). For experiments, mice aged 6-8 weeks were used These mice show abnormal myeloblast morphology/development and lung inflammation (151).

5.2.2.5. BALB/c mice

BALB/cJ is a commonly used inbred mouse strain (152). These mice are generally resistance to experimental autoimmune encephalomyelitis (EAE) and susceptible to develop demyelinating disease upon infection with Theiler's murine encephalomyelitis virus. They are also susceptible to parasites such as Listeria several species of Trypanosoma (153–155).

5.2.3. Generation of anti-mouse COL7 IgG

This protocol has previously established in the laboratory (29). For my thesis, I expressed and purified the NC1 domain of murine COL7 protein using bacterial clones in the laboratory (29). In detail, cDNA fragments of COL7 were cloned into linearized pGEX-6P-1 (Amersham Biosciences) plasmids resulting in the recombinant vectors coding for COL7 fragments. Ligation and in-frame insertion of the various DNA fragments were confirmed by DNA sequence analysis. These vectors are trasnfected into bacterial strain *Escherichia coli*-BL21 and recombinant fusion proteins were expressed and purified using glutathione-agarose affinity chromatography. The obtained protein was sent to a commercial supplier (Eurogentec GmBH, Germany) for immunization of rabbits. Form the rabbit immune sera, I regularly purified the IgG for the experiments in passive transfer EBA using Protein-G sepharose Fast Flow affinity column chromatography (Amersham Biosciences). Antibodies were eluted with 0.1M glycine buffer (pH 2.8) and neutralized with 1M Tris-HCl (pH 9). Obtained antibody fraction was concentrated in extensive washing with PBS (pH 7.2) using 30kD Millipore filters (Merck Millipore, Darmstadt, Germany). Purified IgG was later filter-sterilized (pore size, 0.22µm; Sarstedt AG&Co., Nuembrecht, Germany) and the protein concentration was measured spectrophotometrically at 280 nm. Reactivity of IgG fractions was analyzed by immunofluorescence microscopy on murine skin. As a control, normal rabbit (NR) IgG was used which was also purified from rabbit sera using same protocol mentioned above.

5.2.4. Induction of experimental EBA

For induction of antibody-transfer (passive) EBA studies published protocols with minor modifications were used for this thesis (29). Briefly, mice of the indicated strains received a total of six s. c. injections of rabbit anti-COL7 IgG (amount of IgG used indicated in the experiment protocols) or corresponding amounts of normal rabbit IgG

every second day. Disease severity was expressed as percent of body surface area affected by skin lesions and determined at 3 time points (day 4, 8, 12). Affected body surface area was calculated by allotting individual fraction to each part of the body [Ear (left)-2.5%, Ear (right)-2.5%, Eye (right)-0.5%, Eye (left)-0.5%, Snout-2.5%, oral mucosa-2.5%, head&neck-9%, front leg (left)-5%,front leg (right)-5%, rear leg (left)-10%, rear leg (right)-10%, tail-10% and trunk-40%)] and calculated together to get total body surface area in percentage. An example of calculation table is shown below in table 4.

A

Mouse number	lesion (%)
Ear (left)	
Ear (right)	
Eye (right)	
Eye (left)	
Snout	
oral mucosa	
head&neck	
front leg (left)	
front leg (right)	
rear leg (left)	
rear leg (right)	
tail	
trunk	
overall score	

B

Mouse number	lesion (%)
Ear (left)	0.2
Ear (right)	0.2
Eye (right)	0.6
Eye (left)	0.8
Snout	0
oral mucosa	0
head&neck	0
front leg (left)	0.2
front leg (right)	0.2
rear leg (left)	0
rear leg (right)	0.4
tail	0.2
trunk	0
overall score	**9.7**

Table 9:- Mouse clinical scoring calculation table.

A. Each body part of the mouse was assigned with individual percentage and total effected body surface was calculated as overall score of lesion on individual body parts. **B.** Filled example table shown with overall score after final calculation.

From these time points, the area under the curve (AUC) was calculated, taking both disease onset and maximal disease activity into account. Blood and tissue samples were collected on day 12. All experiments were repeated in more than 3 independent experiments using different batches of purified anti-COL7 and normal IgG. This autoantibody transfer EBA duplicates the clinical, histological, and immunopathological findings of the inflammatory variant of the human disease (156).

5.2.5. Generation of vWFA protein

Expression and purification of vWFA protein was performed at Institute of Chemistry, University of Lübeck (157). Together with Dr. Hiroaki Iwata, protein was expressed and purified at Department of Dermatology. In detail, I used a codon optimized sequence of mvWFA2 of COL7, which was commercially synthesized (Mr. Gene, Regensburg, Germany) and cloned in pTWIN1 (NEB, Frankfurt, Germany). Protein expression in *E. Coli*-ER2566 followed by purification as described (157).

5.2.6. Induction of immunization induced EBA

In this thesis, C57Bl/6, B6.s and GM-CSF deficient mice aged, 6-10 weeks were used for experiments with immunization-induced EBA. All clinical examinations, biopsies and bleedings were performed under anesthesia with i.p. administration of a mixture of ketamine (100µg/kg) and xylazine (15µg/kg). In detail, mice were immunized at the hind footpad with 60 µg of recombinant murine COL7 (vWFA2 domain) emulsified in the non-ionic block copolymer adjuvant TiterMax (ALEXIS Biochemicals, Norcross, Georgia). Subsequently, mice were evaluated every week for presence of skin lesions (i.e., erythema, blisters, erosions, alopecia and crusts) until 10 weeks after immunization. Clinical evaluation was performed as described for antibody transfer-induced EBA. Serum and tail skin samples were collected every week. Serum, ear skin, tail skin, spleen and lymph node (form the lymph node draining the area where the mice were immunized) samples were obtained on final day of the experiment and stored until further analysis.

5.2.7. Determination of serum cytokine concentrations

Serum from EBA patients and normal controls were analyzed for expression of 23 cytokines (TNF-α, MIP-1α, MIP-1β, GM-CSF, G-CSF, IL-1α, IL-1β, IL-2, IL-3, IL-4, IL-5,

IL-6, KC, IL-9, IL-10, IL-12p40, IL-12p70, IL-13, IL-17, Eotaxin, RANTES, IFN-γ and MCP-1) using bipolar (Bioglobe GmbH, Hamburg, Germany). In addition, serum concentrations of all the above cytokines or their corresponding homologs were determined in mice with experimental EBA and appropriate controls at the indicated time points using bioplex (Bioglobe GmbH). Murine data was analyzed before starting thesis by me and human data analysis was then again performed within the thesis.

5.2.8. Direct immunofluorescence (IF) microscopy

Direct IF microscopy for detection of rabbit IgG and murine C3 in experimental EBA was performed as described (158). Briefly, frozen sections were prepared from tissue biopsies and incubated with goat anti-rabbit antibodies reactive with rabbit IgG (DAKO, Dako Deutschland GmbH, Germany), and murine C3 (MP Biomedicals LLc, Keyseberg, France), both labeled with fluorescein isothiocyanate (FITC). For IF staining of draining lymph nodes, the inguinal lymph nodes were obtained from immunized mice at week 6. Lymph node sections (6µm) were fixed in acetone at -20°C for 10 min and blocked using 5% BSA. Sections were stained with Ly6G coupled with PE (Clone R35-95, BD Pharmingen™, Germany) at 4°C for detection of neutrophils. Simultaneously recombinant murine vWFA2 protein conjugated with DyLight488 (according to manufacturer's protocol; Thermo scientific, Rockford, IL) was added to detect COL7 specific B cells. After washing slides were counterstained with DAPI (Life Technologies GmbH, Germany) and mounted for microscopy. Cell numbers with positive staining in the Images were analyzed using ImageJ software (National Institutes of Health, USA).

5.2.9. Treatments with anti-IL-6, sgp130Fc and recombinant IL-6

Rat anti-mouse IL-6 monoclonal antibody (clone: MP5-20F3) was obtained from In Vivo Biotech Services, Henningsdorf, Germany. Recombinant IL-6 and sgp130Fc were expressed, and purified as described (142), and both were kindly provided by Prof. Rose-John (Institute of Biochemistry, Christian-Albrechts-University, Kiel, Germany). Mice were treated with either 250µg anti-IL6 or sgp130Fc one day prior, 4 and 8 days after the first IgG injection. Recombinant IL-6 was administered i.p. at daily doses of either 5 or 20µg/animal. Injection of PBS served as control. PBS or isotype antibody (Rat IgG2a k Isotype, Clone: eBR2a, eBioscience, Frankfurt, Germany) treatment was initiated on day 0 and maintained throughout the experiment.

5.2.10. Detection of serum IL-1Ra, sTNF-R1, IL-4, IL-10 and TGF-β concentrations

For analysis of IL-1Ra levels in mice serum, ELISA was performed using a kit from Quantikine® (Cat No: MRA00, R&D Systems) and for mouse sTNF-R1 analysis in serum, a kit was obtained from Hycult Biotech (Cat No HK201). For analyzing serum levels of IL-4 (Cat No: 88-7044-22), IL-10 (Cat No: 88-7104-22) and TGF-β (Cat No: 88-8350-22) levels, kits were obtained from eBioscience Inc, Germany. Experiments were performed according to the protocols provided by the manufacturers.

5.2.11. TUNEL staining

Presence and quantity of apoptotic (TUNEL positive) cells in the epidermis was assessed using TUNEL In situ Cell Death Detection Kit (Fluorescien, Roche). In principle, The In Situ Cell Death Detection Kit- Fluorescein is based on the detection of single- and double-stranded DNA breaks that occur at the early stages of apoptosis (159). During apoptosis, DNA is degraded and in early stages of degradation, DNA is

selective to the inter-nucleosomal DNA linker regions and yields double-stranded and single-stranded DNA breaks called “nicks”. The enzyme, terminal *deoxynucleotidyl transferase* (TdT) catalyzes the template-independent polymerization of deoxyribonucleotides to the 3'-end of single- and double-stranded DNA and this method has also been termed TUNEL (TdT-mediated dUTP-X nick end labeling). This method is considered to be more sensitive and faster to detect early stages of apoptosis (160). For TUNEL staining, frozen skin sections from perilesional area was fixed in 4% phosphate-buffered formaldehyde solution at pH 7.4 for 15 min and washed in PBS for 30 min. Subsequently slides were kept in ice for 5 min followed by treatment with *DNase* I and TUNEL staining mixture provided by the manufacturer. For measurements, I used ImageJ software and calculated the number of cells and represented as percentage of TUNEL+ cells/ DAPI+ cells.

5.2.12. Differential blood counts in mice

EDTA anti-coagulated blood was collected from mice on day 12 of the experiment and samples were evaluated by a commercial supplier (Laboklin, Bad Kissingen, Germany). Obtained data was analyzed by me for differential blood counts and statistical evaluation.

5.2.13. RT-PCR from mouse skin

For analysis of cytokine mRNA expression, cryosections of ear skin were dissolved in 700µl lysis buffer. Total RNA was isolated according to the manufacturer’s protocol (InnuPrep RNA Mini Kit, Analytic Jena AG) and reverse transcribed. The cDNA was added to qPCR Master Mix Plus (Eurogentec GmbH, Cologne, Germany) and amplified using the SDS ABI 7900 system (Applied Biosystems, Darmstadt, Germany). TaqMan probes, forward and reverse primers were designed using the computer

software CloneManager (version 7.01; Sci Ed Central). The same batch of cDNA (20µl) was used to determine the cycles of threshold. The amount of cDNA copies was normalized to the housekeeping gene MLN51. Optimal primer concentrations used were 900nM each for the forward and reverse primers and 200nM for the TaqMan probe (Biomers.net, Ulm, Germany). For IL-1Ra primers, sequences were kindly provided by Prof. Cem Gabay and Dr. Celine Lamacchia (Division of Rheumatology, University Hospitals of Geneva, Geneva, Switzerland). All the data expressed as relative expression x 100 in relation to MLN51. All used primers are listed in table 10. All RT-PCR experiments were performed by Dr. Kathrin Kalies (Institute of Anatomy, University of Lübeck). I obtained the samples from mice, prepared samples for RT-PCR and analyzed the data obtained from Dr. Kathrin Kalies.

Name	Primer sequence
mMLN51 probe e7/8	5’ CACGGGAACTTCGAGGTGTGCCTAAC 3'
mMLN51 for e7a	5’ CCAAGCCAGCCTTCATTCTTG 3'
mMLN51rev e9a	5’ TAACGCTTAGCTCGACCACTCTG 3'
mBCL2 for	5' GAACCGGCATCTGCACAC 3'
mBCL2 rev	5' AGGTATGCACCCAGAGTGATG 3'
mTimp1 for	5' CTCTGGCATCTGGCATCCTC 3'
mTimp1 rev	5' CGGCATTTCCCACAGCCTTG 3'
mIL-1Ra (soluble)	5‘ TTGC TGTG GCCT CGGG ATGG 3‘
mIL-1Ra (intracellular)	5‘AGAC ACTG CCTG GGTG CTCC T 3‘
mIL-1Ra rev	5‘GTTT GATATTTGGTCC TTGTAAG 3‘
mIL-6 for	5' CTCCCAACAGACCTGTCTATAC 3'
mIL-6 rev	5' GTGCATCATCGTTGTTCATAC 3'
m IL10 probe e3/4	5' CTGAGGCGCTGTCATCGATTTCTCCC 3'
m IL10 for e3	5' TCCCTGGGTGAGAAGCTGAAG 3'
m IL10 rev e4	5' CACCTGCTCCACTGCCTTG 3'
m IL4 probe e3/4	5' CCTGGATTCATCGATAAGCTGCACCATG 3'
m IL4 e3 for	5' GAGACTCTTTCGGGCTTTTCG 3'
m IL4 e4 rev	5' AGGCTTTCCAGGAAGTCTTTCAG 3'
m Tgfb 1 probe e6/7	5' CACAGTACAGCAAGGTCCTTGCCCTCTACA 3'
m Tgfb e6 for	5' GACCCTGCCCCTATATTTGGAG 3'
m Tgfb e7 rev	5' GCGACCCACGTAGTAGACGATG 3'

Table 10: List of primers used in the study.

This table was self-published in Samavedam et al (70).

5.2.14. Histopathology & immunohistochemistry (IHC) studies

For histopathological studies in mouse, specimens were stained using standard staining protocol for Hematoxylin and Eosin staining (H&E). The staining method involves application of *hemalum*, an oxidation product of haematoxylin. *Hemalum* colors nuclei of cells into deep purple-blue. The nuclear staining is followed by counterstaining with an aqueous or alcoholic solution of *eosin Y*, that stains the cytoplasmic material and leaves an orange-pink counter stain which colors other, including connective tissue and collagen, eosinophilic structures in various shades of red, pink and orange depending on the type of granules in the cells (161). Extend of leukocyte infiltration in these sections were scored semi-quantitatively in a blinded fashion as previously described (162). Immunohistochemistry (IHC) in human skin biopsies were performed using 6µm thick frozen skin sections obtained from EBA patients and were fixed in ice-cold acetone for 10 min. Endogenous H_2O_2 was inactivated using Enzyme Block (DAKO) for 10min. Sections were incubated in blocking solution (5% BSA in PBS) for one hour. To evaluate IL-6 expression in human skin, sections were incubated with Leaf™ purified rat anti-human IL-6 antibodies (Clone MQ2-13A5, BioLegend GmbH, Germany). To exclude unspecific staining, sections were additionally stained with appropriate isotype control antibodies. Sections were rinsed and incubated with HRP labeled goat anti-rat secondary antibodies (clone-Poly4054, BioLegend GmbH, Germany). To evaluate the expression of GM-CSF in mouse, 6µm of tissue sections were incubated with goat anti-mouse GM-CSF antibody (sc-52532, Santacruz Biotechnology INC) at 1:50 dilution. For controls, isotype (goat total IgG) was used. Sections were rinsed and incubated with HRP labeled donkey anti-goat secondary antibodies (sc-Santacruz Biotechnology, INC) at 1:200 dilutions for 1 hour. Color was developed using Histoprime® HistoGreen (Cat No E109, AbCys s.a, Paris, France) using the protocol provided by the manufacturer.

5.2.15. Reactive oxygen species release assay on human PMNs

Blood for isolation of polymorphonuclear cells (PMNs) was obtained from EDTA anti-coagulated blood drawn from healthy blood donors. PMN activation was assessed by determination of immune-complex (IC) induced reactive oxygen species (ROS) release using a slightly modified protocol. In brief, human PMNs were isolated using Polymorphoprep™ (Axis-Shield, Heidelberg, Germany) following the protocol provided by the manufacturer. Isolated PMN cells were incubated on a 96 welled plate coated with IC formed by monoclonal anti-COL7 antibodies and recombinant fragments located within the human NC1 domain. These fragments and monoclonal antibodies are cloned, expressed and isolated by Dr. Andreas Recke in the lab (163). ROS release with GM-CSF at different concentrations was analyzed using luminol (5-Amino-2, 3-dihydro-1, 4-phthalazinedione). Luminol exhibits chemi-luminescence in blue when reacts with oxidative agents, such as reactive oxygen species, which are released by activated PMNs. For positive control, fMLPs (Formyl-Methionyl-Leucyl-Phenylalanine) were added in order to activate the PMNs in an immune complex-independent manner (164).

5.2.16. Detection of circulating vWFA2 specific antibodies

To detect circulating vWFA2 specific Abs, ELISA was performed. I optimized the working conditions of the assay by using chessboard titrations with dilutions of antigen and secondary antibody, as previously described (165). The optimized ELISA was performed in 96–well microtiter plates (Maxisorb; Nunc, Roskilde, Denmark) which were coated with 250ng murine vWFA2. Nonspecific binding was reduced by blocking plates with 1% BSA in PBS-T (PBS-tween) at RT for 60 min. Subsequently, plates were incubated with mouse sera at RT for 60 min. Serum from mice diluted in 1:1000. Plates were incubated with anti-mouse IgG conjugated with HRP (Santa Cruz, CA, dilution 1:20,000) and anti-mouse IgG subclasses conjugated with biotin - IgG1 (clone,

A85-1), IgG2a/c (clone, 5.7), IgG2b (clone, R12-3) and IgG3 (clone, R4-82) (BD Biosciences, CA, dilution 1:20,000) for 1 h at RT. Plates were incubated with Ultra-sensitive ABC peroxidase Staining Kit (Thermo Scientific, Rockford, IL) for IgG subclasses for 0.5 h at RT. One-step Turbo^{TM} - ELISA (Thermo Scientific, Rockford, IL) substrate was added for visualization. Negative cut off line was determined by average of negative controls + (3x STDEV of negative controls).

5.2.17. GM-CSF neutralization and neutrophil depletion using antibodies

Endogenous GM-CSF in mice was neutralized using 50 µg of anti-GM-CSF antibodies (Clone MP1-22E9, Cat: 16-7331-1317, eBioscience, Frankfurt, Germany) were given i.p. on alternate days in the autoantibody transfer model of EBA. For GM-CSF blockade in immunization-induced EBA, 100µg anti-GM-CSF antibodies (Clone MP1-22E9, eBioscience, Frankfurt, Germany) were administered i.p., 3 times per week after 2% or more of the body surface areas were covered with skin lesions. Injection of an appropriate isotype antibody served as control (Rat IgG2a k Isotype, Clone: eBR2a, eBioscience, Frankfurt, Germany). Both treatments were carried out over a period of 4 weeks. Extend of skin blistering was expressed as the percentage of body surface area affected by skin lesions every week in relation to the score at the beginning of treatment. Total disease severity during observation period was calculated as area under the curve (AUC) of the recorded disease severity. Neutrophils were depleted using 1A8 antibodies as described elsewhere with minor modifications. Antibodies were obtained from BioXCell, West Lebanon, USA (Cat No: BE0075-1, clone 1A8). Mice were injected with 200µg/mouse/ injection of antibodies, 3 times per week in mice with immunization-induced EBA.

5.2.18. Statistical analysis

Unless otherwise noted, data is presented as mean ± standard error. For comparisons of two groups, t-test or Mann-Whitney Rank Sum Test was used, whenever appropriate. For comparison of more than two groups, ANOVA was used. For equally distributed data One-Way ANOVA, followed by Bonferroni t-test for multiple comparisons were used; if data was non-parametric, ANOVA on ranks (Kruskal-Wallis) was applied, followed by Bonferroni t-test for multiple comparisons. Pearson Product Moment Correlation was used to test for correlations. In all tests, a $p<0.05$ was considered significant. All statistical analysis was performed using SigmaPlot 12.0 (Systat Software, Erkrath, Germany) and or R statistical package version 3.0 (URL: http://www.r-project.org).

6. Results

6.1. Serum levels and cutaneous expression of GM-CSF and IL-6 in human EBA patients

In samples from blood donors and EBA patients, a great variation of cytokine concentrations was noted, especially in the patient samples. Mean GM-CSF concentrations were several-fold increased. Yet, most likely, due to the high variation, these changes were not significantly different. For IL-6, levels were significantly increased in EBA patients compared with the control population. In detail, in most of serum samples from healthy donors, IL-6 was below the detectable levels, whereas it was detected in most EBA sera. Overall, IL-6 serum concentration was 8-fold higher in EBA patients (table 11).

Cytokine	HBD	EBA patients	p value*
GM-CSF	210 ±154	338 ±156	0.059
IL-6	2.0±1.3	16.0±3.4	0.024

Table 11: Increased expression of GM-CSF and IL-6 in EBA patients' serum

Serum form EBA patients (n=17) and healthy controls (n=21) was used to determine the concentrations of GM-CSF and IL-6 (among several other cytokines). For this analysis, samples were sent to a commercial supplier for multiplex analysis of cytokines. There was a trend (p=0.059) for increased GM-CSF concentrations in patients compared to controls. In contrast, a significant increase of IL-6 was noted in EBA patients compared to controls. All concentrations in the table are indicated as pg/ml. *Mann-Whitney Rank Sum Test. Part of this table was published in Samavedam et al (70).

In line with the results shown in table 11, IL-6 expression was detected in 3 out of 4 EBA skin specimens from patients; while only 1 of 6 specimens from healthy control skin had detectable IL-6 expression as detected by IHC (figure 6).

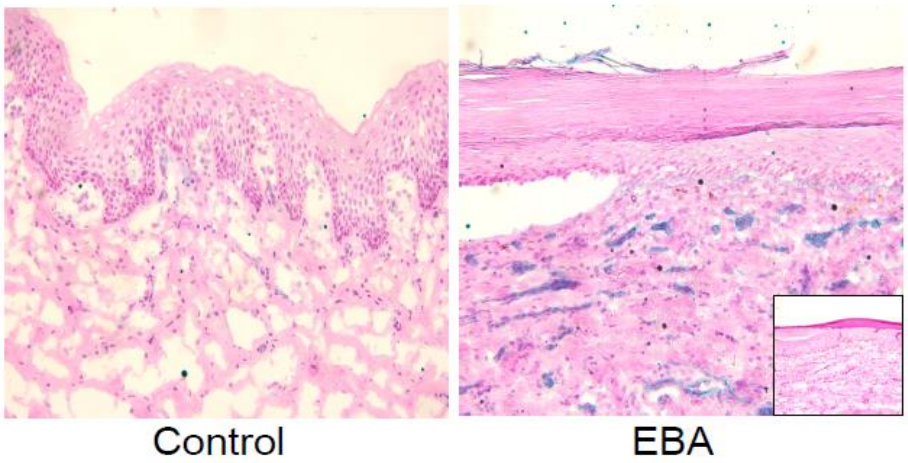

Figure 6: Increased expression of IL-6 in human EBA patient's skin

Representative Immunohistochemistry staining of IL-6 in one of the skin samples of EBA patients or donors. In specimens from EBA patients, 3 of 4 specimens stained positive for IL-6. No IL-6 staining was detected in isotype controls (insert). This figure was published in, Samavedam et al (70).

6.2. Increased expression of GM-CSF and IL-6 in experimental EBA

I here confirmed that repetitive injections of anti-COL7 IgG into either C57Bl/6 or BALB/c mice induce experimental EBA as described (29). In both strains, comparable and equally distributed serum concentrations of GM-CSF and IL-6 were noted in control mice. In contrast, induction of experimental EBA lead to significant increase of both cytokines in the tested mouse strains. A significant increase of serum levels was evident for GM-CSF and IL-6, in BALB/c mice after EBA induction (table 3). In C57Bl/6 mice, serum was collected before the initial anti-COL7 IgG injection, 3, 6 and 12 days post IgG injection. Cytokine serum concentrations strongly correlated with the clinical severity of the disease, expressed as the body surface area affected by EBA skin lesions (table 3). These findings were in line with increased GM-CSF expression in immunohistochemistry staining of EBA skin obtained from C57Bl/6 mice (figure 7) and

increased IL-6 mRNA expression (pooled) in lesional EBA skin obtained from both BALB/c and C57Bl/6 mice (table 12).

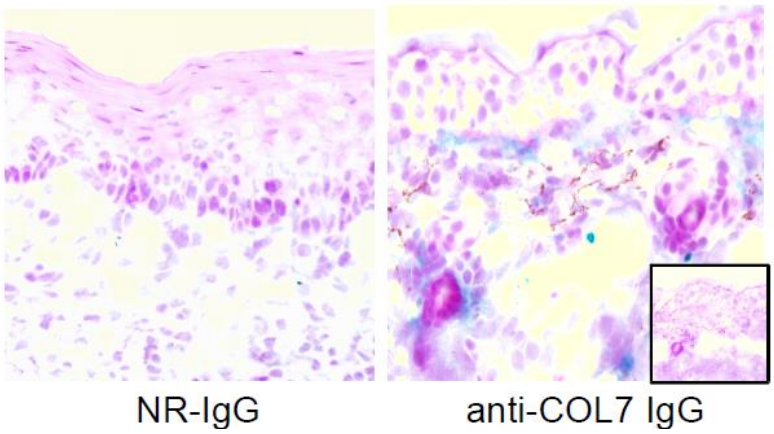

Figure 7. Increased expression of GM-CSF in experimental EBA

Representative staining from skin specimens obtained from mice injected with NR-IgG or anti-COL7 IgG, 12 days after the initial IgG injection. GM-CSF was stained using anti-GM-CSF antibodies and counterstained with HRP labeled secondary antibodies. Color was developed using HistoGreen. Stained GM-CSF was shown in blue (Insert: isotype control staining of anti-COL7 injected mouse).

Injections	IL-6 mRNA copies per copy of MLN51			
	BALB/c		C57BL/6	
	Day 0	Day 12	Day 0	Day 12
NR-IgG	0	0.006	0	0.071
Anti-Col7 IgG	0	0.779	0	0.246

Table 12: Increased expression of IL-6 in mice with experimental EBA

Increased mRNA expression in EBA mouse skin in comparison to the mice injected with normal rabbit (NR) IgG (n=3 mice/group, pooled mRNA data from both BALB/c and C57Bl/6 mice). This table was in own publication, Samavedam et al (70).

6.3. Role of GM-CSF in EBA

6.3.1. Induction of skin blistering in antibody transfer-induced EBA is hindered in GM-CSF deficient mice

To test if the increased serum and cutaneous GM-CSF expression in experimental EBA is of functional relevance, anti-COL7 IgG was injected into mice lacking GM-CSF expression (n=12) and wild type control C57Bl/6 mice (n=12). Skin lesions were evident in 11 of 12 C57Bl/6 mice with a median of 0.2% (range 0-0.6%) of affected body surface area, as early as 4 days after the initial anti-COL7 IgG injection. A similar disease incidence and severity was observed in GM-CSF$^{-/-}$ mice. In detail, 11 of 12 mice presented with skin lesions with a median of 0.4% (range 0-1.4%) affected body surface area. This difference in median disease severity was not statistically significant. Eight days after the initial anti-COL7 IgG injection blister formation affected all mice. Although not statistically significant (p=0.053), a trend towards a lower disease scores in GM-CSF$^{-/-}$ mice was observed. Mean affected body surface area in C57Bl/6 mice was 2.9% (0.6-10.3%), as opposed to 1.3% (0.3-2.6%) in mice lacking GM-CSF expression. This trend was validated 12 days after the initial anti-COL7 IgG injection. While C57Bl/6 mice 8.4% (1.6-14.1%) of the body surface area were affected by blistering, this was significantly lower ($p<0.001$) in GM-CSF$^{-/-}$ mice, which had a mean of 3.0% (0.6-6.1%) affected body surface area (figure 8A). Calculation of the overall clinical disease activity, taking onset and maximum severity into account, disease activity expressed as the area under the curve (AUC) in C57Bl/6 mice reached a median of 29 (4-97). In GM-CSF$^{-/-}$ mice AUC was reduced to 26% of wild type mice (median 8, range 3-20, figure 8B and C). These clinical changes were accompanied by unaltered deposition of IgG and C3 at the DEJ (figure 8C). Injection of NR-IgG did not lead to the development of skin lesions in both strains (n=5/strain) throughout the entire observation period.

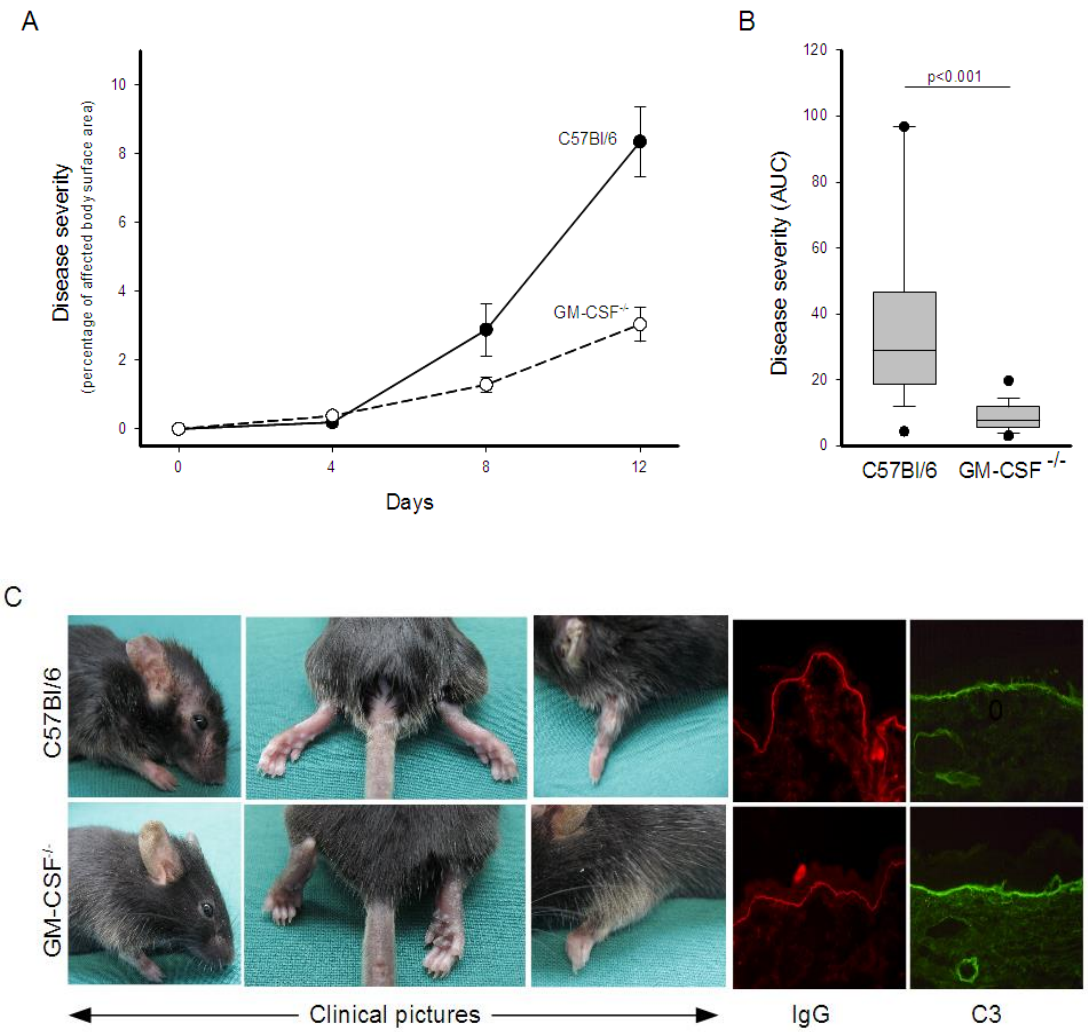

Figure 8. Reduced blister formation in GM-CSF deficient mice after injection of anti-COL7 IgG

Experimental EBA was induced by repetitive injections of anti-COL7 IgG into either C57Bl/6 or GM-CSF deficient (GM-CSF$^{-/-}$) mice. **A**. Clinical EBA severity assessed by the percentage of body surface area covered by skin lesions, 4, 8 and 12 days after the initial anti-COL7 IgG injection. Reduction of affected body surface area in GM-CSF deficient mice is evident 12 days after the initial anti-COL7 IgG injection. **B**. Overall disease severity, expressed as the area under the curve (AUC) show as graphs. Panel A indicate significant reduction in GM-CSF$^{-/-}$ mice (n=12 mice/group, p<0.001, Mann-Whitney Rank Sum Test). Due to the non-parametric distribution, data is presented as median (black line), 25/75-percentiles (boxes), 5/95-percentiles (error bars) and values outside the 95 percentile (dots). **C**. Representative clinical presentations, IgG and C3 deposition 12 days after the initial anti-COL7 IgG injection.

6.3.2. Decreased skin blistering in antibody-transfer-induced EBA after anti-GM-CSF injection

We further tested the impact of GM-CSF in experimental EBA by using neutralizing antibodies against GM-CSF. Anti-COL7 IgG was injected into C57Bl/6 mice (n=5) and anti-GM-CSF antibodies (50µg/mouse) were simultaneously administered. Control mice were injected with anti-COL7 IgG and appropriate isotype control antibody (n=5). Skin lesions were evident in control mice with a median of 0.3% (range 0-0.6%) of affected body surface area as early as 4 days after the initial anti-COL7 IgG injection. In anti-GM-CSF treated mice, no blisters were observed at the same time point (figure 9A). Overall clinical disease severity expressed as area under the curve (AUC) reached a median of 36.2 (26.2-45.3) in isotype antibody injected mice, while extend of blister formation was more than 2-fold decreased in mice treated with anti-GM-CSF, reaching a median AUC of 13.1 (10.2-18.4, p=0.008, Mann-Whitney Rank Sum Test; figure 9B, C). Differences in clinical disease activity were independent of IgG or C3 deposition at the DEJ, which was similar between both treatment groups (figure 9D & E).

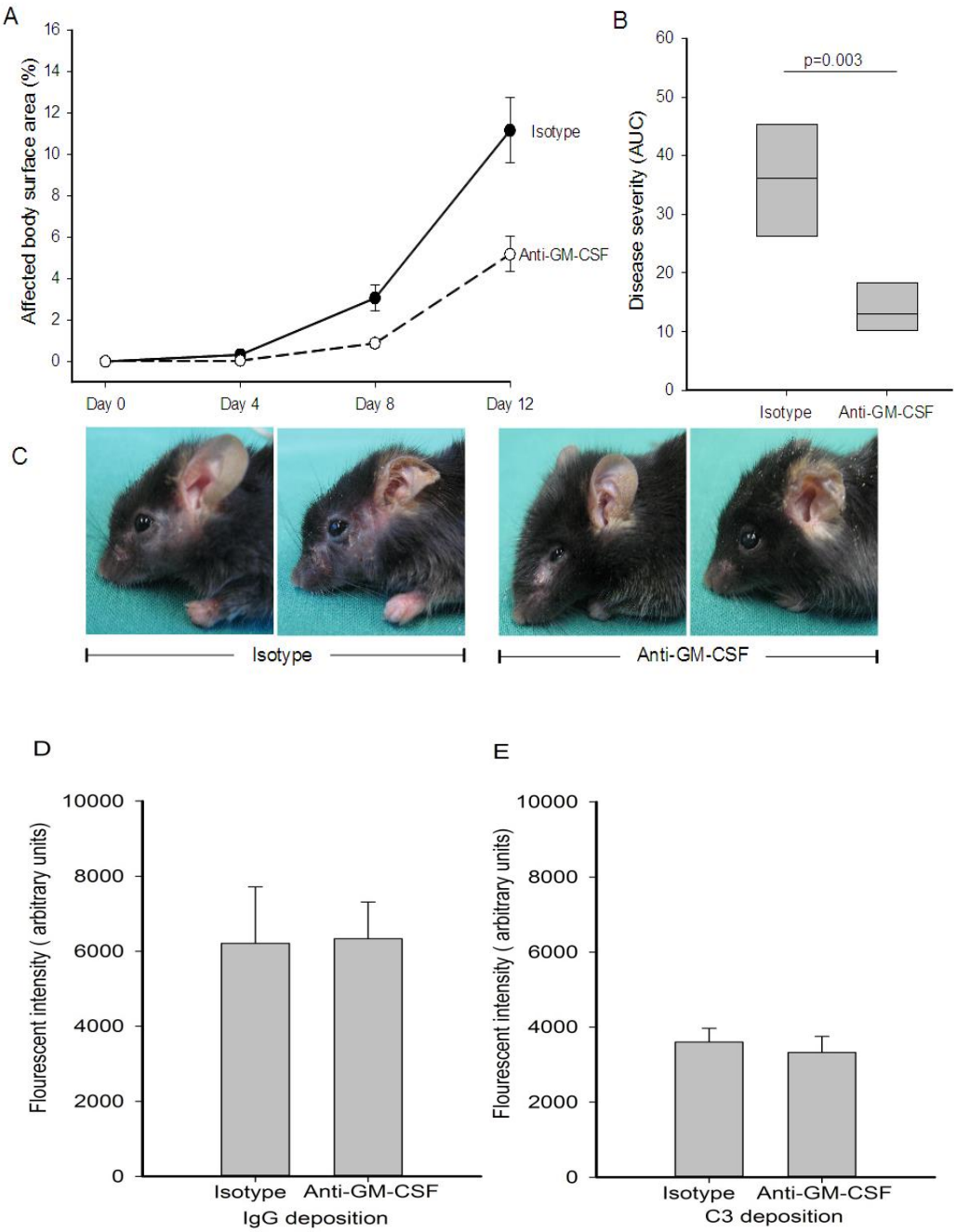

Figure 9. Decreased blister formation in experimental EBA after GM-CSF blocking

Experimental EBA was induced by repetitive injections of anti-COL7 IgG into either anti-GM-CSF or isotype control injected C57Bl/6 mice. **A**. Clinical EBA severity assessed by the percentage of body surface area covered by EBA skin lesions, 4, 8 and 12 days after the initial anti-COL7 IgG injection. Reduction of affected body surface area in anti-GM-CSF treated mice is evident 12 days after the initial anti-COL7 IgG injection. **B**. Overall clinical disease severity, expressed as the area under the curve (AUC) shown as graph indicates significant reduction after GM-CSF neutralization using antibodies (n=5 mice/group, p=0.003, Mann-Whitney Rank Sum Test). Due to the non-parametric distribution, data is presented as median (black line), 25/75-percentiles (boxes). **C**. Representative clinical presentations, 12 days after the initial anti-COL7 IgG injection. **D & E.** In both groups, no difference was detected in the IgG and C3 deposition at the DEJ. Fluorescence intensity was measured using ImageJ software and represented as arbitrary units.

6.3.3. Absence of EBA-associated neutrophilia in GM-CSF deficient mice

Given the pivotal role of neutrophils such as Reactive oxygen species (ROS) and proteolytic enzymes release in the development of autoantibody-induced tissue injury in the EBA model (15, 16, 20) and the effects of GM-CSF on neutrophil activation (76, 80) levels of circulating neutrophils were determined in both mouse strains 12 days after the injection of either anti-COL7 or NR-IgG. In NR-IgG injected C57Bl/6 and GM-CSF$^{-/-}$ mice the proportion of circulating neutrophils was comparable; 16.6±2.2% and 13.4±1.4%, respectively. Compared to NR-IgG, injection of anti-COL7 IgG into C57Bl/6 mice was associated with a marked and statistically significant ($p<0.001$, Mann-Whitney Rank Sum Test) increase in circulating neutrophils (31.5±2.3%). This increase was not observed in GM-CSF$^{-/-}$ mice, which showed similar neutrophil counts after injection of either NR- or anti-COL7 IgG (table 13). In line, in the differential blood count, the proportion of circulating neutrophils is significantly decreased in GM-CSF$^{-/-}$ mice after injection of anti-COL7 IgG compared to wild type controls ($p=0.015$, Mann-Whitney Rank Sum Test).

Strain/ IgG	NR-IgG	Anti-COL7 IgG
C57Bl/6	16.6±2.2	31.5±2.3
GM-CSF$^{-/-}$	13.4±1.4	17.4±4.3

Table 13. EBA-associated neutrophilia is absent in GM-CSF deficient mice

Numbers in table correspond to the percentage of circulating neutrophils, determined by differential blood count 12 days after the injection of the respective IgG preparation (mean ± SEM). Significant differences are observed comparing NR-IgG and anti-COL7 IgG injected C57Bl/6 mice, as well as comparison of anti-COL7 IgG injected C57Bl/6 with GM-CSF deficient mice. Data is from 5-6 mice per group. NR-IgG: normal rabbit IgG, anti-COL7 IgG: rabbit anti-murine type VII collagen IgG.

6.3.4. Decreased dermal infiltration in GM-CSF deficient mice after injection of anti-COL7 IgG

In parallel to the effects of GM-CSF deficiency on circulating neutrophil counts after the injection of anti-COL7 IgG, the impact of lacking GM-CSF expression on the neutrophil rich dermal leukocyte infiltration in experimental EBA (16) was analyzed. Induction of experimental EBA in C57Bl/6 mice led to a pronounced increase in dermal leukocyte infiltration ($p=0.001$, Mann-Whitney Rank Sum Test). This phenomenon was also observed in GM-CSF$^{-/-}$ mice ($p=0.003$, Mann-Whitney Rank Sum Test). However, compared to C57Bl/6 mice with a mean semi-quantitative infiltration score of 1.9±0.2 after injection of anti-COL7 IgG, dermal leukocyte infiltration was significantly lower in GM-CSF$^{-/-}$ mice (1.1±0.1, $p=0.003$, Mann-Whitney Rank Sum Test; figure 10A). Representative H&E staining pictures are shown in figure 10B.

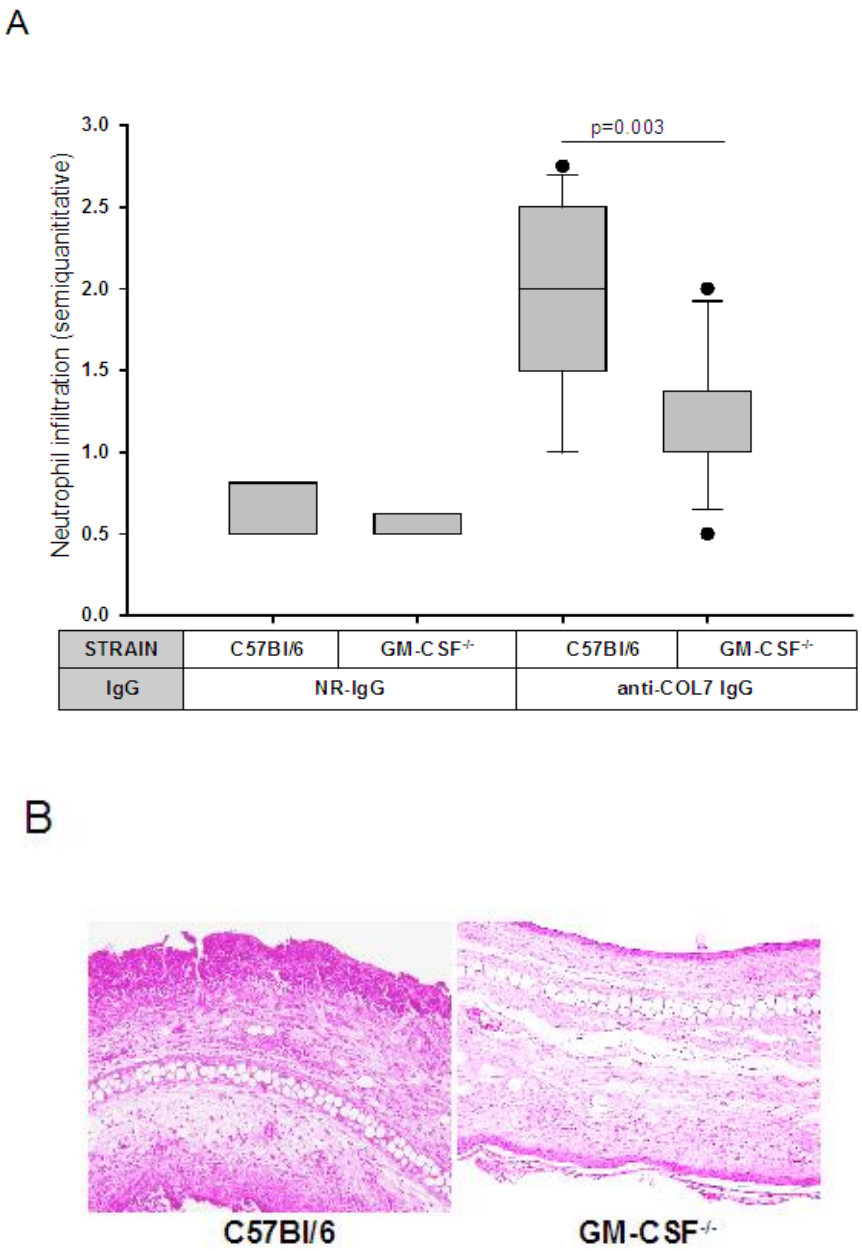

Figure 10. Decreased dermal infiltration in GM-CSF deficient mice after injection of anti-COL7 IgG

A. Extend of dermal leukocyte infiltration is similar in C57Bl/6 and GM-CSF deficient ($^{-/-}$) mice 12 days after injection if normal rabbit IgG (NR-IgG). Likewise, injection of anti-COL7 IgG into both strains of mice induces a significant increase in dermal leukocyte infiltration. The later is however more pronounced in C57Bl/6 compared to GM-CSF$^{-/-}$ mice. Data is from 11 (C57Bl/6) and 12 (GM-CSF$^{-/-}$) scored sections obtained 12 days after the initial IgG injection. **B**. Representative H&E stained sections from both strains injected with anti-COL7 IgG.

6.3.5. GM-CSF enhances IC-induced neutrophil activation

To test if IC-induced neutrophil activation is modulated by GM-CSF, ROS release from IC-activated neutrophils was measured in the absence and presence of GM-CSF. Incubation of neutrophils with GM-CSF in the presence of either monoclonal anti-COL7 antibodies, or corresponding proteins located within the NC1 domain, had no effect on neutrophil ROS release. In contrast, ROS was readily released from neutrophils, after incubation with IC of anti-COL7 antibody and COL7 protein. This IC-induced neutrophil activation was further enhanced by addition of GM-CSF in a dose-dependent fashion (figure 11).

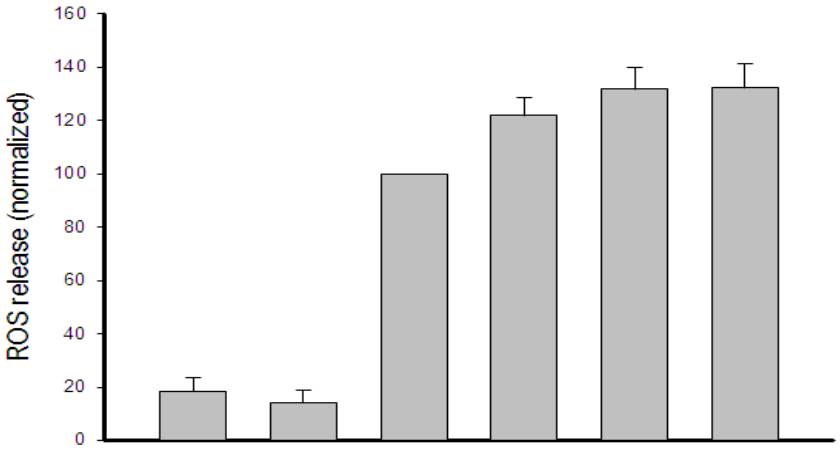

Antigen	+	-	+	+	+	+
Antibody	-	+	+	+	+	+
GM-CSF	1.0ng/ml	1.0ng/ml	-	0.1ng/ml	0.5ng/ml	1.0ng/ml
p (vs. IC only)	<0.001	<0.001	N/A	ns	=0.008	=0.007

Figure 11. GM-CSF increases IC-induced neutrophil activation

Reactive oxygen species release was measured from immune complex activated PMNs. Human COL7 was coated on ELISA plate and IgG1 antibodies specific to COL7 were added to the plate to form immune complex. On to these immune complexes in the plate, PMNs were added with or without recombinant GM-CSF and ROS release was measured using luminol assay. Normalized ROS release of neutrophils after incubation with the indicated combinations of COL7 antigen, anti-COL7 monoclonal antibodies, and different doses of GM-CSF. Data is from 5 independently performed experiments.

6.3.6. Anti-GM-CSF treatment delays disease progression in already established immunization-induced EBA

To test, if modulation of GM-CSF function could be potentially used as a treatment, experimental EBA was induced in 16 B6.s mice by immunization with an immunodominant protein located within murine COL7. Thereafter, mice were scored every week and allocated into anti-GM-CSF-treatment and isotype groups if 2% or more of the body surface area showed skin lesions in individual mice. Mice were randomly allocated to anti-GM-CSF (100µg / 3 times per week, n=8), or appropriate isotype control antibody (n=8). Clinical Disease progression was monitored weekly and expressed in relation to the score at allocation to treatment [median clinical score at allocation was 2.3 (2.1±2.8)]. No difference in disease severity was detected one week after treatments had been initiated. At later time points, clinical disease manifestation in isotype injected mice increased close to 7-fold (figure 12A). In contrast, mice treated with anti-GM-CSF showed a significantly lower disease progression at these time points (figure 12A). In line, overall disease activity expressed as AUC reached a median of 47.6 (38.7-54.4) in isotype treated mice, while disease severity was significantly decreased in mice treated with anti-GM-CSF presented with a median AUC of 33.2 (26.1-37.4, $p \leq 0.001$, Mann-Whitney Rank Sum Test, figure 12B). Differences in clinical disease activity were independent of circulating antigen-specific IgG antibodies, IgG or C3 deposition at the DEJ, which were similar between both treatment groups. Representative clinical pictures are shown in figure 12C.

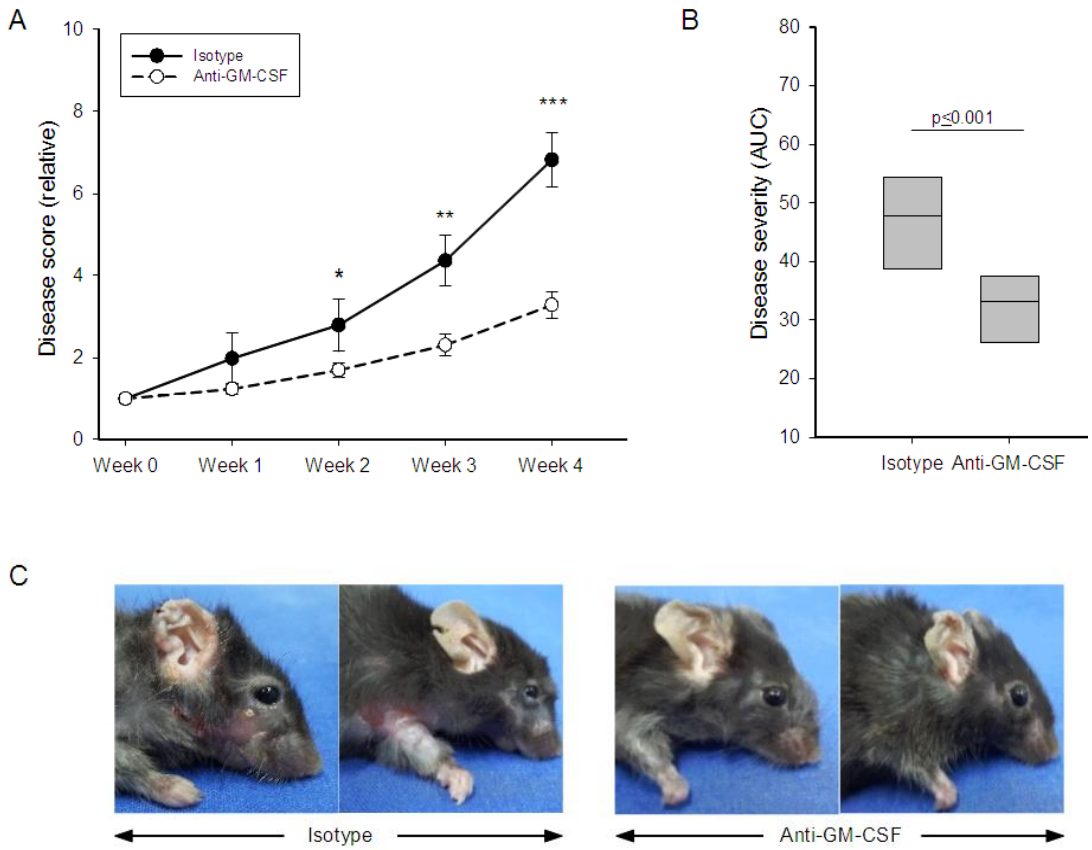

Figure 12. Treatment with anti-GM-CSF impairs clinical disease progression in mice with already established immunization-induced EBA

Experimental EBA was induced in B6.SJL-H2s (B6.s) mice. Mice were treated with anti-GM-CSF or isotype antibody, if 2% or more of the body surface area showed skin blistering. **A**. Clinical disease activity assessed by the percentage of body surface area covered by skin lesions during the 4-week treatment period. With the exception of the first week of treatment, the affected body surface area was significantly lower in GM-CSF-deficient mice throughout the observation period (***p≤0.001,**p=0.001,*p=0.04, t-test) **B**. Overall disease severity, expressed as area under the curve (AUC), indicates significant reduction of skin blistering after anti-GM-CSF treatment. Due to the non-parametric distribution, data is presented as median (black line) and 25/75-percentiles (boxes). **C**. Representative clinical presentations 4 weeks after the initial injection with GM-CSF neutralizing or isotype antibody.

6.3.7. Lower levels of antigen-specific autoantibody concentrations after immunization of GM-CSF deficient mice with recombinant murine COL7: Correlation with neutrophil numbers in draining lymph nodes

Due to the long half life of auto-reactive anti-COL7 producing B cells (*Ben Tiburzy and Hiroaki Iwata, personal communication*), as well as the long persistence of circulating and tissue bound COL7 autoantibodies (166), we investigated if GM-CSF is required for autoantibody production. To address this, C57Bl/6 and GM-CSF$^{-/-}$ mice (n=8/group) were immunized with immunodominant protein located within murine vWFA2 and levels of circulating antibodies were determined by ELISA until 6 weeks after immunization. Autoantibodies against COL7 were detected as early as 2 weeks after immunization at equal titers in both strains of mice. After this time point, C57Bl/6 mice developed significantly higher autoantibody concentrations compared with GM-CSF$^{-/-}$ mice ($p \leq 0.001$,One-Way ANOVA, figure 13). This effect of GM-CSF deficiency on specific autoantibody production affected all antibody subclasses (figure 14).

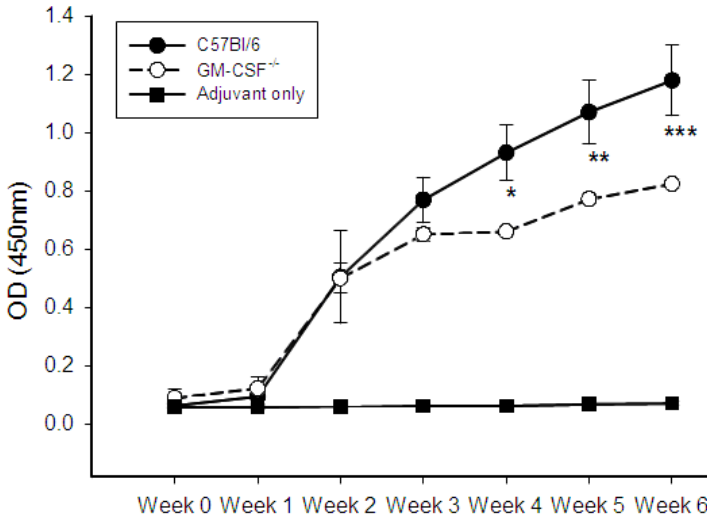

Figure 13. Reduced autoantibody serum levels in GM-CSF-deficient mice after immunization

COL7-specific antibody serum levels in C57Bl/6 or GM-CSF $^{-/-}$ mice were analyzed weekly after immunization using ELISA. GM-CSF$^{-/-}$ mice mounted a significantly lower autoantibody response compared to C57Bl/6 mice from week 4 until the end of the experiment (*$p \leq 0.001$, One-Way ANOVA).

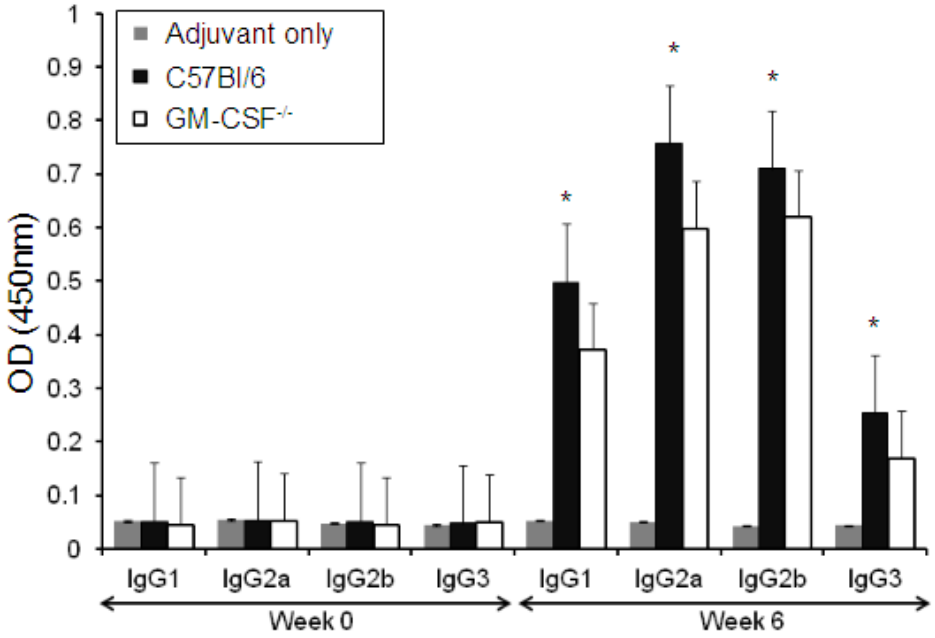

Figure 14. Reduced levels of IgG autoantibody subclasses in GM-CSF-deficient mice serum after immunization

COL7-specific antibody serum levels in C57Bl/6 or GM-CSF $^{-/-}$ mice were analyzed weekly after immunization using ELISA. Comparison of autoantibody IgG subclasses in mice showed a significantly decreased production at week 6 (*p≤0.001, One-Way ANOVA).

Recently, GM-CSF had been shown to contribute for the formation of anti-influenza IgG (167). Furthermore, antibody generation in humans has been demonstrated to be modulated by B cell helper neutrophils (168). Due to the long persistence of circulating and tissue-bound anti-COL7 antibodies (166), we investigated, if neutrophil homing to draining lymph nodes is changed in GM-CSF$^{-/-}$ mice after immunization. Interestingly, at the end of the experiment period, we observed significantly lower neutrophil numbers in the draining lymph nodes of GM-CSF$^{-/-}$ mice compared with C57Bl/6 mice (figure 15A). The ratio of neutrophils versus total number of cells (Ly6G/DAPI) showed significant reduction in GM-CSF$^{-/-}$ mice compared with C57Bl/6 mice (n=5/ group, p=0.001, student's t-test, figure 15B). Presence of antigen in the lymph node, reflecting the total number of COL7 specific B cells (169), was identical in both groups (figure 15C). Furthermore, number of Ly6G positive cells in lymph nodes significantly

correlated with the circulating anti-mCOL7-IgG at the end of experiment (figure 15D; r=0.917; p≤0.0001, Pearson correlation test).

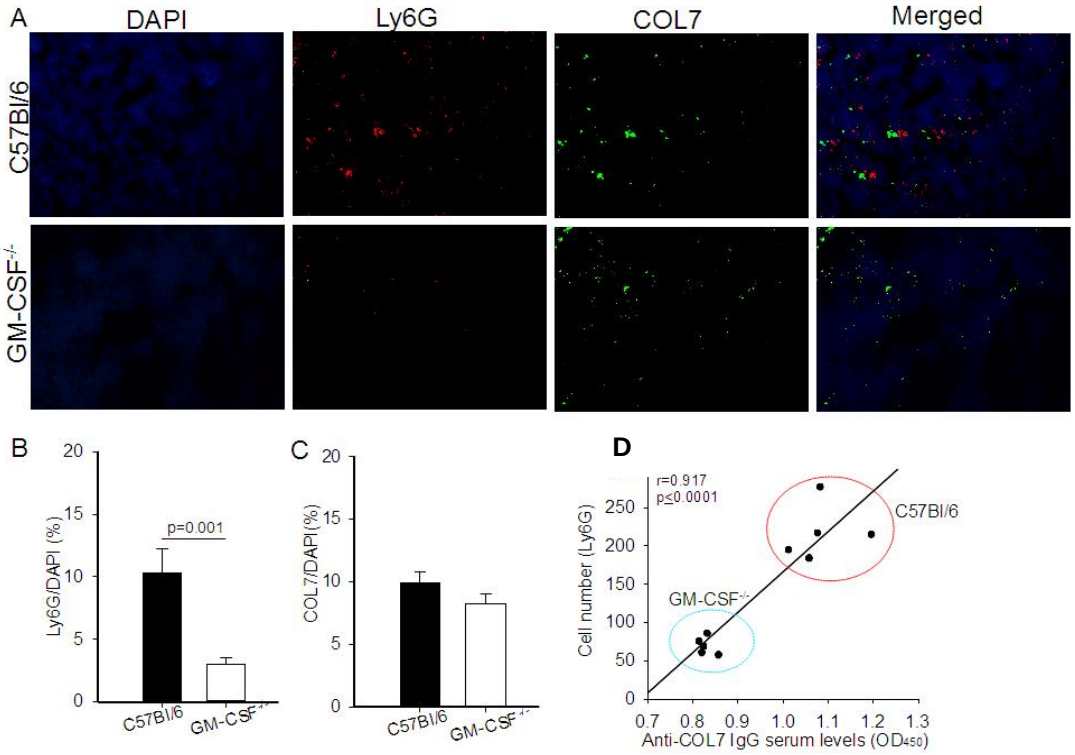

Figure 15. Reduced autoantibody serum levels in GM-CSF-deficient mice correlates with reduced neutrophil numbers in draining lymph nodes

A. Representative sections of staining of draining lymph nodes stained with DAPI (blue), Ly6G (red) and COL7 (green). **B.** Percentage of neutrophil numbers in lymph nodes (Ly6G/DAPI) of C57Bl/6 and GM-CSF$^{-/-}$ mice at the end of the experiment showed a significant reduction of the Ly6G/DAPI ratio in GM-CSF$^{-/-}$ mice (n=5, p=0.001, t-test). **C**. Percentage of COL7-specific B cells in lymph nodes (COL7/DAPI) of C57Bl/6 and GM-CSF$^{-/-}$ mice (n=5) showed no significant difference. **D.** Neutrophil numbers in lymph nodes correlate with anti-mCOL7 IgG serum levels after 6 weeks of immunization in C57Bl/6 and GM-CSF$^{-/-}$ mice (r=0.917; p≤0.0001, Pearson correlation test).

6.3.8. Lower levels of antigen-specific autoantibody concentrations after immunization of neutrophil-depleted mice with COL7

To evaluate the impact of neutrophils on production of specific autoantibodies, we depleted neutrophils in C57Bl/6 mice and GM-CSF$^{-/-}$ mice (n=5 mice/ group). In these mice, EBA was induced by immunization with COL7. As observed before (figure 13), autoantibodies were detected 2 weeks after immunization (figure 16A). At this time

point, equal serum levels of anti-COL7 antibodies were observed in neutrophil-depleted and isotype control mice. After this time point, isotype antibody-injected C57Bl/6 mice mounted a significantly higher immune response compared with neutrophil-depleted mice ($p \leq 0.001$, One-Way ANOVA). Three weeks after immunization, GM-CSF$^{-/-}$ mice (both isotype- or 1A8-injected) showed a similar antibody response, that was significantly lower than observed in C57Bl/6 mice (both isotype- and 1A8-injected, $p \leq 0.001$, One-Way ANOVA). The difference in mounting a specific immune response was even more pronounced 6 weeks after immunization. At this time point, GM-CSF$^{-/-}$ mice injected with 1A8 showed a very low specific autoantibody response (figure 16A). Furthermore, C57Bl/6 mice (1A8-injected) and GM-CSF$^{-/-}$ mice (isotype-injected) had serum levels of anti-COL7 IgG significantly lower compared to isotype-injected C57Bl/6 mice ($p \leq 0.001$, One-Way ANOVA, figure 8A) and significantly higher compared to 1A8-injected GM-CSF$^{-/-}$ mice ($p=0.01$; $p=0.02$ respectively, One-Way ANOVA, figure 16A).

Analysis of the total amount of anti-COL7 IgG produced during the 6-week observation period (expressed as area under the curve, AUC, figure 16B) revealed significant inhibition of autoantibody production in neutrophil-depleted C57Bl/6 mice (1A8-injected, mean AUC 3.4±0.3) compared to C57Bl/6 (isotype-injected, 4.5±0.2, $p \leq 0.001$, Two Way ANOVA). Furthermore, neutrophil depletion using 1A8 in GM-CSF$^{-/-}$ (mean 2.5±0.1) mice showed significantly lower autoantibody levels in sera compared to C57Bl/6 mice (1A8-injected, mean 3.4±0.3, $p=0.003$ Two Way ANOVA) or compared to C57Bl/6 (isotype-injected, 4.5±0.2, $p \leq 0.001$, Two Way ANOVA) or compared to GM-CSF$^{-/-}$ mice (isotype-injected, mean 3.2±0.2, $p=0.002$, Two Way ANOVA)). The effect of neutrophil depletion in GM-CSF$^{-/-}$ mice on autoantibody production is cumulative but not synergistic, as interaction analysis of genotype (C56Bl/6 or GM-CSF$^{-/-}$) and treatment (isotype or 1A8) showed no significance ($p=0.236$, Two Way ANOVA).

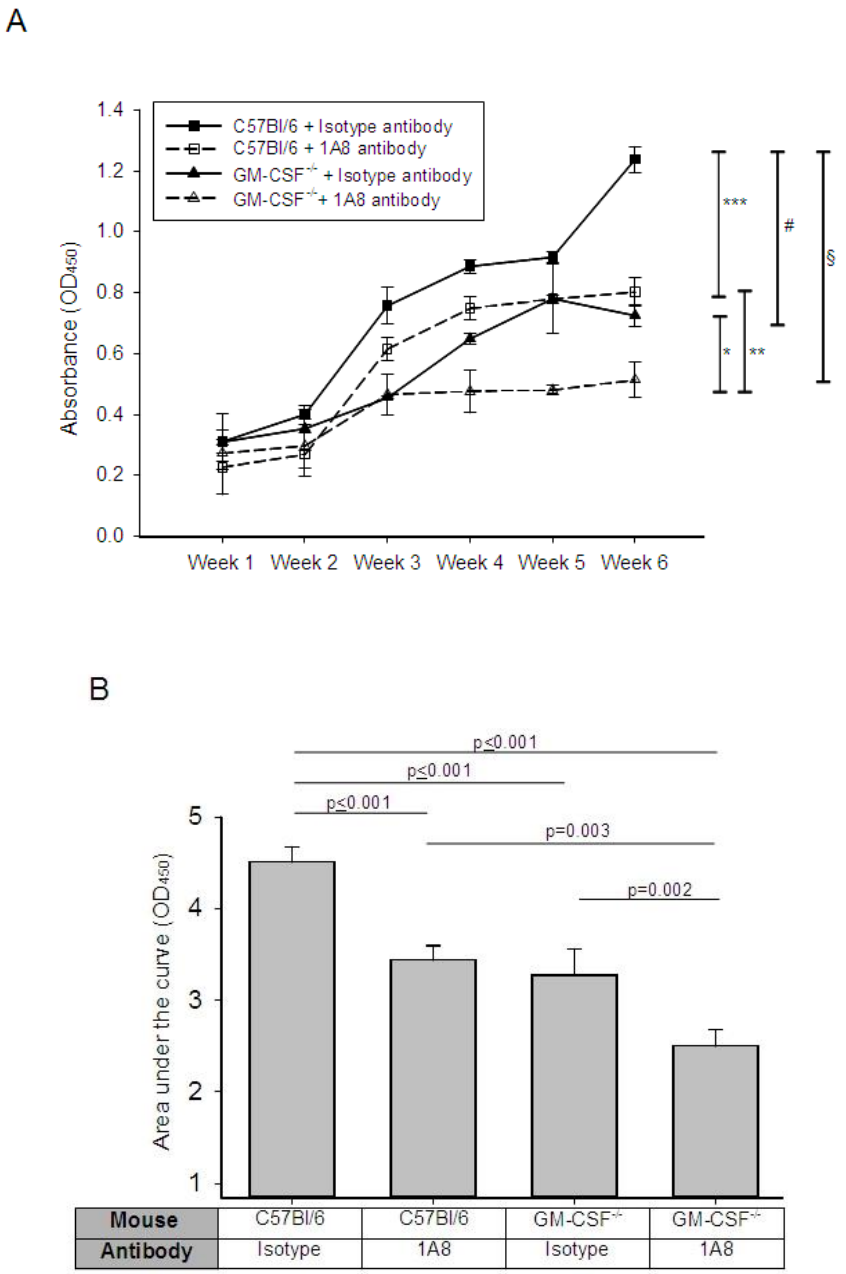

Figure 16. Neutrophil depletion has additive effects on specific antibody production in GM-CSF$^{-/-}$ mice

Specific autoantibody serum levels in COL7-immunized C57Bl/6 or GM-CSF$^{-/-}$ mice with (1A8 antibody) or without (isotype antibody) neutrophil depletion was analyzed weekly by ELISA. **A.** Control mice (C57Bl/6 mice injected with isotype antibody, filled black squares) mount a significantly higher autoantibody response compared to neutrophil-depleted C57Bl/6 mice (empty black squares). Compared to isotype-injected C57Bl/6 mice, autoantibody production is similarly decreased in isotype-injected GM-CSF$^{-/-}$ mice (filled black triangles). Neutrophil depletion in GM-CSF$^{-/-}$ mice (empty black triangles) has additive effects, i.e. a significantly lower autoantibody response compared to the 3 other experimental groups of the experiment (*p=0.02; **p=0.01; ***p≤0.001; $^{\#}$p≤0.001; §p ≤0.001, n=5/group, Two Way ANOVA). **B**. Box plot of summarized OD_{450} readings of autoantibody serum levels (area under curve). Neutrophil depletion (p≤0.001) and GM-CSF deficiency (p≤0.001) both cumulatively reduce autoantibody serum levels, but not synergistically (interaction p=0.236).

6.4. Role of IL-6 in EBA

6.4.1. Increased disease severity in IL-6$^{-/-}$ mice after induction of experimental EBA

To test if increased serum levels and cutaneous IL-6 expression in experimental EBA are of functional relevance, anti-COL7 IgG was injected into mice lacking IL-6 expression (n=14) and wild type control C57Bl/6 mice (n=12). Skin lesions were evident in C57Bl/6 mice with a median of 0.05% (range 0-1.3%) of affected body surface area as early as 4 days after the initial anti-COL7 IgG injection. Interestingly, an even higher disease severity was observed in IL-6$^{-/-}$ mice where skin lesions affected a median of 1.7% (0.5%-3.7%) body surface area (p=0.043, Mann-Whitney Rank Sum Test, figure 17A). In line, overall disease activity expressed as area under the curve (AUC) reached a median of 37.2 (24.5-53.2) in C57Bl/6 mice, while disease severity was more than 2-fold increased in IL-6$^{-/-}$ mice, reaching a median AUC of 75.0 (52.6 - 96.6; figures 17B, C) at the end of experiment. Differences in clinical disease activity were independent of IgG or C3 deposition at the DEJ, which was similar between both strains (figure 17C), and no difference in neutrophil infiltration was observed. Injection of control IgG did not lead to the development of skin lesions in both strains (n=5/strain) throughout the entire observation period.

Similar results were obtained in mice injected with function blocking anti-IL-6 antibody. In detail, skin lesions occurred at a similar frequency and severity in mice injected with anti-COL7 IgG alone and in mice additionally treated with anti-IL-6, as early as 4 days after the initial IgG injection. At later time points, mice receiving the anti-IL-6 antibody showed a significantly enhanced disease severity compared to non-treated EBA mice (figure 18A). Overall disease activity, expressed as AUC, reached a median of 15.8 (10.2-19.8) in control mice, 13.2 (8.9-15.7) in mice additionally injected with isotype

control antibody, and 22 (16.3-26.3) in mice receiving the neutralizing IL-6 antibody (p=0.028, One-Way ANOVA, figure 18B).

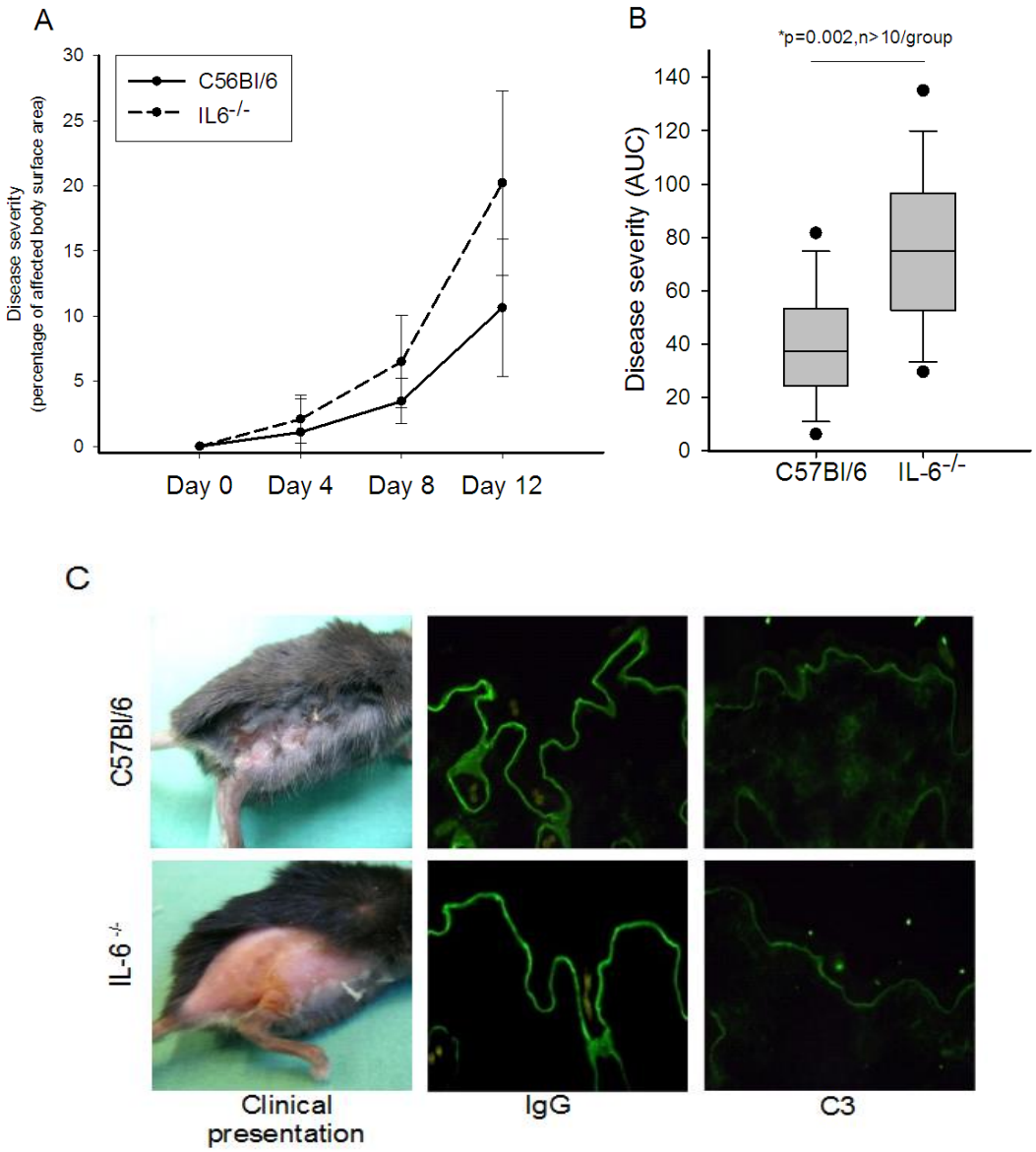

Figure 17: Enhanced EBA severity in IL-6 deficient mice

Experimental EBA was induced by repetitive injections of anti-COL7 IgG into either C56Bl/6 or IL-6 deficient mice (n>10 mice/group). (**A**) Clinical EBA severity assessed by the percentage of body surface area covered by EBA skin lesions, 4, 8 and 12 days after the initial anti-COL7 IgG injection. A statistically significant increase of affected body surface area in IL-6 deficient mice is evident at all evaluated time points. (**B**) Overall disease severity, expressed as the area under the curve (AUC) from the graphs shows a significant increase in IL-6 deficient mice. Due to the nonparametric distribution, data is presented as median (black line), 25/75-percentiles (boxes), 5/95-percentiles (error bars) and each result (blue dots). (**C**) Representative clinical presentations, IgG and C3 deposition 12 days after the initial anti-COL7 IgG injection. This figure has been published as part of own publication, Samavedam et al (70).

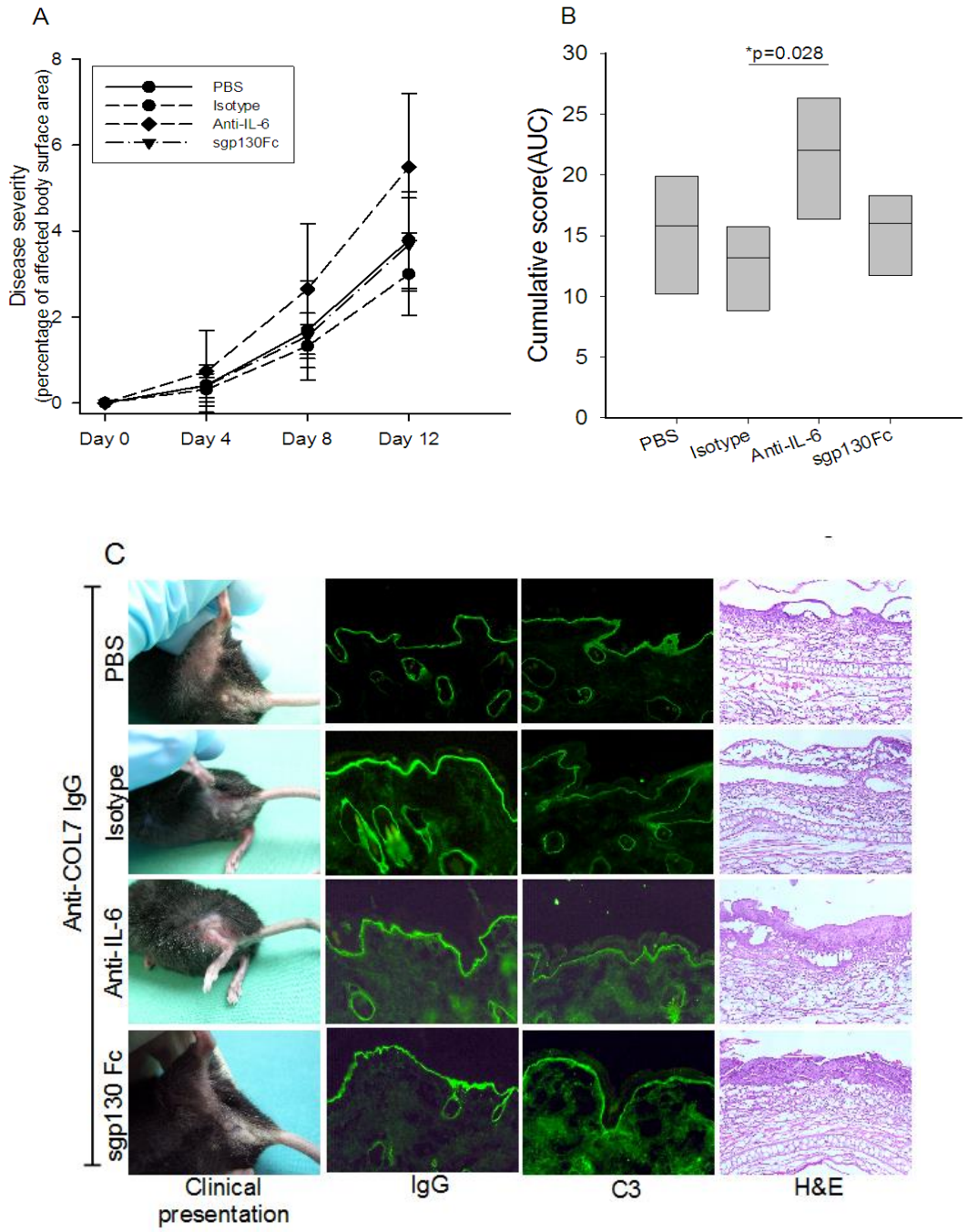

Figure 18: Enhanced EBA severity after IL-6 neutralization

Experimental EBA was induced by repetitive injections of anti-COL7 IgG into control (PBS) treated, isotype antibody treated, anti-IL-6 and sgp-130Fc-treated mice (n=8 mice/ group). (**A**) Clinical EBA severity assessed as percentage of body surface area covered by EBA skin lesions, 4, 8 and 12 days after the initial anti-COL7 IgG injection. No significant different was observed with isotype and sgp-130Fc treated mice. (**B**) Overall disease severity, expressed as the area under the curve (AUC) from the graphs showed in mice injected with anti-IL-6 antibodies [*p= 0.028 (ANOVA)]. Due to the nonparametric distribution, data is presented as median (black line), 25/75-percentiles (boxes). Blue dots represent reads for each sample tested (**C**) Representative clinical presentations, IgG, and C3 deposition and H&E stained sections 12 days after the initial anti-COL7 IgG injection. This figure has been published as part of own publication, Samavedam et al (70).

In contrast to IL-6 neutralization, inhibition of IL-6 trans-signaling using sgp130Fc had no effect on EBA manifestation [AUC: 16 (11.7-18.3), figure 18B]. Throughout the entire observation period, disease severity was similar for isotype- and sgp130Fc-treated mice (figures 18A, 1B). Differences in clinical disease activity were independent of IgG or C3 deposition at the DEJ, which was similar among untreated and sgp130Fc-treated EBA mice (70) (figure 18C).

6.4.2. Treatment with IL-6 impairs induction of experimental EBA

To investigate a potential protective role of IL-6 in experimental EBA, mice were treated with recombinant IL-6. Treatment with recombinant IL-6 dose-dependently impaired the induction of experimental EBA. Mice injected with 20µg recombinant IL-6 per day were almost completely protected from EBA induction (median 1.6, range 1.1-2.7, $p<0.001$, One-Way ANOVA). Lower doses of recombinant IL-6 (5µg/day) had no effect on EBA disease severity (median 11.6 range 11.4-14.2, $p=0.37$, One-Way ANOVA, figures 19A, B). Again, no changes in IgG and C3 deposition were observed among all groups (figure 19C). Injection of normal rabbit IgG did not lead to the development of skin lesions (n=5) throughout the entire observation period (70).

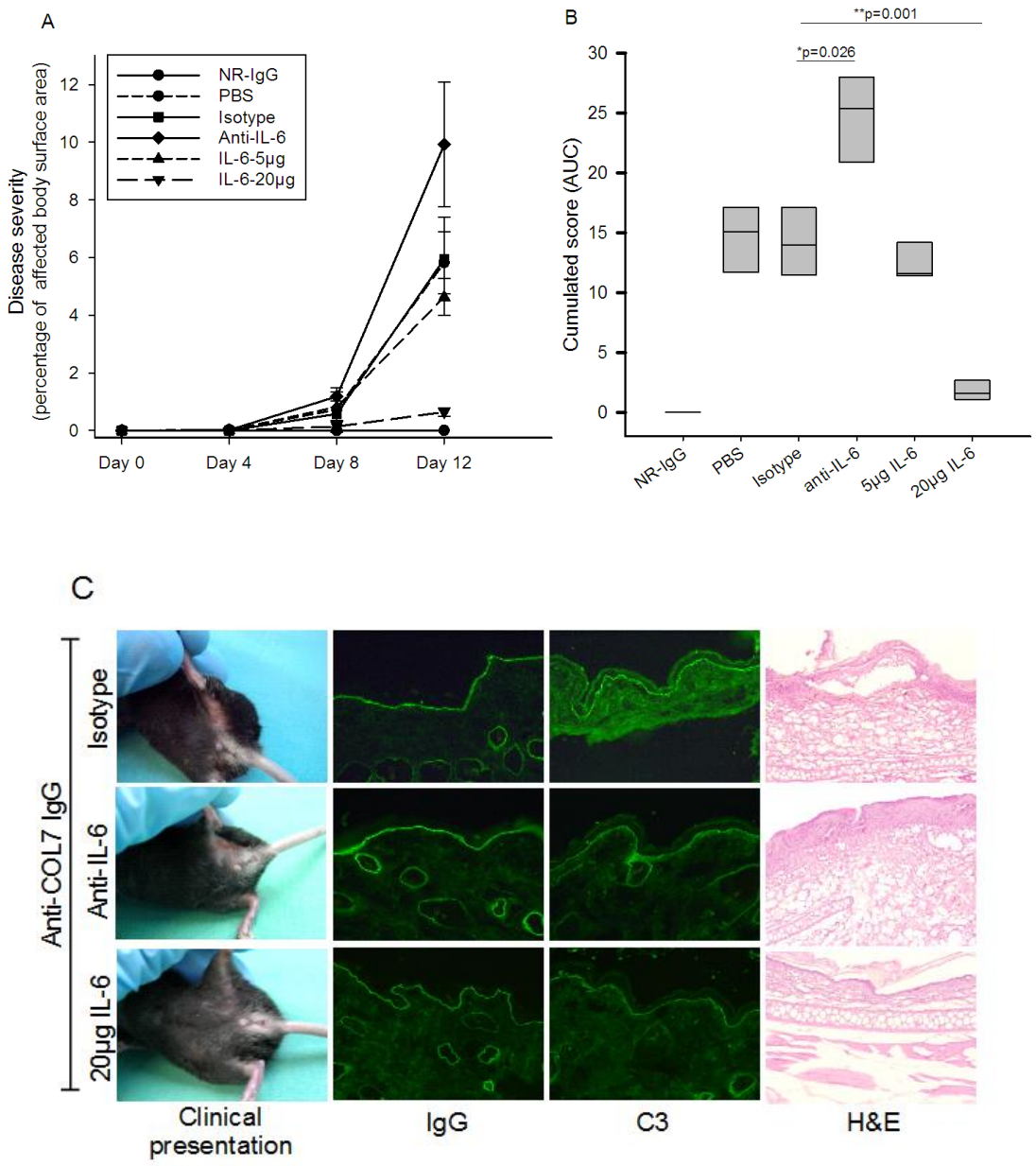

Figure 19: IL-6 treatment protected mice from experimental EBA

Experimental EBA was induced by repetitive injections of anti-COL7 IgG into PBS, isotype, anti-IL-6 injected and recombinant IL-6 (5µg and 20µg) treated mice (n=5 mice/group). Mice injected with NR-IgG (n=5) used as negative control (**A**) Clinical EBA severity assessed by the percentage of body surface area covered by EBA skin lesions, 4, 8 and 12 days after the initial anti-COL7 IgG injection. A statistically significant increase of affected body surface area in IL-6 neutralized mice is evident 12 days after the initial anti-COL7 IgG injection. In contrast, IL-6 (20µg) treated mice were significantly protected from disease. (**B**) Overall disease severity, expressed as the area under the curve (AUC) from the graphs showed a significant increase in mice treated with anti-IL-6 antibodies and opposite effects were shown in mice treated with recombinant IL-6 (20µg) [(*p &**p=0.001, ANOVA)]. Due to the nonparametric distribution, data is presented as median (black line) and 25/75-percentiles (boxes). Results for each sample represented as blue dot. (**C**) Representative clinical presentations, IgG and C3 deposition and H&E stained sections. This figure was published as part of own publication, Samavedam et al (70).

6.4.3. IL-6 treatment leads to increased IL-1Ra expression in skin and serum

As IL-6 has previously been implemented to regulate IL-1Ra in vitro, IL-1Ra concentration in serum and IL-1Ra mRNA expression in the skin were determined. IL-1Ra serum concentrations were significantly increased after induction of experimental EBA (median 138.4 pg/ml, 95.2-170.1), compared with mice injected with normal rabbit IgG (median 73.5pg/ml, 67.4-91.1; p=0.003, Mann-Whitney Rank Sum Test). Interestingly, this EBA-associated increase in serum IL-1Ra levels was absent in IL-6$^{-/-}$ mice injected with anti-COL7 IgG (median 90.2pg/ml, 71.8-125.6pg/ml), which also showed levels similar to those in EBA mice treated with IL-6 antibodies (median 85.5pg/ml, 70.4-98.8pg/ml). In contrast, highest IL-1Ra levels were detected in mice treated with recombinant IL-6 (median 254.5pg/ml, 239.1-274pg/ml, p=0.001, One-Way ANOVA, figure 20).

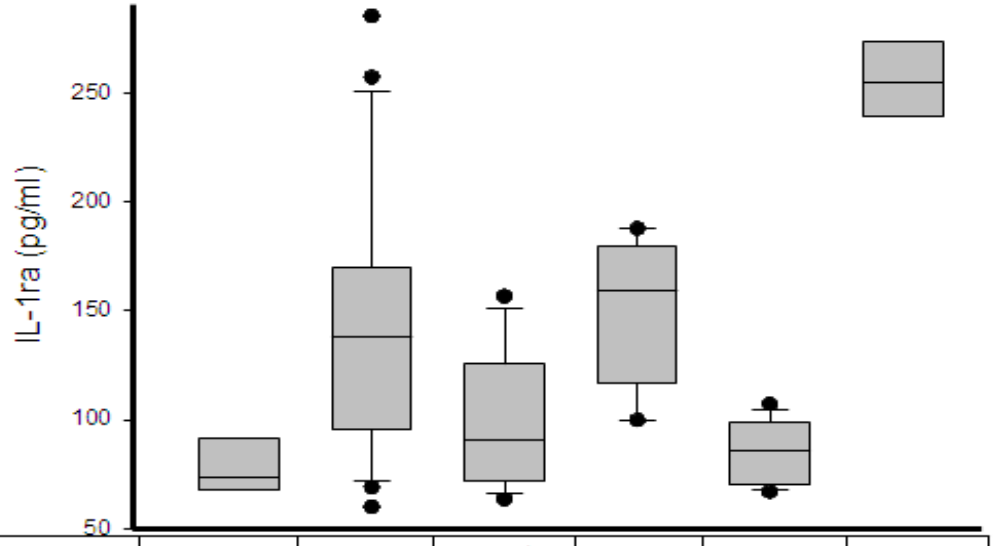

Strain	B6	B6	IL-6$^{-/-}$	B6	B6	B6
IgG	NR	anti-COL7	anti-COL7	anti-COL7	anti-COL7	anti-COL7
antibody	-	-	-	isotype	anti-IL6	-
20µg IL-6	-	-	-	-	-	+
p	N/A	0.003 (NR IgG)	0.027 (isotype)	<0.001 (NR IgG)	<0.001 (isotype)	<0.001 (isotype)

Figure 20: IL-6 treatment increased expression of IL-1Ra in serum

Serum concentrations of IL-1Ra in the indicated treatment groups. Of note, induction of experimental EBA by injection of anti-COL7 IgG led to a significant increase of serum IL-1Ra concentrations (p=0.003). If IL-6 function is blocked either in knockout mice or by injection of a functional blocking antibody, IL-1Ra serum levels remain at basal levels after EBA induction. In contrast, administration of recombinant IL-6 leads to a significant increase of IL-1Ra serum concentrations, exceeding those observed in untreated C57Bl/6 control mice with experimental EBA (p<0.001). Due to the non-parametric data distribution, data is presented as median (black line), 25/75-percentiles (boxes), 5/95-percentiles (error bars). This figure was published as part of own publication, Samavedam et al (70).

To further confirm these findings, analysis of IL-1Ra mRNA expression in skin was performed. Soluble isoform of IL-1Ra (IL-1Ra^{sol}) was significantly increased in mice with experimental EBA (fold change 0.1±0.09) compared with mice injected with normal rabbit IgG (fold change 0±0, p<0.05, student t test). Expression of both IL-1Ra isoforms was significantly increased in IL-6 treated mice (10.1±1.26 for IL-1Ra^{sol} and 2.2±0.01 for IL-1Ra^{int} respectively, p<0.005, One-Way ANOVA, table 14).

	NR-IgG	anti-COL7 IgG	anti-COL7 IgG	anti-COL7 IgG	anti-COL7 IgG	anti-COL7 IgG
	-	-	Isotype	anti-IL-6	5µg IL-6	20µg IL-6
Timp-1	1.02±0.6	0.3±0.01*	0.2±0.02	0.1±0.06**	6.02±1.3	9.3±2.3§
IL-1ra (sol)	0	0.1±0.086*	0.15±0.021	0.1±0.01**	4.9±0.49	10.1±1.26§
IL-1ra (int)	3.1±0.9	0.6±0.01*	0.7±0.2	0.6±0.12	1.6±0.7	2.2±0.01§
Bcl-2	0.19±0.05	0.14±0.03	0.17±0.05	0.14±0.03	0.12±0.03	0.13±0.4

Table 14: Increased expression of IL-1Ra and anti-apoptotic factors in mice skin

Messenger RNA data from the mice sections showed IL-1Ra^{sol} was significantly lowered in IL-6 antibody treated mice compared with isotype ($p<0.02$) but IL-1Ra^{int} does not show any significant difference. In IL-6 (20µg) treated mice, the difference was significant in both the isoforms ($p<0.002$). Timp-1 mRNA expression showed significant reduction in IL-6 antibody treated mice compared with isotype. ($p<0.021$) Mice treated with 20µg IL-6 showed significantly increased expression of Timp-1($p=0.014$).*$p<0.05$ (compared to NR-IgG), **$p<0.02$(compared to Isotype), §$p<0.005$ (compared to Isotype). Expression of Bcl-2 in the different experimental groups showed no significant change. This table has been published as part of own publication, Samavedam et al (70).

Serum levels of IL-10 and TGF-β significantly decreased in mice treated with anti-IL-6 and use of recombinant IL-6 restored levels to those of isotype antibody treated mice. Levels of serum sTNF-R1 and IL-4 remained unaltered in all groups. Similar to changes of serum levels, mRNA expression of IL-10 and TGF-β decreased significantly in mice treated with anti-IL-6 and expression was restored after treatment with recombinant IL-6 (table 15) (70).

Cytokine		NR-IgG	Anti-Col7 IgG	Anti-Col7 IgG		
				Isotype	Anti-IL-6	20µg IL-6
IL-4	Serum	-	-	-	-	-
	Skin (mRNA)	0	0.01±0.005	0.01±0.009	ND	0.01±0.004
IL-10	Serum	0	249.1±92.8*	218.2±58.5	138±68.6§	218.1±28.9
	Skin (mRNA)	0.01±0.002	0.15±0.007*	0.17±0.04	0.1±0.03§	0.21±0.012
TGF-β	Serum	108.9±4.3	308.2±150.3*	385±42.5	166.1±38.4§	325.1±35.5
	Skin (mRNA)	0.56±0.12	1.12±0.32*	2.86±0.45	0.61±0.08§	2.33±0.19
sTNFR-1	Serum	115.2±15.2	101.8±23.3	124.7±34.5	112.8±35.8	118.2±28.8
	Skin (mRNA)	ND	ND	ND	ND	ND

Table 15: Anti-inflammatory cytokine expression after IL-6 treatment in experimental EBA

All serum concentrations are indicated as pg/ml and mRNA expression as relative expression x 100 in relation to MLN51. NR: normal rabbit, ND: not done, -: Below detection threshold. *) Compared with NR-IgG group, $p<0.01$; §) Compared with Isotype, $p<0.02$; $) Compared with NR-IgG, $p<0.05$. This table has been published as part of own publication, Samavedam et al (70).

6.4.4. IL-6 treatment is associated with reduced TUNEL+ basal keratinocytes and increased mRNA expression of Timp-1

Induction of EBA leads to an increased rate of apoptosis in basal keratinocytes. In mice injected with normal rabbit IgG, 19.6% (15.9%-2 2.3%) TUNEL+ cells were detected. After induction of experimental EBA, the proportion of TUNEL+ cells significantly increased to 31.8% (29.0%-33.1%, p=0.016, Student t-test; figure 21A). In line with the clinical observation, the proportion of TUNEL+ cells increased in mice injected with anti-IL-6 antibody (median 58%, 48%-68%). In contrast, mice treated with 20µg of recombinant IL-6 presented with significantly reduced number of TUNEL+ cells (median 16%, 11%-22%, p=0.001, One-Way ANOVA; figure 21B). Data for Timp-1 mRNA expression were in line with findings from TUNEL staining; e.g., decrease in Timp-1 expression to 0.3±0.0 in mice induced with EBA compared with 1.0±0.6 in mice injected with normal rabbit IgG. Furthermore, compared to isotype-injected mice (0.2±0.02), Timp-1 expression was significantly reduced (0.1±0.1) in IL-6 antibody injected mice, and increased in IL-6 treated mice (9.3±2.3; table 13). Expression of Bcl-2 mRNA showed no significant change in all experimental groups (Table 14).

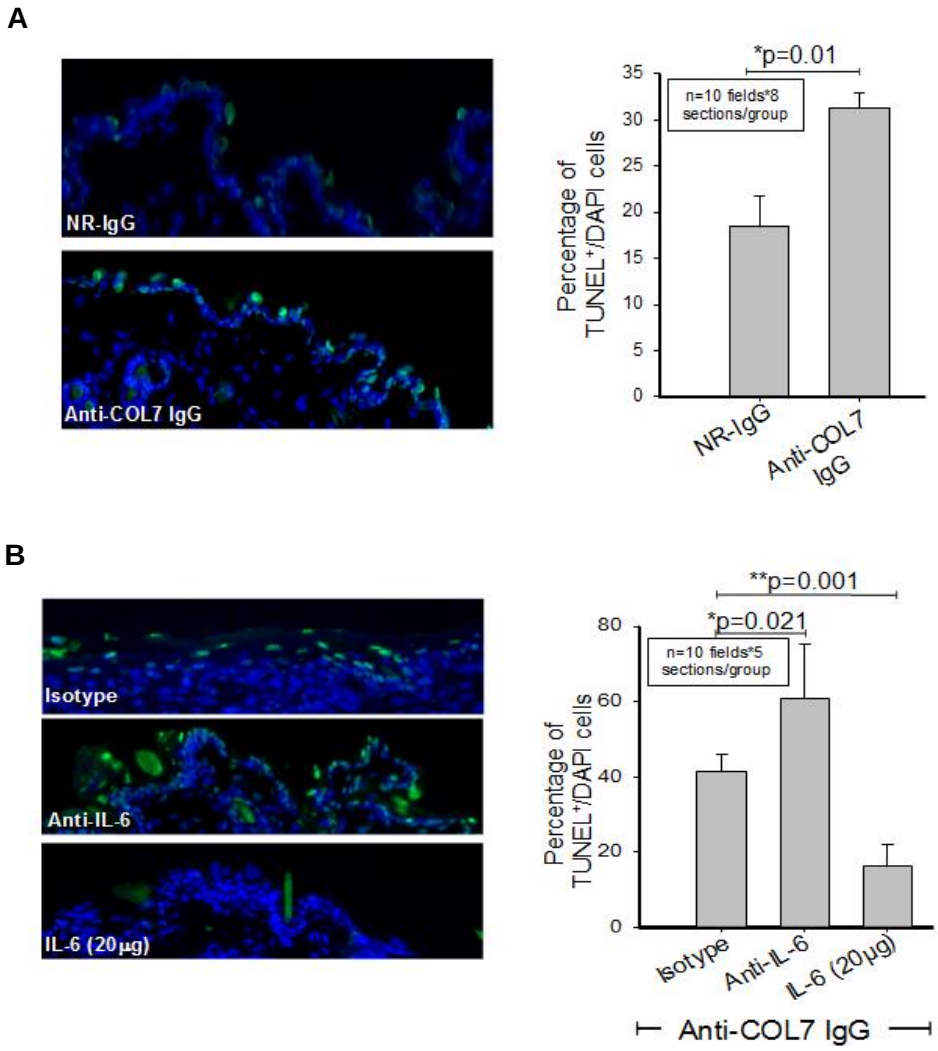

Figure 21: IL-6 treatment protected mice from apoptosis

Representative TUNEL (green) and DAPI (blue) stained skin sections from mice 12 days after injection of either normal rabbit (NR) IgG or anti-COL7 IgG. (**A**) The induction of experimental EBA leads to an increase of apoptosis of basal keratinocytes (p=0.01, Student t-test, n=10 fields*8 sections/group) in anti-COL7 IgG treated mice. (**B**) While blocking of IL-6 function leads to an enhanced number of apoptotic keratinocytes, treatment with recombinant IL-6 significantly reduces the apoptosis rate (p=0.001, One-Way ANOVA, n=10 fields*5 sections/group). This figure has been published as part of own publication, Samavedam et al (70).

7. Discussion

7.1. Clinical presentation of epidermolysis bullosa acquisita

Over 100 years ago, the phrase “epidermolysis bullosa acquisita’’ (EBA) was used to clinically describe patients with late onset and features resembling those of hereditary dystrophic epidermolysis bullosa (13). Several years later, EBA was distinguished from other bullous diseases using distinctive clinical and histological features. The clinical presentation of EBA is very heterogeneous. In descriptive clinical terms, EBA patients can be classified into two major clinical forms: non-inflammatory (classical or mechano-bullous) and inflammatory EBA (11, 15, 170). In addition, clinical presentation of an EBA patient may change during the disease or the same patient may present with two different EBA presentations simultaneously. Mechanobullous (non-inflammatory or classical) variant of EBA is diagnosed in approximately 1/3rd of the patients and patients suffer from skin fragility, tense blisters, scarring and milia formation, localized on trauma-prone sites. Moreover, patients with mechano-bullous EBA frequently develop nail dystrophy, post-inflammatory hyper- and hypopigmentation, and involvement of the oral mucosa is commonly observed (143, 171, 172). Inflammatory variants of EBA, account for most of EB cases. This disease is clinically mimics other AIBD such as bullous pemphigoid (143, 172).

7.2. Extra-cutaneous manifestations of EBA

In addition to muco-cutaneous lesions, EBA can also affect several extra-cutaneous sites. These include ocular, oral mucosa, esophagus, anal, vaginal, tracheal and laryngeal lesions (15, 170). Ocular involvement in EBA resembles lesions in mucous

membrane pemphigoid (MMP) patients and may lead to blindness (173–178). In EBA, erosions and blistering can also affect the oral mucosa and are commonly observed in patients with non-inflammatory, MMP-like or LAD-like inflammatory EBA (179, 180). Patients may not be able to swallow foods and may require endoscopic esophageal dilations (181–183). In some singular cases, laryngeal involvement may cause hoarseness, impaired phonation (dysphonia) and loss of voice, and may lead to irreversible respiratory distress (184, 185).

7.3. Diseases associated with EBA

EBA is associated with other diseases such as systemic lupus erythematosus, cryoglobulinemia, diabetes mellitus, and psoriasis (15, 170). Most commonly, EBA is associated with inflammatory bowel disease (IBD), i.e., ulcerative colitis (UC) and Crohn's disease (CD) (186–188). As of now, association of EBA with Crohn's disease has been noted in several patients and 4 cases in ulcerative colitis (189). Conversely, in patients with active IBD, circulating antibodies to COL7 have been noted at higher frequencies than expected (190). This clinical observation has recently been also duplicated in EBA mouse models: In antibody transfer-induced EBA and in immunization-induced EBA gastrointestinal inflammation was noted (29, 30). This gastrointestinal tissue injury in experimental models of EBA is of functional relevance, as weight loss or failure to gain weight was observed in diseased mice (158).

7.4. Epidemiology of EBA

EBA is a rare disease. The incidence ranges from 0.2 to 0.5 new cases/million/year (191, 192). Due to the chronic nature of the disease, EBA prevalence is most likely higher, but no data on the prevalence has been published. Data from a large collection

of EBA patients from 3 recent epidemiological reports indicates that EBA affects females slightly more often than men. The median age of onset is 47 years (75-percentile: 30-66 years). However EBA has also been described in children (171, 172, 193).

7.5. Pathogenesis of EBA

Like all other AIBD, in EBA, autoantibodies targeting antigens located in the skin cause tissue injury (11, 194). Since the identification of COL7 as the autoantigen in EBA, development of model systems mirroring the human disease has significantly contributed to the current understanding of EBA pathogenesis (195). In most EBA patients, the autoantibodies are of the IgG subclass. In addition to IgG, IgA anti-COL7 autoantibodies have been detected either as the only immunoglobulin class or in combination with IgG. Epitope mapping studies with sera from EBA demonstrated that the vast majority of autoantibodies bind to epitopes located within the non-collagenous (NC) 1 domain of COL7 (33, 196, 197). In very few patients antibody reactivity to either the collagenous domain or to the NC2 domain has been described (198, 199). Of note, so far these epitope mapping studies have been performed for IgG. Epitopes targeted by anti-COL7 IgA antibodies are currently not known.

7.5.1. Demonstration of pathogenic relevance of anti-COL7 antibodies

The pathogenicity of anti-COL7 antibodies has been documented in vitro and in vivo. In vitro pathogenicity was demonstrated by incubation of cryosections of human skin with serum, total IgG or NC1-affinity purified IgG isolated from EBA patients. This leads to linear IgG deposition along the dermal-epidermal junction. When these sections are subsequently incubated with neutrophils from healthy human blood donors, this induces location of neutrophils along the dermal-epidermal junction, followed by

release of *matrix-metalloproteinase* and reactive oxygen species (ROS) from neutrophils and ultimately to dermal-epidermal separation, i.e., the parting of the epidermis from the underlying dermis (23). The addition of neutrophils is required to induce this dermal-epidermal separation, as antibody binding alone does not induce dermal-epidermal separation. Based on these findings an additional in vitro model of EBA has been developed: Neutrophils from healthy blood donors were isolated and incubated with fixed immune-complexes of anti-COL7 IgG and recombinant COL7 leading to neutrophil activation, measured by release of ROS by chemiluminescence and *elastase* from the supernatant by ELISA (200).

Later, the in vivo pathogenic relevance of autoantibodies targeting COL7 has been documented. Injection of total IgG isolated from rabbits immunized with recombinant protein of COL7 into wild type mice of several inbred stains induces subepidermal skin blisters, reproducing human EBA at the clinical, histological, electron microscopical, and immunopathological levels (29). At the same time point, another group independently generated rabbit anti-human COL7 IgG, which also induced experimental EBA after injection into genetically diverse SKH1 mice (32). Later on further animal models were developed, all documenting the pathogenic contribution of antibodies directed against COL7 (31, 33–36). For example, to model all aspects of the human disease, including loss of tolerance, as well as autoantibody-induced tissue injury, several mouse strains were immunized with a protein spanning the amino acid residues 757-967, which contains a GST-tag for isolation, termed GST-mCOL7C. Mice were immunized with the protein and were subsequently boosted 3 times at 3-week intervals. This led to the induction of clinical disease in close to 80% of SJL/J, and approximately 50% in BALB/c and Fc gamma receptor IIB-deficient mice on a C57Bl/6 genetic background. Contrary, genetically diverse SKH1 and wild type C57Bl/6 mice did not develop skin blistering, despite the presence of circulating anti-COL7 IgG; although with the presence of another isoclass (30). Experimental EBA can also be induced by immunization in susceptible inbred mouse strains (SJL/J, B6.SJL-H2s,

B10.s and MRL/MpJ) by single immunization with GST-mCOL7C, in an autoimmune-prone advanced intercross mouse line (AIL) by single immunization with GST-mCOL7C and in SJL/J and B6.SJL-H2s mice by single immunization with another immunodominant protein corresponding to the vWFA2-like sub-domain of COL7-NC1 (38, 39).

7.5.2. Loss of tolerance to COL7 in EBA

7.5.2.1. Genetic control of EBA susceptibility

Clinical observations and MHC genotyping in patients with EBA point towards a genetic control of EBA, which is also observed in EBA animal models. In more detail, EBA susceptibility was associated to certain MHC alleles in patients. One study documented an association with HLA-DR2 and a later study found HLA-DRB1*15:03 to be associated with EBA (172, 201). In addition to these studies, the observation of co-occurrence of EBA cases in one family (uncle-nephew) points towards a genetic control of EBA (202). Like in EBA patients, an MHC restriction is also observed in immunization-induced experimental murine EBA: After immunization with GST-mCOL7C almost all inbred mouse strains developed anti-COL7 antibodies. Interestingly, only few strains also develop a subepidermal blistering disease. Among several tested mouse strains, SJL/J and B6.SJL-H2s mice show a high incidence of severe disease, while C57Bl/10.s and MRL/MpJ mice develop mild EBA at a low incidence. NOD/Sh/J and C57Bl10.q mice were resistant to both anti-COL7 autoantibody production and clinical disease development (38). Moreover, immunization-induced EBA-resistant C57Bl/6 mice become susceptible if they lack expression of the inhibitory Fc gamma IIB receptor (29). Overall, these differences indicate that genes outside the MHC locus contribute to EBA susceptibility. In order to define this genetic control of EBA susceptibility, a genetically diverse out bred AIL mice were immunized with GST-mCOL7C. Mice of the 4th offspring generation (G4) were

immunized with the protein. Of these immunized AIL mice, one-third developed clinically manifest experimental EBA, while the remaining majority of mice remained clinically healthy. All immunized and phenotyped AIL mice were genotyped for 1400 single-nucleotide polymorphisms (SNP) to identify those regions within the genome that control EBA susceptibility. These susceptibility loci are also termed quantitative trait locus (QTL). This identified several non-MHC QTL controlling EBA susceptibility (39).

7.5.2.2. T-cells are required for autoantibody production in experimental EBA

T cell-deficient SJL^{nude} mice are completely protected from induction of immunization-induced EBA. SJL^{nude} mice, disease susceptibility could be restored by transfer of T cells from wild type SJL/J mice, which have been immunized with COL7 (37). Therefore, T cells are required for induction of autoantibody production, and possibly also for the maintenance of autoantibody production. To further define T cell subsets involved in generation of anti-COL7 antibodies in experimental murine EBA, CD4- and CD8 T cells were depleted in a time-restricted fashion. Cell depletion was achieved at the time of immunization and maintained for at least 2 weeks thereafter. Depletion of CD4 T cells for within this period significantly delayed both autoantibody production and onset of clinical disease. In contrast, depletion of CD8 T cells for the same time period had no effect on anti-COL7 IgG production and clinical disease manifestation (203).

7.5.2.3. HSP90 is required for autoantibody production in experimental EBA

Heat-shock proteins (HSPs), or stress proteins, are highly conserved molecular chaperones, play crucial roles in folding/unfolding of proteins, protein complex assembly, sub cellular transport and also controls cell-cycle and apoptosis (204). Several HSPs are studied in the context of inflammation and autoimmunity such as

autoimmune arthritis, type 1 diabetes mellitus, atherosclerosis, multiple sclerosis, and other autoimmune reactions (205). Based on these considerations, Dr. Kasperkiewicz from our laboratory challenged the hypothesis that inhibition of heat-shock protein 90 (Hsp90) induces cell death of auto-reactive plasma cells. In these experiments, mice were treated with HSP90 inhibitors before induction of immunization-induced EBA. Additionally, in a therapeutic setting, mice with already clinically manifest immunization-induced EBA were injected with 2 different HSP90 inhibitors. Both HSP90 inhibitors prevented the onset of immunization-induced EBA. In the therapeutic experimental setting, blockade of HSP90 also ameliorated clinical disease along with suppression of autoantibody production and a reduction of the leukocyte infiltration in the skin. Unexpectedly, B cell function was not affected after HSP90 blockade. However, T-cell proliferation was significantly inhibited, as shown by a reduced response of isolated lymph node cells from immunized mice to in vitro restimulation with anti-CD3/CD28 antibody or autoantigen in presence of HSP90 inhibitors (169).

7.5.2.4. The production of anti-COL7 IgG is restricted to peripheral lymph nodes in experimental EBA

In immunization-induced EBA, antigen-specific T cells can be detected in almost all secondary lymphoid organs. Of note, antigen-specific B cells can however only be detected in the peripheral lymph nodes proximal to the sites of immunization; i.e. popliteal and inguinal lymph nodes (169). Hence, anti-COL7 IgG are exclusively produced at this anatomical location. In human EBA patients, the location of auto-reactive B cells is largely unknown. In other AIBD, such as pemphigus vulgaris, antigen-specific B cells can be isolated from blood (206). In EBA patients, COL7 specific T cells have been found and IgG reactivity is associated with T cell recognition of identical sub-domains of COL7 (207). Therefore, it is tempting to speculate, that anti-COL7 producing B cells are also found in the circulation of EBA patients.

7.5.2.5. Production of disease-inducing anti-COL7 IgG is linked with a Th1 polarization in peripheral lymph nodes in experimental EBA

As outlined above, most mouse strains develop circulating and tissue-bound anti-COL7 antibodies after immunization with COL7. However, only few strains develop a clinical manifestation of a subepidermal blistering skin disease. Comparison of the autoantibody response in clinically healthy versus diseased mice after COL7 immunization showed that IgG2 antibodies are associated with clinical EBA manifestation, indicative of a Th1 polarization of the induced immune response. The detected increased IFN-γ / IL-4 ratio in the draining lymph nodes of EBA-susceptible mice also reflects this Th1-polarization of the immune response in mice with clinically manifestations of immunization-induced EBA (30, 208).

7.5.3. The neonatal Fc receptor controls the half-life of anti-COL7 autoantibodies

After the autoantibodies are produced and released into the circulation, their half-life is controlled by the neonatal Fc receptor (FcRn). The FcRn is a MHC class I like molecule that, among other functions, protects IgG from catabolism (209). FcRn-IgG interaction also modulates antigen presentation and cross-presentation in immune cells (209, 210). Hence, one would expect that blockade of the FcRn protects from EBA induction. Indeed, in animal models of AIBD, including pemphigus, bullous pemphigoid and EBA, mice are completely blocked from disease induction, although this protection can be overcome by injection of high amounts of anti-COL7 (211, 212).

7.6. Autoantibody-induced tissue injury in EBA

7.6.1. Anti-COL7 antibodies rapidly bind to their target antigen

Detailed morphological studies on anti-COL7 IgG deposition after injection into mice by direct immunofluorescence (IF) microscopy showed linear antibody deposits along the dermal-epidermal junction within 24 hours (158). To obtain more insights into the dynamics of anti-COL7 IgG deposition in the skin, these autoantibodies were fluorescently labeled. These labelled-anti-COL7 autoantibodies retained their pathogenic ability, i.e., after transfer into mice DyLight488-anti-COL7 IgG induced cutaneous blistering. Next, labeled anti-COL7 IgG were injected (i.v.) into mice and their binding to the skin was observed by multi-photon in vivo microscopy. After injection, anti-COL7 IgG bound to the dermal-epidermal junction within minutes. Interestingly, an inhomogeneous binding pattern was observed, i.e. tissue-bound IgG was observed at some, but not all parts of the skin (*Hiroaki Iwata, personal communication*). Other work found that in addition to the skin, COL7 expression is confined to the basement membranes beneath other stratified squamous epithelium; for example esophagus, and buccal, anal, and vaginal mucosa, but not in colonic mucosa (213). In mice, COL7 mRNA and protein can be detected in the skin and in all organs of the gastrointestinal tract. Of note, COL7 expression decreases from proximal to distal parts of the gastrointestinal tract (15).

7.6.2. F (ab) - and Fc-mediated effects on blister formation

As detailed above (chapter 7.5), IgG antibodies from EBA patients bind to numerous epitopes located with the NC1 domain of COL7. In other AIBD, F(ab)-mediated effects on blister formation have been described. For example in pemphigus, F(ab) mediated effects alone induce blister formation (214) In addition, in bullous pemphigoid a weakening of cell attachment after binding of anti-BP180 antibodies to keratinocytes

has been described (215). In contrast, no data on F(ab) mediated effects of anti-COL7 antibodies on keratinocyte adhesiveness has been reported, and several lines of evidence suggest that the Fc-portion of anti-COL7 antibodies is a key molecular prerequisite to lead to blister formation (23). The importance of the Fc fragment in modulating blister formation in EBA is further highlighted by the finding that not all isotype-classes of anti-COL7 have the potential to induce dermal-epidermal separation. Specifically, only IgG1 and IgG3, but not IgG2 and IgG4, induced ex vivo blister formation (163). Absence of skin lesions in mice injected with chicken anti-mouse COL7 IgY, which does not bind murine complement and Fc receptors, further underlines the importance of Fc – Fc receptor interactions for blister formation in experimental EBA (216).

7.6.3. Immuno-modulatory role of GM-CSF in the pathogenesis of EBA

There is ample evidence for an increased expression of several cytokines in AIBD. Despite these findings, and in contrast to other chronic inflammatory diseases (50, 53, 55, 217) a cytokine-targeting therapy has not been established in EBA or any other AIBD – with the exception of the relatively well documented beneficial effects of TNF-α inhibition in mucous membrane pemphigoid (218). In experimental EBA, induced by transfer of anti-COL7 IgG into C57Bl/6 or BALB/c mice, increased serum concentrations of several cytokines were noted (70). The contribution of CXCR1 and CXCR2 ligands, such as CXCL1 and CXCL2 has also been addressed in animal models of EBA. Both, CXCL1 and CXCL2 cutaneous expression in increased after induction of experimental EBA in mice (219). The current study provides strong evidence for pro-inflammatory functions of GM-CSF in an experimental model of a prototypic organ-specific autoantibody-mediated disease. Both genetic and pharmacological blockade of GM-CSF led to significant decrease in clinical disease severity in two different models of EBA. Interestingly, blockade of GM-CSF not only

impaired neutrophil functions, but also significantly contributed to autoantibody production. More specifically, induction of experimental EBA led to increased levels of GM-CSF, both locally (skin) and systemically (serum). These increased GM-CSF levels are of functional relevance, as in GM-CSF$^{-/-}$ mice induction of skin blistering by antibody transfer is significantly impaired. Furthermore, in already established EBA, blockade of GM-CSF significantly attenuated clinical disease progression. Our findings are in line with observations in experimental models of arthritis (67, 68, 220); yet in contrast to data obtained in murine models of contact hypersensitivity, where GM-CSF deficiency alone has no effect on disease manifestation (221), despite increased GM-CSF expression (222). These observations underscore the importance of validating morphologic findings or expression data in appropriate experimental systems to fully understand their contribution to disease pathogenesis.

For the effector phase of experimental EBA, i.e. autoantibody-induced tissue injury, neutrophil depletion has been shown to protect mice from induction of skin blisters(20). In line, CD18-deficient mice with impaired leukocyte extravasation into the skin (223) are also completely resistant to blister induction. In addition, impaired release of reactive oxygen species or proteolytic enzymes from neutrophils has similar protective effects (20, 24). In this context, our findings provide novel insights into EBA pathogenesis: GM-CSF contributes to EBA-associated tissue injury by modulating several neutrophil functions: (**i**) GM-CSF is required to induce the autoantibody-induced neutrophilia. It is tempting to speculate that the increase in circulating neutrophils allows a higher number of neutrophils to migrate into the skin. In general, both G- and GM-CSF are capable to recruit neutrophils from the bone marrow into the blood(224, 225). Interestingly, in experimental EBA, this recruitment is only mediated by GM-CSF, as neutrophil numbers remained completely unaltered in GM-CSF$^{-/-}$ mice after EBA induction. (**ii**) GM-CSF is required for neutrophil extravasation from the blood

into the skin, as after EBA induction, the dermal leukocyte infiltrate was significantly reduced in GM-CSF$^{-/-}$ compared to C57Bl/6 mice. Based on the observation of a significant increase in dermal leukocyte infiltration in GM-CSF$^{-/-}$ mice, neutrophil extravasation into the skin, in contrast to recruitment into the blood, is not solely mediated by GM-CSF. Furthermore, given that GM-CSF deficiency led to impaired blistering, the effect of GM-CSF on neutrophil recruitment into the skin may be indirect, rather than a direct enhancement of neutrophil migration(226). More specifically, we hypothesize that GM-CSF activates neutrophils in the skin, resulting in the release of pro-inflammatory mediators by neutrophils, which lead to continued and increased neutrophil migration into the skin (227). Immune complex-mediated activation of neutrophils is also enhanced by GM-CSF, like described for many, but not all known neutrophil agonists (80). This enhancement of IC-induced neutrophil activation contributes to reactive oxygen release by neutrophils, which is required for autoantibody-induced tissue injury in different models of EBA. In addition, GM-CSF may also enhance other effector functions of neutrophils, such as release of pro-inflammatory mediators or proteolytic enzymes.

These findings confirm and extend previous reports on GM-CSF inhibition in the effector phase of arthritis. However, in these models, GM-CSF inhibition had no effect on autoantibody production (67, 68). In contrast, in the context of infection, GM-CSF (together with IL-4) was shown to stimulate an antibody response to avian influenza in immunodeficient mice engrafted with human hematopoietic stem cells by promoting T, B, and dendritic cell maturation(167). Furthermore, neutrophils, which are among the main target cells of GM-CSF (76), have profound effects on B cell functions. More specifically, neutrophils induced immunoglobulin class switching, somatic hyper mutation and antibody production by activating B cells through mechanisms involving BAFF, APRIL and IL-21(168). However, the precise mechanism through which

neutrophils modulate the antibody response is unclear. I here present a reduced autoantibody response in GM-CSF$^{-/-}$ mice in immunization-induced EBA, which is associated with lower, but not completely absent, neutrophil numbers and unchanged number of COL7-specific B cells in draining lymph nodes compared to C57Bl/6 mice. Based on these findings, I hypothesize that GM-CSF is an important, but not the only driving factor leading to neutrophil recruitment into draining lymph nodes after immunization. In addition to GM-CSF, prostaglandins have been demonstrated to recruit neutrophils into lymph nodes after immunization with protein antigens emulsified in adjuvants (89). However, neutrophils recruited by prostaglandins into lymph nodes inhibited CD4 T cell functions (89). Therefore, the contribution of innate immune cells, such as neutrophils seem to have a differential contribution on adaptive immune functions; most likely in the context of location and timing.

7.6.4. Anti-inflammatory role of IL-6 in EBA

The data presented here provides strong evidence for anti-inflammatory functions of IL-6 in an experimental model of a prototypic organ-specific autoantibody-mediated disease. In contrast to GM-CSF blockade, both genetic and pharmacological blockade of IL-6 led to significant increase in disease severity after injection of anti-COL7 IgG compared to untreated EBA mice. As the specific IL-6 trans-signaling inhibitor sgp130Fc had no effect on EBA manifestation, these effects are attributed to *classical IL-6 signaling* rather than to *trans-signaling*. Administration of recombinant IL-6 almost completely protected mice from disease. Cells responsive to classic signaling include hepatocytes, monocytes, macrophages and some leukocyte populations. Since blockade of IL-6 trans-signaling by sgp130Fc did not change the severity of EBA and administration of recombinant IL-6 improved the disease, it can be concluded that the cells responsible for the IL-6 effect express a membrane-bound IL-6R. At the molecular level, IL-6 reduced the pro-inflammatory effects of IL-1 *(personal communication,*

Hengameh Sadeghi) by inducing IL-1Ra. In line, administration of IL-1Ra reduced clinical EBA severity (70). Yet, extent of reduction accompanied with the use of IL-1Ra was lower compared to treatment with IL-6. This may be due to different pharmacokinetics of the two compounds and/or due to additional effects of IL-6. The later assumption is supported by our demonstration, that IL-6 also affected the expression of Timp-1 and the apoptosis of basal keratinocytes.

This anti-inflammatory activity of IL-6 in experimental EBA is in sharp contrast to the clear pro-inflammatory effects of IL-6 in other chronic inflammatory diseases such as rheumatoid arthritis, where IL-6 deficiency protects from both the induction and effector phase (65, 66), and treatment with the anti-IL-6R antibody tocilizumab is effective in patients (64). Like in experimental models of rheumatoid arthritis (228, 229), we observed an increased IL-6 serum and skin expression in experimental EBA. Furthermore, again paralleling the findings in rheumatoid arthritis patients (230), increased IL-6 expression was noted in EBA patients. Yet, while inhibition of IL-6 in animal models of arthritis as well as in patients has profound inhibitory effects (231). Among the pro-inflammatory cytokine milieu developed after EBA induction, IL-1 contributes significantly to the autoantibody-induced tissue injury, as inhibition of IL-1 function hinders EBA induction *(personal communication, Hengameh Sadeghi)*. In the present study, demonstrated that these pro-inflammatory events mediated by IL-1 are counter-balanced by IL-6 through induction of IL-1Ra (70). This activity of IL-6 also leads to significant changes in levels of TGF-β and IL-10 where anti-IL6 treatment significantly reduced levels of both cytokines. Treatment of mice with recombinant IL-6 restored levels of TGF-β and IL-10 to those in isotype antibody injected animals. Both anti-IL-6 treatment and recombinant IL-6 treatment had no effect on serum IL-4 and sTNF-R1, which remained constant in all our experimental groups. In EBA, this activity of IL-6 attributed to counteract the so far unrecognized apoptosis of basal

keratinocytes in the skin. Although, Bcl-2 expression is indeed controlled by IL-6, regulation of other anti-inflammatory and anti-apoptotic pathways (both IL-1Ra and Timp-1 expression) may be more important, given the pro-inflammatory activity of IL-1 *(personal communication, Hengameh Sadeghi)* in EBA manifestation. Anakinra, recombinant IL-1Ra treatment of mice (as part of the thesis of Ms. Sadeghi) provide further in-vivo evidence for in vitro and in vivo evidence obtained within my thesis. Furthermore, the inclusion of this data here adds to the overall understanding of the effects of IL-6 in EBA (70). One may speculate that *neutrophil derived enzymes* are inhibited by the observed IL-6-induced up-regulation of Timp-1. Anti-apoptotic effects of IL-6 have been well characterized and are mediated by STAT3 signaling. This effect of IL-6 has evolved as a possible target to treat cancer (232, 233). In colitis-associated cancer, the IL-6-STAT3-mediated cascade is required for survival of intestinal epithelial cells (233). The different pathogenic events in diseases in which IL-6 has been shown to have either anti- or pro-inflammatory activities, may explain the opposing effects of IL-6 treatment. In EBA IL-6 acts anti-inflammatory, as IL-6 counteracts crucial pathogenic events in the disease's pathogenesis. In contrast, in rheumatoid arthritis the pro-inflammatory activities of IL-6 play a more predominant role than the anti-inflammatory properties of this cytokine. Therefore, inhibition of IL-6 function rheumatoid arthritis does have therapeutic effects.

7.6.5. Generation of pro-inflammatory milieu in EBA

In the current study, I here employed preclinical murine models of epidermolysis bullosa acquisita (EBA), to systematically analyze the contribution of GM-CSF and IL-6 in the pathogenesis of EBA using both patient material and experimental in vivo models. In EBA, binding of autoantibodies to COL7, located at the dermal-epidermal junction, leads to formation of a pro-inflammatory milieu including expression and up-regulation of different cytokines including GM-CSF and IL-6 as shown in this thesis.

This pro-inflammatory cytokine milieu activates complement through alternative pathway leading to deposition of C3 at the DEJ (19). This leads to the CD18-dependent recruitment of neutrophils into the skin (20). After Fc gamma receptor-dependent binding to the immune complexes, neutrophils and other immune effector cells are activated (200, 234). These effector cells release reactive oxygen species and proteolytic enzymes leading to blister formation (20, 24).

8. Conclusion

In the present study, cytokine response in EBA patients and experimental models has been characterized. From 23 different cytokines analyzed, 10 correlated with disease activity in experimental EBA. From these, GM-CSF and IL-6 were selected for further evaluation. The data provided here also demonstrates that EBA induction prompts anti-inflammatory events. Modulation of these pathways, by **(i)** recruitment and activation of neutrophils and modulating autoantibody production by GM-CSF and **(ii)** IL-6 mediated classical signaling, able to regulate EBA disease activity. While established to be a pathogenic event in pemphigus diseases (235), induction of apoptosis by autoantibodies had also been described for EBA.

In EBA, blister formation is known to be initiated by the binding of autoantibodies to COL7 located at the dermal-epidermal junction (DEJ) (16). The formation of these immune-complexes induces an inflammatory cascade, which is required for clinical disease manifestation. GM-CSF not only inhibits innate, but also adaptive immune functions. A similar inhibitory effect on autoantibody production was also observed in neutrophil-depleted mice. Combining GM-CSF inhibition and neutrophil depletion showed additive effects. Our findings extend the potential therapeutic spectrum of GM-CSF inhibition to autoantibody-mediated diseases.

Based on the clearly demonstrated anti-inflammatory role of IL-6 in experimental EBA, adds to our understanding of IL-6 biology and shows its complex contribution to the pathogenesis of autoantibody-mediated tissue injury. In contrast to rheumatoid arthritis, inhibition of IL-6 using tocilizumab should not be considered in patients with treatment-refractory and relapsing EBA or with other subepidermal AIBD associated

with increased IL-6 levels. However, due to the potent pro-inflammatory and tumorogenic activities of IL-6 (236), treatment of patients with IL-6 is not a promising therapeutic approach. On the other hand, the recapitulation of the anti-inflammatory properties of IL-6, e.g. induction of IL-1Ra release from basal keratinocytes, or administration of anakinra may be potential therapeutic options.

9. Perspectives

Given the immuno-modulatory role of GM-CSF and IL-6 in the pathogenesis of EBA, the contribution of other cytokines in the pathogenic milieu is also prime importance in understanding the sequence of events leading to blister formation. It is also worthwhile to execute interaction studies of different cytokines in experimental models, which could provide thorough understanding of the complex biology of cytokines. Moreover, contribution of other immune cells, such as dendritic cells and (or) keratinocytes or tissue macrophages at the site of autoantibody binding in the skin could be evaluated as these cells might influence and presumably could play significant role in the formation of local inflammatory response, which leads to cellular influx and inflammatory loop leading to tissue injury.

10. References

1. Hiroshi Shimizu. *Shimizu's Textbook of Dermatology [Internet]*

2. Christiano AM, Uitto J. Molecular complexity of the cutaneous basement membrane zone. Revelations from the paradigms of epidermolysis bullosa. *Exp Dermatol*. 1996;5(1):1–11.

3. Carroll DL, Stephan MJ, Hays GL. Epidermolysis bullosa--review and report of case. *J Am Dent Assoc*. 1983;107(5):749–751.

4. Mackay IR. Travels and travails of autoimmunity: A historical journey from discovery to rediscovery. *Autoimmunity Reviews*. 2010;9(5):A251–A258.

5. Smadel JE. EXPERIMENTAL NEPHRITIS IN RATS INDUCED BY INJECTION OF ANTI-KIDNEY SERUM : I. PREPARATION AND IMMUNOLOGICAL STUDIES OF NEPHROTOXIN. *J Exp Med*. 1936;64(6):921–942.

6. K. Landsteiner. The Specificity of Serological Reactions 2nd ed 1945

7. R.B. Gallagher, J. Gilder, G.J.V. Nossal, G. Salvatore. Roots of and routes to autoimmunity. In: *Immu,nology: The Making of a Modern Science*. Academic Press, London and San Diego; 1995:49–62

8. WITEBSKY E, ROSE NR, TERPLAN K, PAINE JR, EGAN RW. Chronic thyroiditis and autoimmunization. *J Am Med Assoc*. 1957;164(13):1439–1447.

9. W. Dameshek, E. Witebsky, F. Milgrom. *Autoimmunity: experimental and clinical aspects*. Ann NY Acad Sci; 1965:

10. Schmidt E, Zillikens D. Modern diagnosis of autoimmune blistering skin diseases. *Autoimmun Rev*. 2010;10(2):84–89.

11. Schmidt E, Zillikens D. Pemphigoid diseases. *Lancet*. 2013;381(9863):320–332.

12. LEVER WF. Pemphigus. *Medicine (Baltimore)*. 1953;32(1):1–123.

13. Elliot, G.T. Two cases of epidermolysis bullosa. *J Cutan genitourin Dis*. 1895;(13:10).

14. Roenigk HH, Ryan JG, Bergfeld WF. Epidermolysis bullosa acquisita. Report of three cases and review of all published cases. *Arch Dermatol*. 1971;103(1):1–10.

15. Ishii N et al. Epidermolysis bullosa acquisita: what's new? *J Dermatol*. 2010;37(3):220–30.

16. Ludwig RJ, Zillikens D. Pathogenesis of epidermolysis bullosa acquisita. *Dermatol Clin*. 2011;29(3):493–501, xi.

17. Sitaru C, Zillikens D. Mechanisms of blister induction by autoantibodies. *Exp Dermatol*. 2005;14(12):861–875.

18. Woodley DT et al. Identification of the skin basement-membrane autoantigen in epidermolysis bullosa acquisita. *N Engl J Med*. 1984;310(16):1007–13.

19. Mihai S et al. The alternative pathway of complement activation is critical for blister induction in experimental epidermolysis bullosa acquisita. *J Immunol*. 2007;178(10):6514–21.

20. Chiriac MT et al. NADPH oxidase is required for neutrophil-dependent autoantibody-induced tissue damage. *J Pathol*. 2007;212(1):56–65.

21. Kasperkiewicz M et al. Genetic identification and functional validation of FcγRIV as key molecule in autoantibody-induced tissue injury. *J Pathol*. 2012;228(1):8–19.

22. Yu X et al. FcγRIIA and FcγRIIIB are required for autoantibody-induced tissue damage in experimental human models of bullous pemphigoid. *J Invest Dermatol*. 2010;130(12):2841–2844.

23. Sitaru C, Kromminga A, Hashimoto T, Bröcker EB, Zillikens D. Autoantibodies to type VII collagen mediate Fcgamma-dependent neutrophil activation and induce dermal-epidermal separation in cryosections of human skin. *Am J Pathol*. 2002;161(1):301–11.

24. Shimanovich I et al. Granulocyte-derived elastase and gelatinase B are required for dermal-epidermal separation induced by autoantibodies from patients with epidermolysis bullosa acquisita and bullous pemphigoid. *J Pathol*. 2004;204(5):519–27.

25. Komorowski L et al. Sensitive and specific assays for routine serological diagnosis of epidermolysis bullosa acquisita. *J Am Acad Dermatol*. 2013;68(3):e89–95.

26. Shigemoto T, Nashiro K, Tsuchida T, Seki Y, Tamaki K. Administration of IgG fraction of epidermolysis bullosa acquisita (EBA) serum into mice. *J Dermatol*. 1988;15(2):123–7.

27. Borradori L et al. Passive transfer of autoantibodies from a patient with mutilating epidermolysis bullosa acquisita induces specific alterations in the skin of neonatal mice. *Arch Dermatol*. 1995;131(5):590–5.

28. Bieber K et al. Animal models for autoimmune bullous dermatoses. *Exp Dermatol*. 2010;19(1):2–11.

29. Sitaru C et al. Induction of dermal-epidermal separation in mice by passive transfer of antibodies specific to type VII collagen. *J Clin Invest*. 2005;115(4):870–8.

30. Sitaru C et al. Induction of complement-fixing autoantibodies against type VII collagen results in subepidermal blistering in mice. *J Immunol*. 2006;177(5):3461–8.

31. Woodley DT et al. Induction of epidermolysis bullosa acquisita in mice by passive transfer of autoantibodies from patients. *J Invest Dermatol*. 2006;126(6):1323–30.

32. Woodley DT et al. Evidence that anti-type VII collagen antibodies are pathogenic and responsible for the clinical, histological, and immunological features of epidermolysis bullosa acquisita. *J Invest Dermatol*. 2005;124(5):958–64.

33. Chen M et al. The cartilage matrix protein subdomain of type VII collagen is pathogenic for epidermolysis bullosa acquisita. *Am J Pathol*. 2007;170(6):2009–18.

34. Wang X. Type IV collagen binding-site within type VII collagen is a pathogenic epitope for EBA autoantibodies. In: Journal of Investigative Dermatology; 2011:

35. Umemoto H et al. Type VII collagen deficiency causes defective tooth enamel formation due to poor differentiation of ameloblasts. *Am J Pathol*. 2012;181(5):1659–1671.

36. Vorobyev A. Human type VII collagen harbors multiple pathogenically relevant epitopes. In: Journal of Investigative Dermatology; 2013:S17–S55

37. Sitaru AG et al. T cells are required for the production of blister-inducing autoantibodies in experimental epidermolysis bullosa acquisita. *J Immunol*. 2010;184(3):1596–603.

38. Ludwig RJ et al. Generation of antibodies of distinct subclasses and specificity is linked to H2s in an active mouse model of epidermolysis bullosa acquisita. *J Invest Dermatol*. 2011;131(1):167–76.

39. Ludwig RJ et al. Identification of quantitative trait loci in experimental epidermolysis bullosa acquisita. *J Invest Dermatol*. 2012;132(5):1409–1415.

40. Iwata H et al. B cells, dendritic cells, and macrophages are required to induce an autoreactive CD4 helper T cell response in experimental epidermolysis bullosa acquisita. *J Immunol*. 2013;191(6):2978–2988.

41. cytokines [Internet]. *Cytokines & Cells Online Pathfinder Encyclopedia (COPE)*. 2013;http://www.copewithcytokines.org/cope.cgi?key=cytokines. Accessed on April 25, 2013

42. Gilman A, Goodman LS, Hardman JG, Limbird LE. *The pharmacological basis of therapeutics.* 2001:

43. Cannon JG. Inflammatory Cytokines in Nonpathological States. *News Physiol Sci*. 2000;15:298–303.

44. Goldszmid RS, Trinchieri G. The price of immunity. *Nat Immunol*. 2012;13(10):932–938.

45. O'Shea JJ, Ma A, Lipsky P. Cytokines and autoimmunity. *Nat Rev Immunol*. 2002;2(1):37–45.

46. Freitas do Rosario AP, Langhorne J. T cell-derived IL-10 and its impact on the regulation of host responses during malaria. *Int J Parasitol*. 2012;42(6):549–555.

47. Buckley CD, Gilroy DW, Serhan CN, Stockinger B, Tak PP. The resolution of inflammation. *Nat Rev Immunol*. 2013;13(1):59–66.

48. Lawrence T, Gilroy DW, Colville-Nash PR, Willoughby DA. Possible new role for NF-κB in the resolution of inflammation. *Nat Med*. 2001;7(12):1291–1297.

49. Brennan FM, Feldmann M. Cytokines in autoimmunity. *Current Opinion in Immunology*. 1996;8(6):872–877.

50. Elliott MJ et al. Randomised double-blind comparison of chimeric monoclonal antibody to tumour necrosis factor alpha (cA2) versus placebo in rheumatoid arthritis. *Lancet*. 1994;344(8930):1105–1110.

51. Suffredini AF et al. Effects of recombinant dimeric TNF receptor on human inflammatory responses following intravenous endotoxin administration. *J Immunol*. 1995;155(10):5038–5045.

52. Den Broeder AA et al. Long term anti-tumour necrosis factor alpha monotherapy in rheumatoid arthritis: effect on radiological course and prognostic value of markers of cartilage turnover and endothelial activation. *Ann Rheum Dis*. 2002;61(4):311–318.

53. Mease PJ et al. Etanercept in the treatment of psoriatic arthritis and psoriasis: a randomised trial. *Lancet*. 2000;356(9227):385–390.

54. Feldman M, Taylor P, Paleolog E, Brennan FM, Maini RN. Anti-TNF alpha therapy is useful in rheumatoid arthritis and Crohn's disease: analysis of the mechanism of action predicts utility in other diseases. *Transplant Proc*. 1998;30(8):4126–4127.

55. Sandborn WJ et al. Adalimumab induction therapy for Crohn disease previously treated with infliximab: a randomized trial. *Ann Intern Med*. 2007;146(12):829–838.

56. Bresnihan B et al. Treatment of rheumatoid arthritis with recombinant human interleukin-1 receptor antagonist. *Arthritis Rheum*. 1998;41(12):2196–2204.

57. Campion GV, Lebsack ME, Lookabaugh J, Gordon G, Catalano M. Dose-range and dose-frequency study of recombinant human interleukin-1 receptor antagonist in patients with rheumatoid arthritis. The IL-1Ra Arthritis Study Group. *Arthritis Rheum*. 1996;39(7):1092–1101.

58. *Anakinra - http://www.clinicaltrials.gov/ct2/results?term=anakinra&recr=Open*. 2013. Accessed on April 23, 2013:

59. Jones SA, Richards PJ, Scheller J, Rose-John S. IL-6 transsignaling: the in vivo consequences. *J Interferon Cytokine Res*. 2005;25(5):241–253.

60. Feliciani C et al. In vitro and in vivo expression of interleukin-1alpha and tumor necrosis factor-alpha mRNA in pemphigus vulgaris: interleukin-1alpha and tumor necrosis factor-alpha are involved in acantholysis. *J Invest Dermatol*. 2000;114(1):71–77.

61. Langan SM et al. Bullous pemphigoid and pemphigus vulgaris--incidence and mortality in the UK: population based cohort study. *BMJ*. 2008;337:a180.

62. Joly P et al. A comparison of oral and topical corticosteroids in patients with bullous pemphigoid. *N Engl J Med*. 2002;346(5):321–327.

63. Joly P et al. A comparison of two regimens of topical corticosteroids in the treatment of patients with bullous pemphigoid: a multicenter randomized study. *J Invest Dermatol*. 2009;129(7):1681–1687.

64. Maini RN et al. Double-blind randomized controlled clinical trial of the interleukin-6 receptor antagonist, tocilizumab, in European patients with rheumatoid arthritis who had an incomplete response to methotrexate. *Arthritis Rheum*. 2006;54(9):2817–2829.

65. Ohshima S et al. Interleukin 6 plays a key role in the development of antigen-induced arthritis. *Proc Natl Acad Sci USA*. 1998;95(14):8222–8226.

66. Sasai M et al. Delayed onset and reduced severity of collagen-induced arthritis in interleukin-6-deficient mice. *Arthritis Rheum*. 1999;42(8):1635–1643.

67. Campbell IK et al. Protection from collagen-induced arthritis in granulocyte-macrophage colony-stimulating factor-deficient mice. *J Immunol*. 1998;161(7):3639–3644.

68. Cook AD, Braine EL, Campbell IK, Rich MJ, Hamilton JA. Blockade of collagen-induced arthritis post-onset by antibody to granulocyte-macrophage colony-stimulating factor (GM-CSF): requirement for GM-CSF in the effector phase of disease. *Arthritis Res*. 2001;3(5):293–298.

69. MorphoSys AG. *A Study of the Safety and Preliminary Efficacy of MOR103, a Human Antibody to Granulocyte Macrophage Colony-stimulating Factor (GM-CSF), in Patients With Active Rheumatoid Arthritis [Internet].*Accessed on April 24, 2013.

70. Samavedam UKSRL et al. Recombinant IL-6 treatment protects mice from organ specific autoimmune disease by IL-6 classical signalling-dependent IL-1Ra induction. *J Autoimmun*. [published online ahead of print: September 11, 2012]; doi:10.1016/j.jaut.2012.08.002

71. Hamilton JA, Stanley ER, Burgess AW, Shadduck RK. Stimulation of macrophage plasminogen activator activity by colony-stimulating factors. *J Cell Physiol*. 1980;103(3):435–445.

72. Burgess AW, Metcalf D. The nature and action of granulocyte-macrophage colony stimulating factors. *Blood*. 1980;56(6):947–958.

73. Handman E, Burgess AW. Stimulation by granulocyte-macrophage colony-stimulating factor of Leishmania tropica killing by macrophages. *J Immunol*. 1979;122(3):1134–1137.

74. Campbell IK, Rich MJ, Bischof RJ, Hamilton JA. The colony-stimulating factors and collagen-induced arthritis: exacerbation of disease by M-CSF and G-CSF and requirement for endogenous M-CSF. *J Leukoc Biol*. 2000;68(1):144–150.

75. Whetton AD, Dexter TM. Myeloid haemopoietic growth factors. *Biochim Biophys Acta*. 1989;989(2):111–132.

76. Griffin JD et al. The biology of GM-CSF: regulation of production and interaction with its receptor. *Int J Cell Cloning*. 1990;8 Suppl 1:35–44; discussion 44–45.

77. Metcalf D. Hematopoietic regulators: redundancy or subtlety? *Blood*. 1993;82(12):3515–3523.

78. Mantovani A, Sozzani S, Locati M, Allavena P, Sica A. Macrophage polarization: tumor-associated macrophages as a paradigm for polarized M2 mononuclear phagocytes. *Trends Immunol*. 2002;23(11):549–555.

79. Fuhler GM, Blom NR, Coffer PJ, Drayer AL, Vellenga E. The reduced GM-CSF priming of ROS production in granulocytes from patients with myelodysplasia is associated with an impaired lipid raft formation. *J Leukoc Biol*. 2007;81(2):449–457.

80. Weisbart RH, Kwan L, Golde DW, Gasson JC. Human GM-CSF primes neutrophils for enhanced oxidative metabolism in response to the major physiological chemoattractants. *Blood*. 1987;69(1):18–21.

81. Stanley E et al. Granulocyte/macrophage colony-stimulating factor-deficient mice show no major perturbation of hematopoiesis but develop a characteristic pulmonary pathology. *Proc Natl Acad Sci USA*. 1994;91(12):5592–5596.

82. Bezbradica JS et al. Granulocyte-macrophage colony-stimulating factor regulates effector differentiation of invariant natural killer T cells during thymic ontogeny. *Immunity*. 2006;25(3):487–497.

83. Menetrier-Caux C et al. Inhibition of the differentiation of dendritic cells from CD34(+) progenitors by tumor cells: role of interleukin-6 and macrophage colony-stimulating factor. *Blood*. 1998;92(12):4778–4791.

84. Willman CL, Stewart CC, Miller V, Yi TL, Tomasi TB. Regulation of MHC class II gene expression in macrophages by hematopoietic colony-stimulating factors (CSF). Induction by granulocyte/macrophage CSF and inhibition by CSF-1. *J Exp Med*. 1989;170(5):1559–1567.

85. Phillips WA, Hamilton JA. Colony stimulating factor-1 is a negative regulator of the macrophage respiratory burst. *J Cell Physiol*. 1990;144(2):190–196.

86. Hamilton JA. Rheumatoid arthritis: opposing actions of haemopoietic growth factors and slow-acting anti-rheumatic drugs. *Lancet*. 1993;342(8870):536–539.

87. Hamilton JA et al. Cytokine regulation of colony-stimulating factor (CSF) production in cultured human synovial fibroblasts. II. Similarities and differences in the control of interleukin-1 induction of granulocyte-macrophage CSF and granulocyte-CSF production. *Blood*. 1992;79(6):1413–1419.

88. Hamilton JA, Campbell IK, Wojta J, Cheung D. Plasminogen activators and their inhibitors in arthritic disease. *Ann N Y Acad Sci*. 1992;667:87–100.

89. Yang YH, Hamilton JA. Dependence of interleukin-1-induced arthritis on granulocyte-macrophage colony-stimulating factor. *Arthritis Rheum*. 2001;44(1):111–119.

90. Marusic S et al. Local delivery of granulocyte macrophage colony-stimulating factor by retrovirally transduced antigen-specific T cells leads to severe, chronic experimental autoimmune encephalomyelitis in mice. *Neurosci Lett*. 2002;332(3):185–189.

91. McQualter JL et al. Granulocyte macrophage colony-stimulating factor: a new putative therapeutic target in multiple sclerosis. *J Exp Med*. 2001;194(7):873–882.

92. Kitching AR et al. The requirement for granulocyte-macrophage colony-stimulating factor and granulocyte colony-stimulating factor in leukocyte-mediated immune glomerular injury. *J Am Soc Nephrol*. 2002;13(2):350–358.

93. Timoshanko JR, Kitching AR, Semple TJ, Holdsworth SR, Tipping PG. Granulocyte macrophage colony-stimulating factor expression by both renal parenchymal and immune cells mediates murine crescentic glomerulonephritis. *J Am Soc Nephrol*. 2005;16(9):2646–2656.

94. Keller M et al. T cell-regulated neutrophilic inflammation in autoinflammatory diseases. *J Immunol*. 2005;175(11):7678–7686.

95. Antman KS et al. Effect of recombinant human granulocyte-macrophage colony-stimulating factor on chemotherapy-induced myelosuppression. *N Engl J Med*. 1988;319(10):593–598.

96. Korzenik JR, Dieckgraefe BK, Valentine JF, Hausman DF, Gilbert MJ. Sargramostim for active Crohn's disease. *N Engl J Med*. 2005;352(21):2193–2201.

97. Sainathan SK et al. Granulocyte macrophage colony-stimulating factor ameliorates DSS-induced experimental colitis. *Inflamm Bowel Dis*. 2008;14(1):88–99.

98. Hirano T et al. Complementary DNA for a novel human interleukin (BSF-2) that induces B lymphocytes to produce immunoglobulin. *Nature*. 1986;324(6092):73–76.

99. Geiger T et al. Induction of rat acute-phase proteins by interleukin 6 in vivo. *Eur J Immunol*. 1988;18(5):717–721.

100. Harris TB et al. Associations of elevated Interleukin-6 and C-Reactive protein levels with mortality in the elderly. *The American Journal of Medicine*. 1999;106(5):506–512.

101. Lipsky PE. Interleukin-6 and rheumatic diseases. *Arthritis Res Ther*. 2006;8 Suppl 2:S4.

102. Teague TK, Marrack P, Kappler JW, Vella AT. IL-6 rescues resting mouse T cells from apoptosis. *J Immunol*. 1997;158(12):5791–5796.

103. Yoshida H, Hashizume M, Suzuki M, Mihara M. Anti-IL-6 receptor antibody suppressed T cell activation by inhibiting IL-2 production and inducing regulatory T cells. *Eur J Pharmacol*. 2010;634(1-3):178–183.

104. Senn JJ, Klover PJ, Nowak IA, Mooney RA. Interleukin-6 Induces Cellular Insulin Resistance in Hepatocytes. *Diabetes*. 2002;51(12):3391 –3399.

105. Nemeth E et al. IL-6 mediates hypoferremia of inflammation by inducing the synthesis of the iron regulatory hormone hepcidin. *J Clin Invest*. 2004;113(9):1271–1276.

106. Taga T, Kishimoto T. Gp130 and the interleukin-6 family of cytokines. *Annu Rev Immunol*. 1997;15:797–819.

107. Scheller J, Rose-John S. Interleukin-6 and its receptor: from bench to bedside. *Med Microbiol Immunol*. 2006;195(4):173–183.

108. Rose-John S, Waetzig GH, Scheller J, Grötzinger J, Seegert D. The IL-6/sIL-6R complex as a novel target for therapeutic approaches. *Expert Opin Ther Targets*. 2007;11(5):613–624.

109. Honda M et al. Human soluble IL-6 receptor: its detection and enhanced release by HIV infection. *J Immunol*. 1992;148(7):2175–2180.

110. Rose-John S, Neurath MF. IL-6 trans-signaling: the heat is on. *Immunity*. 2004;20(1):2–4.

111. Schirmacher P et al. Hepatocellular hyperplasia, plasmacytoma formation, and extramedullary hematopoiesis in interleukin (IL)-6/soluble IL-6 receptor double-transgenic mice. *Am J Pathol*. 1998;153(2):639–648.

112. Scheller J, Chalaris A, Schmidt-Arras D, Rose-John S. The pro- and anti-inflammatory properties of the cytokine interleukin-6. *Biochim Biophys Acta*. 2011;1813(5):878–888.

113. Narazaki M et al. Soluble forms of the interleukin-6 signal-transducing receptor component gp130 in human serum possessing a potential to inhibit signals through membrane-anchored gp130. *Blood*. 1993;82(4):1120–1126.

114. Jostock T et al. Soluble gp130 is the natural inhibitor of soluble interleukin-6 receptor transsignaling responses. *Eur J Biochem*. 2001;268(1):160–167.

115. Nowell MA et al. Therapeutic targeting of IL-6 trans signaling counteracts STAT3 control of experimental inflammatory arthritis. *J Immunol*. 2009;182(1):613–622.

116. Mees ST et al. Inhibition of interleukin-6-transsignaling via gp130-Fc in hemorrhagic shock and sepsis. *J Surg Res*. 2009;157(2):235–242.

117. Houssiau FA, Devogelaer JP, Van Damme J, de Deuxchaisnes CN, Van Snick J. Interleukin-6 in synovial fluid and serum of patients with rheumatoid arthritis and other inflammatory arthritides. *Arthritis Rheum*. 1988;31(6):784–788.

118. Mahida YR, Kurlac L, Gallagher A, Hawkey CJ. High circulating concentrations of interleukin-6 in active Crohn's disease but not ulcerative colitis. *Gut*. 1991;32(12):1531–1534.

119. Yokoyama A et al. Circulating interleukin-6 levels in patients with bronchial asthma. *Am J Respir Crit Care Med*. 1995;151(5):1354–1358.

120. Grossman RM et al. Interleukin 6 is expressed in high levels in psoriatic skin and stimulates proliferation of cultured human keratinocytes. *Proc Natl Acad Sci USA*. 1989;86(16):6367–6371.

121. Eriksson U et al. Interleukin-6-deficient mice resist development of autoimmune myocarditis associated with impaired upregulation of complement C3. *Circulation*. 2003;107(2):320–325.

122. Alonzi T et al. Interleukin 6 is required for the development of collagen-induced arthritis. *J Exp Med*. 1998;187(4):461–468.

123. Samoilova EB, Horton JL, Hilliard B, Liu TS, Chen Y. IL-6-deficient mice are resistant to experimental autoimmune encephalomyelitis: roles of IL-6 in the activation and differentiation of autoreactive T cells. *J Immunol*. 1998;161(12):6480–6486.

124. Deng C, Goluszko E, Tüzün E, Yang H, Christadoss P. Resistance to experimental autoimmune myasthenia gravis in IL-6-deficient mice is associated with reduced germinal center formation and C3 production. *J Immunol*. 2002;169(2):1077–1083.

125. Nowell MA et al. Soluble IL-6 receptor governs IL-6 activity in experimental arthritis: blockade of arthritis severity by soluble glycoprotein 130. *J Immunol*. 2003;171(6):3202–3209.

126. Waetzig GH, Rose-John S. Hitting a complex target: an update on interleukin-6 trans-signalling. *Expert Opin Ther Targets*. 2012;16(2):225–236.

127. Poffenberger MC et al. Lack of IL-6 during coxsackievirus infection heightens the early immune response resulting in increased severity of chronic autoimmune myocarditis. *PLoS ONE*. 2009;4(7):e6207.

128. Xing Z et al. IL-6 is an antiinflammatory cytokine required for controlling local or systemic acute inflammatory responses. *J Clin Invest*. 1998;101(2):311–320.

129. Kopf M et al. Impaired immune and acute-phase responses in interleukin-6-deficient mice. *Nature*. 1994;368(6469):339–342.

130. Fattori E et al. Defective inflammatory response in interleukin 6-deficient mice. *J Exp Med*. 1994;180(4):1243–1250.

131. Tilg H, Trehu E, Atkins MB, Dinarello CA, Mier JW. Interleukin-6 (IL-6) as an anti-inflammatory cytokine: induction of circulating IL-1 receptor antagonist and soluble tumor necrosis factor receptor p55. *Blood*. 1994;83(1):113–118.

132. De Benedetti F et al. Effect of IL-6 on IGF Binding Protein-3: A Study in IL-6 Transgenic Mice and in Patients with Systemic Juvenile Idiopathic Arthritis. *Endocrinology*. 2001;142(11):4818 –4826.

133. Gabay C, Smith MF, Eidlen D, Arend WP. Interleukin 1 receptor antagonist (IL-1Ra) is an acute-phase protein. *Journal of Clinical Investigation*. 1997;99(12):2930–2940.

134. Pedersen BK, Fischer CP. Beneficial health effects of exercise--the role of IL-6 as a myokine. *Trends Pharmacol Sci*. 2007;28(4):152–156.

135. Croker BA et al. IL-6 promotes acute and chronic inflammatory disease in the absence of SOCS3. *Immunol Cell Biol*. 2012;90(1):124–129.

136. Razzaque MS, Kumari S, Foster CS, Ahmed AR. Expression profiles of collagens, HSP47, TGF-beta1, MMPs and TIMPs in epidermolysis bullosa acquisita. *Cytokine*. 2003;21(5):207–13.

137. Guo S-Y et al. TIMP-1 mediates the inhibitory effect of interleukin-6 on the proliferation of a hepatocarcinoma cell line in a STAT3-dependent manner. *Braz J Med Biol Res*. 2007;40(5):621–631.

138. Silacci P et al. Interleukin (IL)-6 and Its Soluble Receptor Induce TIMP-1 Expression in Synoviocytes and Chondrocytes, and Block IL-1-induced Collagenolytic Activity. *Journal of Biological Chemistry*. 1998;273(22):13625 –13629.

139. Lotz M, Guerne PA. Interleukin-6 induces the synthesis of tissue inhibitor of metalloproteinases-1/erythroid potentiating activity (TIMP-1/EPA). *Journal of Biological Chemistry*. 1991;266(4):2017 –2020.

140. Waxman AB, Kolliputi N. IL-6 Protects against Hyperoxia-Induced Mitochondrial Damage via Bcl-2-Induced Bak Interactions with Mitofusions. *Am J Respir Cell Mol Biol*. 2009;41(4):385–396.

141. Garcia-Tuñón I et al. IL-6, its receptors and its relationship with bcl-2 and bax proteins in infiltrating and in situ human breast carcinoma. *Histopathology*. 2005;47(1):82–89.

142. Tenhumberg S et al. Structure-guided optimization of the interleukin-6 trans-signaling antagonist sgp130. *J Biol Chem*. 2008;283(40):27200–27207.

143. Kim JH, Kim YH, Kim SC. Epidermolysis bullosa acquisita: a retrospective clinical analysis of 30 cases. *Acta Derm Venereol*. 2011;91(3):307–12.

144. Jonkman MF et al. Inflammatory variant of epidermolysis bullosa acquisita with IgG autoantibodies against type VII collagen and laminin alpha3. *Arch Dermatol*. 2000;136(2):227–31.

145. C57Bl/6. JAX mice Database [Internet]. *C57BL/6J*. http://jaxmice.jax.org/strain/000664.html. Accessed on April 28, 2013

146. B6.SJL-H2s mice. JAX mice Database [Internet]http://jaxmice.jax.org/strain/000966.html. Accessed on April 28, 2013

147. B6.129S2-Il6tm1Kopf/J. JAX mice data base [Internet]http://jaxmice.jax.org/strain/002650.html. Accessed on April 28, 2013

148. Dranoff G et al. Involvement of granulocyte-macrophage colony-stimulating factor in pulmonary homeostasis. *Science*. 1994;264(5159):713–716.

149. Huffman JA, Hull WM, Dranoff G, Mulligan RC, Whitsett JA. Pulmonary epithelial cell expression of GM-CSF corrects the alveolar proteinosis in GM-CSF-deficient mice. *J Clin Invest*. 1996;97(3):649–655.

150. Reed JA et al. Aerosolized GM-CSF ameliorates pulmonary alveolar proteinosis in GM-CSF-deficient mice. *Am J Physiol*. 1999;276(4 Pt 1):L556–563.

151. Robb L et al. Hematopoietic and lung abnormalities in mice with a null mutation of the common beta subunit of the receptors for granulocyte-macrophage colony-stimulating factor and interleukins 3 and 5. *Proc Natl Acad Sci USA*. 1995;92(21):9565–9569.

152. BALB/cJ. JAX mice Database [Internet]http://jaxmice.jax.org/strain/000651.html. Accessed on April 28, 2013

153. Pearson LD, Osebold JW. Effects of antithymocyte and antimacrophage sera on the survival of mice infected with Listeria monocytogenes. *Infect Immun*. 1973;7(3):479–486.

154. Galvao-Castro B, Hochmann A, Lambert PH. The role of the host immune response in the development of tissue lesions associated with African trypanosomiasis in mice. *Clin Exp Immunol*. 1978;33(1):12–24.

155. Roderick TH, Langley SH, Leiter EH. Some unusual genetic characteristics of BALB/c and evidence for genetic variation among BALB/c substrains. *Curr Top Microbiol Immunol*. 1985;122:9–18.

156. Ludwig RJ. Model systems duplicating epidermolysis bullosa acquisita: A methodological review. *Autoimmunity*. 2011;

157. Leineweber S, Schönig S, Seeger K. Insight into interactions of the von-Willebrand-factor-A-like domain 2 with the FNIII-like domain 9 of collagen VII by NMR and SPR. *FEBS Lett*. 2011;585(12):1748–1752.

158. Ishii N et al. Autoantibody-induced intestinal inflammation and weight loss in experimental epidermolysis bullosa acquisita. *J Pathol*. 2011;224(2):234–44.

159. Roche Applied Science. In Situ Cell Death Detection Kit, Fluorescein [Internet]http://www.roche-applied-science.com/shop/en/us/products/%3Ci%3Ein-situ%3C-i%3E-cell-death-detection-kit-fluorescein. Accessed on April 28, 2013

160. Gavrieli Y, Sherman Y, Ben-Sasson SA. Identification of programmed cell death in situ via specific labeling of nuclear DNA fragmentation. *J Cell Biol*. 1992;119(3):493–501.

161. Brown H.S. HEMATOXYLIN & EOSIN [Internet]http://www.sigmaaldrich.com/img/assets/7361/Primer-H&Emay04.pdf. Accessed on April 29, 2013

162. Ludwig RJ et al. Junctional adhesion molecules (JAM)-B and -C contribute to leukocyte extravasation to the skin and mediate cutaneous inflammation. *J Invest Dermatol*. 2005;125(5):969–976.

163. Recke A et al. Pathogenicity of IgG subclass autoantibodies to type VII collagen: induction of dermal-epidermal separation. *J Autoimmun*. 2010;34(4):435–444.

164. Torres M, Hall FL, O'Neill K. Stimulation of human neutrophils with formyl-methionyl-leucyl-phenylalanine induces tyrosine phosphorylation and activation of two distinct mitogen-activated protein-kinases. *J Immunol*. 1993;150(4):1563–1577.

165. Zillikens D et al. A highly sensitive enzyme-linked immunosorbent assay for the detection of circulating anti-BP180 autoantibodies in patients with bullous pemphigoid. *J Invest Dermatol*. 1997;109(5):679–683.

166. Kasperkiewicz M et al. Clearance rates of circulating and tissue-bound autoantibodies to type VII collagen in experimental epidermolysis bullosa acquisita. *Br J Dermatol*. 2010;162(5):1064–70.

167. Chen Q, He F, Kwang J, Chan JKY, Chen J. GM-CSF and IL-4 Stimulate Antibody Responses in Humanized Mice by Promoting T, B, and Dendritic Cell Maturation. *J Immunol*. [published online ahead of print: October 22, 2012]; doi:10.4049/jimmunol.1201789

168. Puga I et al. B cell-helper neutrophils stimulate the diversification and production of immunoglobulin in the marginal zone of the spleen. *Nat Immunol*. 2012;13(2):170–180.

169. Kasperkiewicz M et al. Heat-shock protein 90 inhibition in autoimmunity to type VII collagen: evidence that nonmalignant plasma cells are not therapeutic targets. *Blood*. 2011;117(23):6135–42.

170. Gupta R, Woodley DT, Chen M. Epidermolysis bullosa acquisita. *Clin Dermatol*. 2012;30(1):60–9.

171. Buijsrogge JJ, Diercks GF, Pas HH, Jonkman MF. The many faces of epidermolysis bullosa acquisita after serration pattern analysis by direct immunofluorescence microscopy. *Br J Dermatol*. 2011;165(1):92–8.

172. Zumelzu C et al. Black Patients of African Descent and HLA-DRB1*15:03 Frequency Overrepresented in Epidermolysis Bullosa Acquisita. *J Invest Dermatol*. 2011;131(12):2386–93.

173. Lang PG, Tapert MJ. Severe ocular involvement in a patient with epidermolysis bullosa acquisita. *J Am Acad Dermatol*. 1987;16(2 Pt 2):439–43.

174. Zierhut M et al. Ocular involvement in epidermolysis bullosa acquisita. *Arch Ophthalmol*. 1989;107(3):398–401.

175. Caux F et al. IgA-epidermolysis bullosa acquisita in a child resulting in blindness. *Br J Dermatol*. 1997;137(2):270–5.

176. Camara A et al. [Resistant acquired bullous epidermolysis with severe ocular involvement: the success of extracorporeal photochemotherapy]. *Ann Dermatol Venereol*. 1999;126(8-9):612–5.

177. Bauer JW et al. Ocular involvement in IgA-epidermolysis bullosa acquisita. *Br J Dermatol*. 1999;141(5):887–92.

178. Vodegel RM, de Jong MC, Pas HH, Jonkman MF. IgA-mediated epidermolysis bullosa acquisita: two cases and review of the literature. *J Am Acad Dermatol*. 2002;47(6):919–25.

179. Kurzhals G et al. Acquired epidermolysis bullosa with the clinical feature of Brunsting-Perry cicatricial bullous pemphigoid. *Arch Dermatol*. 1991;127(3):391–5.

180. Wieme N et al. Epidermolysis bullosa acquisita with combined features of bullous pemphigoid and cicatricial pemphigoid. *Dermatology*. 1999;198(3):310–3.

181. Taniuchi K, Inaoki M, Nishimura Y, Mori T, Takehara K. Nonscarring inflammatory epidermolysis bullosa acquisita with esophageal involvement and linear IgG deposits. *J Am Acad Dermatol*. 1997;36(2 Pt 2):320–2.

182. Harman KE, Whittam LR, Wakelin SH, Black MM. Severe, refractory epidermolysis bullosa acquisita complicated by an oesophageal stricture responding to intravenous immune globulin. *Br J Dermatol*. 1998;139(6):1126–7.

183. Shipman AR et al. Epidermolysis bullosa acquisita requiring multiple oesophageal dilatations. *Clin Exp Dermatol*. 2008;33(6):787–9.

184. Luke MC et al. Mucosal morbidity in patients with epidermolysis bullosa acquisita. *Arch Dermatol*. 1999;135(8):954–9.

185. Hester JE, Arnstein DP, Woodley D. Laryngeal manifestations of epidermolysis bullosa acquisita. *Arch Otolaryngol Head Neck Surg*. 1995;121(9):1042–4.

186. Raab B et al. Epidermolysis bullosa acquisita and inflammatory bowel disease. *JAMA*. 1983;250(13):1746–8.

187. Schattenkirchner S et al. Localized epidermolysis bullosa acquisita of the esophagus in a patient with Crohn's disease. *Am J Gastroenterol*. 1996;91(8):1657–9.

188. Labeille B, Gineston JL, Denoeux JP, Capron JP. Epidermolysis bullosa acquisita and Crohn's disease. A case report with immunological and electron microscopic studies. *Arch Intern Med*. 1988;148(6):1457–9.

189. Hughes BR, Horne J. Epidermolysis bullosa acquisita and total ulcerative colitis. *J R Soc Med*. 1988;81(8):473–5.

190. Licarete E et al. Prevalence of collagen VII-specific autoantibodies in patients with autoimmune and inflammatory diseases. *BMC Immunol*. 2012;13:16.

191. Bernard P et al. Incidence and distribution of subepidermal autoimmune bullous skin diseases in three French regions. Bullous Diseases French Study Group. *Arch Dermatol*. 1995;131(1):48–52.

192. Bertram F, Bröcker EB, Zillikens D, Schmidt E. Prospective analysis of the incidence of autoimmune bullous disorders in Lower Franconia, Germany. *J Dtsch Dermatol Ges*. 2009;7(5):434–40.

193. Bordier-Lamy F et al. [Epidermolysis bullosa acquisita of childhood]. *Ann Dermatol Venereol*. 2009;136(6-7):513–7.

194. Stanley JR, Amagai M. Pemphigus, bullous impetigo, and the staphylococcal scalded-skin syndrome. *N Engl J Med*. 2006;355(17):1800–1810.

195. Woodley DT et al. Epidermolysis bullosa acquisita antigen is the globular carboxyl terminus of type VII procollagen. *J Clin Invest*. 1988;81(3):683–7.

196. Lapiere JC et al. Epitope mapping of type VII collagen. Identification of discrete peptide sequences recognized by sera from patients with acquired epidermolysis bullosa. *J Clin Invest*. 1993;92(4):1831–9.

197. Gammon WR et al. Autoantibodies to type VII collagen recognize epitopes in a fibronectin-like region of the noncollagenous (NC1) domain. *J Invest Dermatol*. 1993;100(5):618–22.

198. Ishii N et al. Some epidermolysis bullosa acquisita sera react with epitopes within the triple-helical collagenous domain as indicated by immunoelectron microscopy. *Br J Dermatol*. 2009;160(5):1090–3.

199. Ishii N et al. Epidermolysis bullosa acquisita sera react with distinct epitopes on the NC1 and NC2 domains of type VII collagen: study using immunoblotting of domain-specific recombinant proteins and postembedding immunoelectron microscopy. *Br J Dermatol*. 2004;150(5):843–51.

200. Kulkarni S et al. PI3Kβ plays a critical role in neutrophil activation by immune complexes. *Sci Signal*. 2011;4(168):ra23.

201. Gammon WR et al. Increased frequency of HLA-DR2 in patients with autoantibodies to epidermolysis bullosa acquisita antigen: evidence that the expression of autoimmunity to type VII collagen is HLA class II allele associated. *J Invest Dermatol*. 1988;91(3):228–32.

202. Noe MH, Chen M, Woodley DT, Fairley JA. Familial epidermolysis bullosa acquisita. *Dermatol Online J*. 2008;14(12):2.

203. Iwata H. CD4+ T cells control loss of self-tolerance in experimental epidermolysis bullosa acquisita. In: Venice: Journal of Investigative Dermatology; S14–S35

204. Li Z, Srivastava P. Heat-shock proteins. *Curr Protoc Immunol*. 2004;Appendix 1:Appendix 1T.

205. Raska M, Weigl E. Heat shock proteins in autoimmune diseases. *Biomed Pap Med Fac Univ Palacky Olomouc Czech Repub*. 2005;149(2):243–249.

206. Colliou N et al. Long-term remissions of severe pemphigus after rituximab therapy are associated with prolonged failure of desmoglein B cell response. *Sci Transl Med*. 2013;5(175):175ra30.

207. Müller R et al. T and B cells target identical regions of the non-collagenous domain 1 of type VII collagen in epidermolysis bullosa acquisita. *Clin Immunol*. 2010;135(1):99–107.

208. Hammers CM et al. Complement-Fixing Anti-Type VII Collagen Antibodies Are Induced in Th1-Polarized Lymph Nodes of Epidermolysis Bullosa Acquisita-Susceptible Mice. *J Immunol*. 2011;187(10):5043–50.

209. Kuo TT et al. Neonatal Fc receptor: from immunity to therapeutics. *J Clin Immunol*. 2010;30(6):777–789.

210. Tzaban S et al. The recycling and transcytotic pathways for IgG transport by FcRn are distinct and display an inherent polarity. *J Cell Biol*. 2009;185(4):673–684.

211. Li N et al. Complete FcRn dependence for intravenous Ig therapy in autoimmune skin blistering diseases. *J Clin Invest*. 2005;115(12):3440–3450.

212. Sesarman A, Sitaru AG, Olaru F, Zillikens D, Sitaru C. Neonatal Fc receptor deficiency protects from tissue injury in experimental epidermolysis bullosa acquisita. *J Mol Med (Berl)*. 2008;86(8):951–9.

213. Paller AS et al. Organ-specific, phylogenetic, and ontogenetic distribution of the epidermolysis bullosa acquisita antigen. *J Invest Dermatol*. 1986;86(4):376–9.

214. Rock B, Labib RS, Diaz LA. Monovalent Fab' immunoglobulin fragments from endemic pemphigus foliaceus autoantibodies reproduce the human disease in neonatal Balb/c mice. *J Clin Invest*. 1990;85(1):296–299.

215. Iwata H et al. IgG from patients with bullous pemphigoid depletes cultured keratinocytes of the 180-kDa bullous pemphigoid antigen (type XVII collagen) and weakens cell attachment. *J Invest Dermatol*. 2009;129(4):919–926.

216. Sesarman A et al. Binding of avian IgY to type VII collagen does not activate complement and leucocytes and fails to induce subepidermal blistering in mice. *Br J Dermatol*. 2008;158(3):463–71.

217. Lovell DJ et al. Adalimumab with or without methotrexate in juvenile rheumatoid arthritis. *N Engl J Med*. 2008;359(8):810–820.

218. John H, Whallett A, Quinlan M. Successful biologic treatment of ocular mucous membrane pemphigoid with anti-TNF-alpha. *Eye (Lond)*. 2007;21(11):1434–1435.

219. Hirose M et al. The Allosteric CXCR1/2 Inhibitor DF2156A Improves Experimental Epidermolysis Bullosa Acquisita [Internet]. *Journal of Genetic Syndromes & Gene Therapy*. 2013;04(03). doi:10.4172/2157-7412.S3-005

220. Campbell IK, Bendele A, Smith DA, Hamilton JA. Granulocyte-macrophage colony stimulating factor exacerbates collagen induced arthritis in mice. *Ann Rheum Dis*. 1997;56(6):364–368.

221. Gillessen S, Mach N, Small C, Mihm M, Dranoff G. Overlapping roles for granulocyte-macrophage colony-stimulating factor and interleukin-3 in eosinophil homeostasis and contact hypersensitivity. *Blood*. 2001;97(4):922–928.

222. Kondo S, Pastore S, Shivji GM, McKenzie RC, Sauder DN. Characterization of epidermal cytokine profiles in sensitization and elicitation phases of allergic contact dermatitis as well as irritant contact dermatitis in mouse skin. *Lymphokine Cytokine Res*. 1994;13(6):367–375.

223. Radeke HH, Ludwig RJ, Boehncke W-H. Experimental approaches to lymphocyte migration in dermatology in vitro and in vivo. *Exp Dermatol*. 2005;14(9):641–666.

224. Roberts AW. G-CSF: a key regulator of neutrophil production, but that's not all! *Growth Factors*. 2005;23(1):33–41.

225. Spitzer G et al. Randomized comparison of G-CSF + GM-CSF vs G-CSF alone for mobilization of peripheral blood stem cells: effects on hematopoietic recovery after high-dose chemotherapy. *Bone Marrow Transplant*. 1997;20(11):921–930.

226. Cairo MS, van de Ven C, Toy C, Mauss D, Sender L. Recombinant human granulocyte-macrophage colony-stimulating factor primes neonatal granulocytes for enhanced oxidative metabolism and chemotaxis. *Pediatr Res*. 1989;26(5):395–399.

227. Barker JN et al. Modulation of keratinocyte-derived interleukin-8 which is chemotactic for neutrophils and T lymphocytes. *Am J Pathol*. 1991;139(4):869–876.

228. Sugita T et al. Enhanced expression of interleukin 6 in rat and murine arthritis models. *Int J Immunopharmacol*. 1993;15(4):469–476.

229. Takai Y et al. Enhanced production of interleukin-6 in mice with type II collagen-induced arthritis. *Arthritis Rheum*. 1989;32(5):594–600.

230. Waage A, Kaufmann C, Espevik T, Husby G. Interleukin-6 in synovial fluid from patients with arthritis. *Clin Immunol Immunopathol*. 1989;50(3):394–398.

231. Smolen JS, Aletaha D, Koeller M, Weisman MH, Emery P. New therapies for treatment of rheumatoid arthritis. *Lancet*. 2007;370(9602):1861–1874.

232. Lesina M et al. Stat3/Socs3 activation by IL-6 transsignaling promotes progression of pancreatic intraepithelial neoplasia and development of pancreatic cancer. *Cancer Cell*. 2011;19(4):456–469.

233. Grivennikov S et al. IL-6 and Stat3 are required for survival of intestinal epithelial cells and development of colitis-associated cancer. *Cancer Cell*. 2009;15(2):103–113.

234. Hellberg L et al. Methylprednisolone Blocks Autoantibody-Induced Tissue Damage in Experimental Models of Bullous Pemphigoid and Epidermolysis Bullosa Acquisita through Inhibition of Neutrophil Activation. *J Invest Dermatol*. [published online ahead of print: February 28, 2013]; doi:10.1038/jid.2013.91

235. Schmidt E, Waschke J. Apoptosis in pemphigus. *Autoimmun Rev*. 2009;8(7):533–537.

236. Neurath MF, Finotto S. IL-6 signaling in autoimmunity, chronic inflammation and inflammation-associated cancer. *Cytokine Growth Factor Rev*. 2011;22(2):83–89.

11. Scientific achievement during the PhD work

11.1 List of own original articles

11.1.1. Related to PhD thesis

1. **Recombinant IL-6 treatment protects mice from organ specific autoimmune disease by IL-6 classical signalling-dependent IL-1Ra induction**. *Samavedam UK, Kalies K, Scheller J, Sadeghi H, Gupta Y, Jonkman MF, Schmidt E, Westermann J, Zillikens D, Rose-John S, Ludwig RJ.* ***Journal of Autoimmunity,*** *Volume 40, February 2013, Pages 74-85, PMID:22980031*

11.1.2. Other publications

1. **Methylprednisolone blocks autoantibody-induced tissue damage in experimental models of bullous pemphigoid and epidermolysis bullosa acquisita through inhibition of neutrophil activation.** *Hellberg L, Samavedam UK, Holdorf K, Hänsel M, Recke A, Beckmann T, Steinhorst K, Boehncke WH, Kirchner T, Möckel N, Solbach W, Zillikens D, Schmidt E, Ludwig RJ, Laskay T.,* ***Journal of Investigative Dermatology****, doi: 10.1038/jid.2013.91, SN: 1523-1747, April 2013, PMID: 23448878 (advanced online publication).*
2. **Genetic identification and functional validation of FcγRIV as key molecule in autoantibody-induced tissue injury.** *Kasperkiewicz M, Nimmerjahn F, Wende S, Hirose M, Iwata H, Jonkman MF, Samavedam U, Gupta Y, Möller S, Rentz E, Hellberg L, Kalies K, Yu X, Schmidt E, Häsler R, Laskay T, Westermann J, Köhl J, Zillikens D, Ludwig RJ****.*** ***Journal of Pathology*****,** *228: 8–19, September 2012, PMID: 2243093.*

11.2. Oral presentations and posters during PhD work

1. May 2013, **"GM-CSF modulates both innate and adaptive immune responses in autoantibody-mediated organ-specific autoimmune disease"**, IID-2013, Edinburgh, Scotland, UK (Poster)
2. May 2013, **"GM-CSF modulates both innate and adaptive immune responses in autoantibody-mediated organ-specific autoimmune disease"**, International pre IID 2013 Satellite Meeting on Autoimmune Bullous Diseases, Lübeck, Germany (Poster)
3. March 2013, **"Distinct contributions of cytokines to autoantibody-induced tissue injury"**, 40th ADF-2013 meeting, Dessau, Germany (Poster)
4. February 2013, **"GM-CSF modulates both innate and adaptive immune responses in an autoantibody-mediated organ-specific autoimmune disease"**, Interdisciplinary Cluster Symposium-Inflammation at Interfaces, Hamburg, Germany (poster)
5. December 2012, **"Distinct contributions of cytokines to autoantibody-induced tissue injury"**, Biofest 2012, Hyderabad, India (Oral presentation)
6. November 2012, **"Recombinant IL-6 treatment protects mice from organ-specific autoimmune disease by induction of IL-1Ra, mediated by classical IL-6 signaling",** 35th symposium of the North-German Immunologists, Borstel, Germany (poster)
7. September 2012, **"Recombinant IL-6 treatment protects mice from organ specific autoimmune disease by IL-6 classical signalling-dependent IL-1Ra induction"**, European Society for Dermatological Research (ESDR), Venice, Italy (Oral presentation & poster)
8. May-2012, **"Role of GM-CSF in the pathogenesis of EBA"**, International congress on Autoimmunity, Granada, Spain (Poster)

9. April-2012, "**Crucial Role of GM-CSF in the pathogenesis of EBA"**, GRK1727-Modulation of Autoimmunity retreat, Lübeck, Germany (Oral presentation)
10. February-2012, **"Role of GM-CSF in the pathogenesis of EBA"**, Arbeitsgemeinschaft Dermatologische Forschung (ADF)-Marburg, Germany (Oral presentation & Poster)
11. November-2011, **"Immune modulation in EBA- Role of keratinocytes"**, GRK1727-Modulation of Autoimmunity retreat, Ahrensburg, Germany (Oral presentation)
12. May-2011, **"Role of GM-CSF in the pathogenesis of EBA"**, *Uni im Dialog* – 5. Lübecker Doktorandentag. Lübeck, Germany (Poster)
13. December-2010, **"IL-6 modulates autoantibody induced tissue injury in EBA"**, Dermatology retreat, University of Lübeck, Boltenhagen, Germany (Oral presentation)

11.3. Published abstracts

1. **GM-CSF modulates both innate and adaptive immune responses in autoantibody-mediated organ-specific autoimmune disease,** *U Samavedam, H Iwata, S Müller, FS Schulze, A Recke, E Schmidt, D Zillikens and RJ Ludwig****, International Investigative Dermatology (IID-2013), Edinburgh, 8–11 May, 2013,*** *J Invest Dermatology 133: S17-S55; doi:10.1038/jid.2013.95.*

2. **Distinct contributions of cytokines to autoantibody-induced tissue injury,** *U Samavedam, Misa Hirose, Hengameh Sadeghi, Michael Kasperkiewicz, Marcel Jonkman, Jürgen Scheller, Kathrin Kalies, Jürgen Westermann, Enno Schmidt, Anike Lockmann, Anna-Carina Hund, Takashi Hashimoto, Michael P. Schön, Detlef Zillikens, Stefan Rose-John and Ralf J. Ludwig,* ***40th Annual Meeting of the Arbeitsgemeinschaft Dermatologische Forschung, Dessau, Germany, 14-16th March, 2013,*** *Experimental Dermatology, Volume 22, Issue 3, DOI: 10.1111/exd.12072.*

3. **Distinct contributions of cytokines to autoantibody-induced tissue injury**, *Unni Krishna SRL Samavedam, Misa Hirose, Hengameh Sadeghi, Michael Kasperkiewicz, Marcel Jonkman, Jürgen Scheller, Kathrin Kalies, Jürgen Westermann, Enno Schmidt, Anike Lockmann, Anna-Carina Hund, Takashi Hashimoto, Michael P. Schön, Detlef Zillikens, Stefan Rose-John and Ralf J. Ludwig,* ***Biofest 2012, Hyderabad, India, 12-13th December,2012.*** *http://www.brightice.org/proceedings.php, Track-2-5: Immunology and Current research*

4. **Recombinant IL-6 treatment protects mice from organ-specific autoimmune disease by induction of IL-1Ra, mediated by classical IL-6 signaling**, *US Samavedam, K Kalies, J Scheller, Y Gupta, MF Jonkman, E Schmidt, J Westermann, D Zillikens, S Rose-John and R Ludwig,* ***42nd Annual meeting of***

the European Society of Dermatological Research (ESDR), Venice, Italy, 19-22 September,2012, *Journal of Investigative Dermatology (2012) 132, S14–S35*

5. **A crucial role of granulocyte-macrophage colony-stimulating factor in the pathogenesis of experimental epidermolysis bullosa acquisita**, *U. Samavedam, S. Müller, A. Recke, E. Schmidt, D. Zillikens and R. J. Ludwig,* ***39th Annual Meeting of the Arbeitzgemeinschaft Dematologische Forschung (ADF), Marburg, Germany - March 01-03****, 2012, Exp. Dermatol. (2012), 21: e11, P062 (V08).*

11.4. Received Awards

1. XI International Society of Dermatology Global Education Award, to be presented at XI International Congress of Dermatology - New Delhi, 4th - 7th December, 2013 (prize value $1000)
2. GRK-1727 publication award “Recombinant IL-6 treatment protects mice from organ specific autoimmune disease by IL-6 classical signaling-dependent IL-1Ra induction”, GRK winter retreat, 9th-10th November 2012 (prize value €1500).
3. Travel grant for 46th annual meeting of the European Society for Dermatological Research (ESDR), Venice, Italy, 19-22nd September 2012 (prize value €500).

12. Acknowledgements

I would like to articulate my utmost gratitude to **Prof. Detlef Zillikens**, Director of Department of Dermatology and Venereology, University of Lübeck for providing me this opportunity to start my scientific career in the cytokine biology of the skin and for his supervision and guidance.

I gratefully acknowledge my supervisor, **Prof. Ralf J Ludwig**, Department of Dermatology. Throughout this research project, I have very gratefully received numerous thoughtful and helpful suggestions and guidance from him.

I am thankful to **Prof. Enno Schmidt,** Department of Dermatology and Venereology, for being my second supervisor in GRK and for his valuable suggestions and guidance.

I am also heartily thankful to **Prof. Jürgen Westermann**, Professor of Institute of Anatomy for providing critical comments and being mentor in GRK & Chairman to my thesis.

I am also thankful to **Prof. Jörg Köhl**, Professor of Institute for Systemic Inflammation Research (ISEF) for providing critical suggestions on my thesis.

I am also very much thankful to **Prof. Stephan Rose-John**, Department of Biochemistry, CAU, Kiel and **Prof. Jürgen Scheller**, Department of Biochemistry, Dusseldorf for their valuable suggestions and guidance.

I am also incredibly thankful to **Prof. Marcel F. Jonkman**, Department of Dermatology, University of Groningen, Groningen, Netherlands, for providing EBA patient sera.

I very sincerely appreciate the valuable assistance and advice given by my peers and supervisors and colleagues in the completion of this project. I have been truly fortunate to work in such a marvelous environment. In particular, I greatly thank Ms. Susen Müller who helped me in the generation of GM-CSF$^{-/-}$ mice used in the study and Dr. Kathrin Kalies, Institute of Anatomy, University of Lübeck, for her assistance in RT-PCR analysis. I sincerely grateful for the assistance given by Ms. Claudia Kauderer and Ms. Rebecca Cames, laboratory technicians in the laboratory, to carry out histology experiments, ROS release assays and ELISA. I am also appreciating the assistance given by Dr. Hiroaki Iwata, M.D, during the studies on the active model of EBA. I am very much thankful to Dr. Andreas Recke and Mr. Yask Gupta who helped me in learning R-packages and statistical analysis.

I dedicate this work to my parents, S.L.N.Sastry & S.S.Lakshmi and to my wife, Samanvitha. With their never-failing support and encouragement, I have been able to pursue this dermatological research.

13. Declarations

No part of the work referred to in this dissertation has been submitted in support of an application for any degree or qualification of The University of Lübeck or any other University or Institute of learning.

14. Copyright Statement